# Manipulating Magnetic Structures in Chiral Metals by Currents

## Manipulation chiraler magnetischer Strukturen in Metallen durch elektrische Ströme

**Diploma Thesis**

**by**

**Karin Everschor**


*Institute of Theoretical Physics, Department of Physics*
*Faculty of Mathematics and Natural Sciences*
*University of Cologne*

Cologne, June 2009

## Abstract

In this thesis, we investigate the influence of electric currents on magnetic structures in bulk materials, such as manganese silicide (MnSi). This research is motivated by recent experiments in spintronics suggesting that electric currents influence magnetic structures by spin transfer torques. The so-called "spin transfer" describes the transfer of angular momentum produced by a flow of electrons through an inhomogeneous magnetization configuration.

We focus on magnets without inversion symmetry, where weak spin-orbit coupling leads to the formation of magnetic helices with a long pitch. These helices pin only very weakly to disorder and the underlying crystalline lattice. Specifically, we study the helimagnet MnSi which exhibits a particularly interesting phase, the so-called "A-phase". It is well described by a superposition of three helices and a uniform magnetic moment forming a lattice of anti-Skyrmions.

To formulate an effective theory for the magnetization direction, we start from the Landau-Lifshitz-Gilbert equation including reactive and dissipative spin transfer torques. In particular, we characterize the different magnetic structures by a few time-dependent variables and determine their equations of motion.

As a main result, we find that the current does not alter the direction of the single helix but has an influence on the A-phase which is slightly anisotropic. Both results are in agreement with experimental observations in MnSi. We find, that on the one hand the direction vectors of the three helices rotate, but on the other hand the plane defined by the direction vectors tilts. Both effects are linear in the strength of the current. Moreover, we illustrate that similar to the topological Hall effect a non-zero Skyrmion density is the significant link between the magnetic structure and the current.

Apparently, our effective theory explains well the experimentally observed distortion of the A-phase by currents.

# Contents

# Introduction

In this thesis, we examine the influence of an electric current on magnetic structures. Motivated by recent experiments performed with manganese silicide (MnSi), which is a chiral itinerant magnet, we study this material as an explicit example. However, most of the displayed formalism is also applicable to other chiral magnetic materials. In particular, helimagnetical structures appear in a lot of materials, e.g. in $Fe_xCo_{1-x}Si$, CrSi and FeGe. Moreover, also the topologically non-trivial magnetic structure of MnSi, the so-called "A-phase", is experimentally detected in a second material: Münzer *et al.* have verified the magnetic structur of the A-phase in $Fe_xCo_{1-x}Si$ for $x = 0.2$ and $x = 0.25$ [1].

Section 1 constitutes a description of some general properties of MnSi. Moreover, we present a temperature versus magnetic field phase diagram of MnSi and describe the different magnetic phases. The phases that appear are the helical phase, the conical phase and the A-phase. The experimental setups to detect these three phases by neutron scattering are explained in Section 2.

In Section 3, we focus on the theoretical description of the different magnetic ground states in the framework of a Ginzburg-Landau theory. First, we recapitulate the results for usual ferromagnets without spin-orbit coupling. Afterwards, we examine magnets without inversion symmetry in general, and we observe that weak spin-orbit coupling leads to the formation of magnetic helices with a long pitch. In the last part of this Section, we give reasons for the stabilization of the A-phase.

In Section 4, we try to motivate the investigation of the influence of a current on magnetic materials. In Section 5, we introduce the Landau-Lifshitz-Gilbert (LLG) equation including reactive and dissipative spin transfer torques. The LLG equation describes the dynamic evolution of the local magnetic moments. Starting from this equation as an ansatz, we determine the equations of motion for a general magnetic structure that can be described by a finite number of variables.

In Sections 6 and 7, we apply the method introduced in the previous Section to the helical phase and the A-phase. As a basic result, we find that a current leads to a drift of the magnetic configuration. Besides in the helical phase, the current does not alter the magnetic texture, but in the A-phase it leads to a rotation and a tilt of the magnetic pattern.

Section 8 discusses the topological Hall effect that occurs in the A-phase and identifies this phase as a lattice of anti-Skyrmions. Finally, in Section 9, we study a derivation of the LLG equation from a variational principle, where the origin of the Berry phase leading to the topological Hall effect becomes evident.

# 1 Properties and Magnetic Phases of MnSi

Manganese silicide (MnSi) is a weakly ferromagnetic itinerant metal with an experimentally measured Curie temperature of $T_c \approx 29\,\mathrm{K}$. It can be produced in ultra-pure form with a mean free path of about 5000 Å. The intermetallic compound forms the cubic crystal structure B20 with four Mn and four Si atoms per unit cell. The atoms are in the positions $(u, u, u; \frac{1}{2}+u, \frac{1}{2}-u, \bar{u}; \frac{1}{2}-u, \bar{u}, \frac{1}{2}+u; \bar{u}, \frac{1}{2}+u, \frac{1}{2}-u)$ with $u_{\mathrm{Mn}} = 0.138$ and $u_{\mathrm{Si}} = 0.845$. In this structure, the Mn and the Si atoms are displaced in opposite $\langle 111 \rangle$ directions from the fcc position [2].

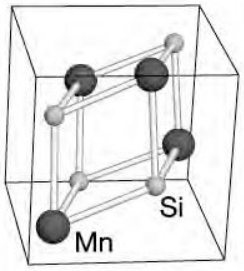


Figure 1: Crystalline structure of MnSi. Picture taken from Ref. [3].

MnSi crystallizes in the noncentrosymmetric cubic space group $P2_13$. The corresponding point group $T$ consists only of cyclic permutations of $\hat{x}, \hat{y}$ and $\hat{z}$, of rotations by $\pi$ around the coordinate axes, and of combinations thereof. However, the crystalline structure of MnSi has *no inversion symmetry*. Other noncentrosymmetric itinerant magnets with B20 crystal structure are, for example, $\mathrm{Fe}_x\mathrm{Co}_{1-x}\mathrm{Si}$, CrSi and FeGe.

Fig. 2 shows the magnetic phases of MnSi as a function of temperature $T$ and applied magnetic field $B$. In addition to the usual ferromagnetic and paramagnetic phases of a ferromagnet, MnSi exhibits three other magnetic phases.

At ambient pressure and small applied magnetic field MnSi develops a left-handed helical magnetic order below a critical temperatur of $T_c = 29.5\,\mathrm{K}$ [7, 8, 9]. The ordered magnetic moment $\vec{M}$ is perpendicular to the propagation vector $\vec{q}$ of the helix, and its low temperature magnitude is of the order of $0.4\,\mu_{\mathrm{B}}$. Its origin is the asymmetric Dzyaloshinskii-Moriya (DM) spin-orbit coupling [9, 10, 11, 12] due to the lack of inversion symmetry in its $B20$-type cubic structure. The DM interaction favors canted spin structures and therefore precludes the establishment of a ferromagnetic ground state. The period of the helix, approximately 190 Å, is large compared to the lattice constant, $a \approx 4.56\,\text{Å}$. This large separation of length scales leads to an effective decoupling of the magnetic and atomic structures. Besides the ferromagnetic and the DM interaction, there are very weak crystalline field

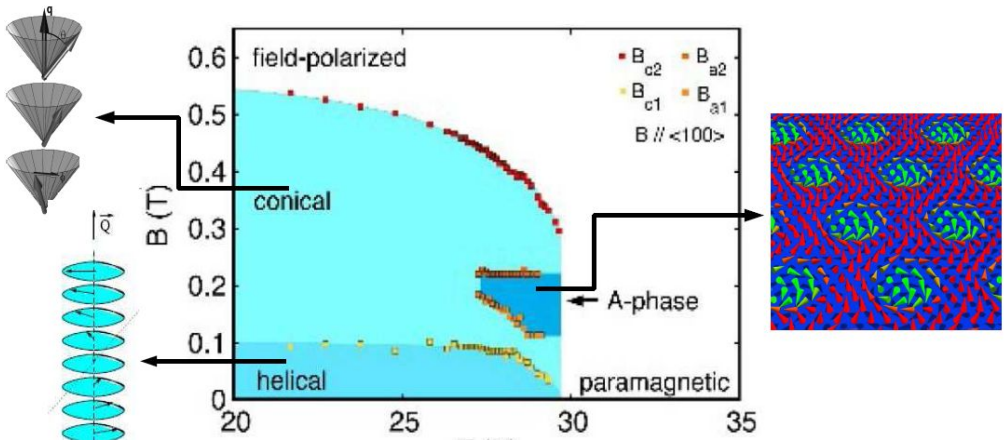


Figure 2: Magnetic phase diagram of MnSi as a function of temperature and applied magnetic field (see text for details). Pictures taken from Ref. [4, 5, 6].

interactions which break the rotational symmetry [9, 10]. These occur only in at least fourth power in the small spin-orbit coupling and align the direction of the helix along the cubic space diagonal $\langle 111 \rangle$. The typical size of magnetic domains in the helical state is about $10^4$ Å.

Below $T_c$, with an applied magnetic field $\vec{B}$ exceeding the critical field $B_{c1} \approx 0.1\,\mathrm{T}$, the helical state evolves into a conical magnetic phase. A conical configuration of the magnetization is basically a helix with an additional uniform magnetization in the direction of the spiral wave vector $\vec{q}$. Furthermore, the magnetic field pins $\vec{q}$ parallel to $\vec{B}$. The cone angle smoothly decreases to zero at field strength $B_{c2} \approx 0.6\,\mathrm{T}$. For a magnetic field exceeding $B_{c2}$, the effects of the DM interaction are suppressed, entailing a ferromagnetic state.

For temperatures just below $T_c$ an additional phase, referred to as the A-phase, is stabilized in a finite field interval for $\vec{B} \parallel \langle 100 \rangle$, as shown in Fig. 2. Measurements of the specific heat and the susceptibility as well as neutron scattering experiments show that the A-phase is a distinct phase with a first-order phase transition separating it from the conical phase [13]. The spin orientation in the A-phase exhibits a hexagonal symmetry perpendicular to the small applied magnetic field. This magnetic structure can be described approximately by a vectorial superposition of three helical states plus a uniform magnetic component, generating an anti-Skyrmion lattice, where the magnetic field vector $\vec{B}$ is perpendicular to the wave vectors of all helices [4].

A real-space picture of such an anti-Skyrmion lattice, almost identical to the spin orientation in the A-phase, is shown in Fig. 3. It illustrates the doubly twisted magnetic structure around an anti-Skyrmion center. In contrast to vortices, Skyrmions

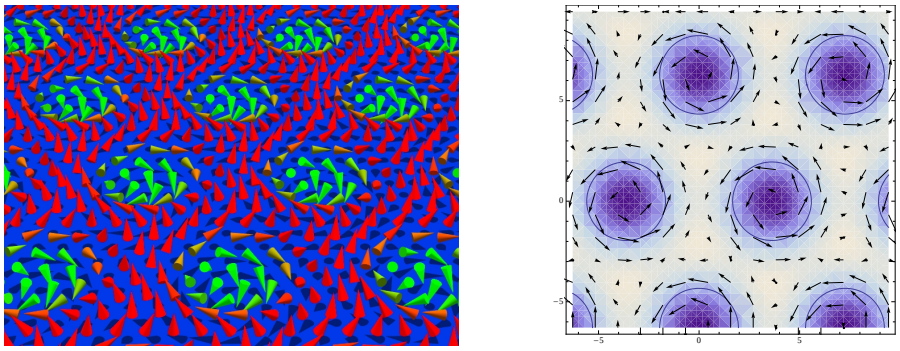


Figure 3: Spin orientation in the A-phase. Left: Three dimensional sideview illustrating the doubly twisted magnetic structure around an anti-Skyrmion center. Right: Projection from above.

do not contain a singularity at the core of the defect, i.e. the spin orientation is smooth everywhere. Furthermore, the magnetic pattern in the A-phase pins very weakly in the $\langle 110 \rangle$ direction of the crystal.

## 2 Neutron Scattering: Experimental Setup and Results

Most of the work reviewed in this Section has been published in Refs. [4, 14]. In general, helimagnetic order can be observed in neutron scattering experiments in the form of Bragg peaks located on a sphere in reciprocal space. The radius of this sphere is proportional to the inverse pitch of the helix. The position of the peaks depends on weak crystalline field interactions, which may lead to a position locking of the peaks.

In MnSi, where the helical wavevector $\vec{q}$ is along a threefold axis of the cubic structure, there are four equivalent magnetic propagation vectors $\vec{q}_1 \parallel (111)$, $\vec{q}_2 \parallel (1\bar{1}\bar{1})$, $\vec{q}_3 \parallel (\bar{1}1\bar{1})$, and $\vec{q}_4 \parallel (\bar{1}\bar{1}1)$. The chirality of the magnetic structure is single-handed as determined from polarized neutron scattering. Consequently, there are no chiral domains. The same helix is observed at $\vec{q}$ and $-\vec{q}$. With unpolarized neutrons there are thus eight magnetic peaks around each nuclear Bragg peak, corresponding to $\pm\vec{q}_k$ $(k = 1, \ldots, 4)$.

Since the direction vector of the helix $\vec{q}$ tends to align parallel to an applied magnetic field in a large part of the magnetic phase diagram, neutron scattering as a function of magnetic field $\vec{B}$ has been performed such that the magnetic field is perperdicular to the indicent neutron beam [15, 16, 17], as shown in Fig. 4.

In contrast, Mühlbauer, *et al.* have prepared the incident neutron beam parallel to the applied magnetic field, as shown in Fig. 5.

Fig. 6 shows typical data recorded for two different samples. The panels (A) to (C) are measurements of sample 1, whereas (D) to (F) are taken from a different sample 2. Panels (A) to (E) are measured in the setup, where the incident neutron beam is parallel to the applied magnetic field $\vec{B}$. Only panel (F) shows data that has been taken using the setup shown in Fig. 4. All data shown represent the sum over rocking scans with respect to the vertical axis through the sample.

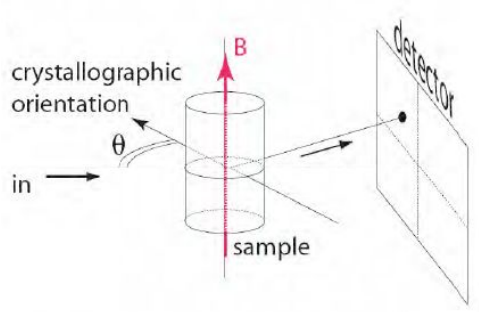


Figure 4: Neutron scattering setup; the applied magnetic field $\vec{B}$ is perpendicular to the incident neutron beam (see Ref. [14]).

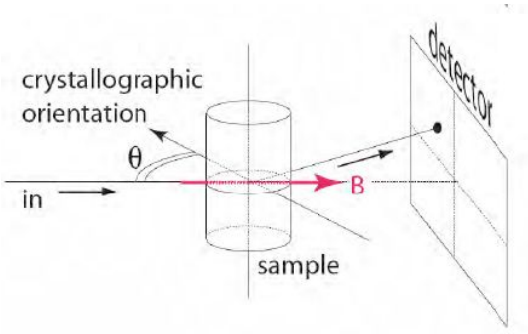


Figure 5: Neutron scattering setup; the applied magnetic field $\vec{B}$ is parallel to the incident neutron beam (see Ref. [4]).

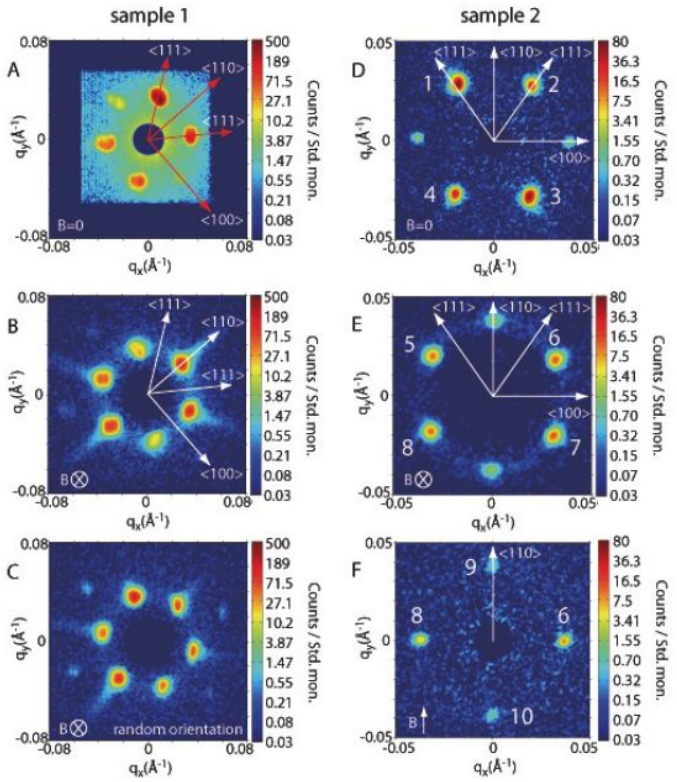


Figure 6: Typical small-angle neutron scattering (SANS) intensities (see text for details); the color scale is logarithmic to make weak features visible. A typical background measurement above $T_c$ and $\vec{B} = 0$ is substracted in all panels except for figure A, light blue square (see Ref. [4]).

(A) shows the scattering intensity in a zero-field-cooled state at temperature $T = 27\,\mathrm{K}$ and $|\vec{B}| = 0$ for a $\langle 110 \rangle$ scattering plane. One observes the helical magnetic order along $\langle 111 \rangle$.

(B) displays the intensity pattern in the A-phase. Six spots emerge on a regular hexagon. The measurement was done with the same orientation as in panel (A), but at temperature $T = 26.45\,\mathrm{K}$ and magnetic field $|\vec{B}| = 0.164\,\mathrm{T}$.

(C) shows the six-fold intensity pattern in the A-phase for a random orientation of the sample measured at temperature $T = 26.77\,\mathrm{K}$ and magnetic field $|\vec{B}| = 0.164\,\mathrm{T}$.

(D) Helical order in sample 2 in the zero-field-cooled state at temperature $T = 16\,\mathrm{K}$ and magnetic field $|\vec{B}| = 0$.

(E) The A-phase in sample 2 with same orientations as in panel (D) at temperature $T = 27.7\,\mathrm{K}$ and magnetic field $|\vec{B}| = 0,162\,\mathrm{T}$.

(F) The A-phase as measured in a conventional setup at temperature $T = 27.7\,\mathrm{K}$ and magnetic field $|\vec{B}| = 0.190\,\mathrm{T}$. A small residual intensity due to the conical phase is observed (spots 9 and 10), whereas spots 6 and 8 correspond to those in panel (E).

The neutron scattering measurements were performed at the diffractometer MIRO at FRM II at the Technische Universität München. All data at finite magnetic field were measured after zero-field-cooling to the desired temperature, followed by a field ramp to the desired field value. However, in the A-phase data were identical also after field-cooling [4].

The key results of the neutron scattering data may be summarized as follows:

- The helical wave-vector aligns perpendicular to the applied magnetic field.
- The fundamental symmetry of the intensity pattern is sixfold suggesting a multi-$\vec{q}$ structure.
- The A-phase stabilizes in a magnetic field strength of order $B_{c_2}/2$. The Bragg spots are located in the plane perpendicular to the magnetic field $\vec{B}$ and form a regular hexagon independent of the orientation of the underlying lattice. Moreover, the pattern aligns very weakly with respect to the $\langle 110 \rangle$ orientation.

# 3 Theoretical Description: Ginzburg-Landau Theory

In the abscence of a current, the magnetic structures can be analyzed in the framework of a continuum Ginzburg-Landau theory, where the Ginzburg-Landau free energy is expanded in terms of the slowly varying magnetization. Taking thermal fluctuations into account, it is also possible to explain the stabilization of the A-phase [4].

## 3.1 Ginzburg-Landau Functional for a Usual Ferromagnet

For a usual ferromagnet, we have the following szenario [18]. Below the critical temperature $T_c$, the system is spontaneously magnetized. The thermodynamic state of the system is, in addition to the external magnetic field $\vec{B}$ and the temperature $T$, characterized by the magnetization $\vec{M}$, which is the thermal average of the microscopic spins.

In the paramagnetic phase, i.e. above the critical temperature $T_c$ the magnetization $\vec{M}$ vanishes. Since $\vec{M}$ is continuous, the phase transition is of second order. Fig. 7 shows a typical temperature versus magnetic field phase diagram of a ferromagnet.

Near the critical temperature $T_c$ the two phases can be explained in the framework of a Ginzburg-Landau theory. In thermal equilibrium, the magnetic state of any system is the one that minimizes its free energy $G$. The free energy is given by the volume integral of the free energy density $F$, which is constructed as a function of the order parameter, the local magnetization $\vec{M}(\vec{r})$. The dimensionless free energy $G$ as a function of the magnetic field and temperature is given by

$$e^{-G} = \int \mathcal{D}\vec{M}\, e^{-F[\vec{M}]}. \tag{1}$$

The free energy functional $F$ is a functional of the magnetization and its derivatives. Near the phase transition the order parameter is small, such that one may expand

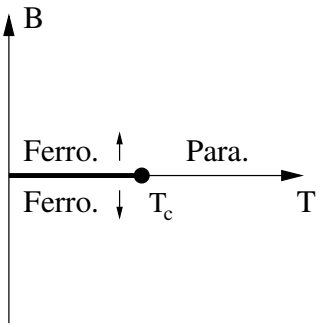


Figure 7: Magnetic phase diagram of a ferromagnet.

$F$ in powers of $\vec{M}$. Moreover, in the low energy limit, we do not expect fast fluctuations of the magnetic moments, therefore we additionally expand $F$ in gradients of the magnetization. Postulating time-reversal symmetry and invariance under the rotation of all spins, these requirements lead to

$$F[\vec{M}(\vec{r})] = \int d\vec{r} \left( r_0 \vec{M}^2 + J \underbrace{\left(\nabla \vec{M}\right)^2}_{:=\partial_\alpha M_\beta \partial_\alpha M_\beta} + U\left(\vec{M}^2\right)^2 + \text{higher order terms} \right).$$

Here, $r_0, J$ and $U$ are parameters with $J, U > 0$, and Einstein summation is understood. In a first step, we will neglect the "higher order terms." Analyzing the Ginzburg-Landau free energy functional, we observe that $F$ is additionally invariant under the following transformations:

- translation: $\vec{r} \quad \to \vec{r} + \vec{o}$ with $\vec{o} \in \mathbb{R}^3$ constant
- rotation of space: $\vec{M}(\vec{r}) \to \vec{M}(R^{-1}\vec{r})$ with $R \in SO(3)$
- full rotation: $\vec{M}(\vec{r}) \to R\vec{M}(R^{-1}\vec{r})$
- inversion: $\vec{r} \quad \to -\vec{r}$ and $\vec{M}(\vec{r}) \to +\vec{M}(-\vec{r})$

Applying an external magnetic field $\vec{B}$, we get the additional term $-\int d\vec{r}\, \vec{B} \cdot \vec{M}(\vec{r})$. In the framework of a mean field approximation, we obtain

$$G \approx \min F[\vec{M}] =: F[\vec{M}_0].$$

Therefore, the basic idea of our approach is to minimize $F$ with respect to the spin structure $\vec{M}(\vec{r})$. Afterwards, one can add fluctuations to the minimum of the free energy functional to improve the mean field solution. Within this approach, the integral in Eq. (1) becomes Gaussian and thus feasible. For a given local minimum $\vec{M}_0(\vec{r})$, the result is

$$G \approx F[\vec{M}_0] + \frac{1}{2} \ln \det \left( \frac{\delta^2 F}{\delta \vec{M} \delta \vec{M}} \right) \Bigg|_{\vec{M}_0}, \tag{2}$$

where we have omitted the additive constant $(3/2)\ln(2\pi)$.

So far, we have not taken spin-orbit coupling into account. In MnSi, spin-orbit coupling is weak, but important for the formation of the magnetic patterns. Thus, we arrange the terms of the free energy funtional according their order of spin-orbit coupling and treat spin-orbit coupling as a small pertubation. For example in the purely ferromagnetic case we may neglect spin-orbit coupling, while for MnSi we have to expand the free energy functional $F$ to higher order.

## 3.2 Ginzburg-Landau Theory for Solids Without Inversion Symmetry

For crystals without inversion symmetry like MnSi, there exist additional terms which are of higher order in spin-orbit coupling. To linear order in spin-orbit coupling there is the so-called "Dzyaloshinskii-Moriya (DM) term"

$$F_{\mathrm{DM}} = \int d\vec{r}\; 2\, D\, \vec{M} \cdot \left(\nabla \times \vec{M}\right)$$

that adds to the quadratic part of the Ginzburg-Landau free energy functional [19, 20]. This term is odd under spatial inversion. Moreover, the spin-orbit coupling term breaks the rotation symmetry. It remains only invariant under rotations in coordinate space combined with a rotation of the magnetization. Because of its relativistic origin, the DM term has a small prefactor, $D \sim v^2/c^2$. This prefactor $D$ is of the order of the spin-orbit coupling strength.

Hence, the Ginzburg-Landau free energy is to quadratic order in the magnetization $\vec{M}(\vec{r})$, given by [9, 10]

$$F_2[\vec{M}(\vec{r})] = \int d\vec{r} \left( r_0 \vec{M}^2 + J \partial_\alpha M_\beta \partial_\alpha M_\beta + 2D\vec{M} \cdot \left(\nabla \times \vec{M}\right)\right). \tag{3}$$

From this functional we may infer the existence of three energy scales: The largest energy scale is the ferromagnetic exchange energy that favors a uniform spin polarization. The second one is the weaker Dzyaloshinskii-Moriya interaction favoring canted spins. The weakest energy scale is not included in the quadratic free energy functional. It originates from very weak crystalline field interactions and is described by higher order spin-orbit interactions. For example, subleading spin-orbit coupling (crystal anisotropy) locks the magnetic structures to the underlying atomic lattice and thus determines the location of magnetic Bragg peaks.

With the additional term $F_{\mathrm{DM}}$ the ground state changes from a ferromagnetic to a helical magnetic structure for an arbitrary small $D$ [7, 21] as the following argument demonstrates . The "large-scale" magnetic structure is determined by the minimization of $F_2$, see Eq. (3). Because this model is still translational invariant, $\vec{M}(\vec{r})$ is a periodic function in space,

$$\vec{M}(\vec{r}) = \frac{M}{\sqrt{2}} \left( \vec{m} e^{i\vec{q}\cdot\vec{r}} + \vec{m}^* e^{-i\vec{q}\cdot\vec{r}} \right).$$

Here, $\vec{m}$ is a complex unit vector, i.e. $\vec{m} \cdot \vec{m}^* = 1$. If $\vec{M}^2 = M^2$ is constant, then $\vec{m}^2$ must be zero. Therefore, we can rewrite $\vec{m}$ as $\vec{m} = (\vec{m}_1 + i\vec{m}_2)/\sqrt{2}$ with two mutually perpendicular real unit vectors $\vec{m}_1$ and $\vec{m}_2$. Using this ansatz we obtain

$$\vec{M}(\vec{r}) = M \left( \vec{m}_1 \cos(\vec{q}\cdot\vec{r}) - \vec{m}_2 \sin(\vec{q}\cdot\vec{r}) \right).$$

Substituting this representation into the DM term leads to

$$2iDM^2\vec{q}\cdot\vec{m}_1\times\vec{m}_2.$$

This expression has a minimun as a function of $\vec{q}$ if the vectors $\vec{q}$ and $\vec{m}_1\times\vec{m}_2$ are collinear, i.e. parallel if $D<0$ and antiparallel if $D>0$. Thus, the additional DM term causes a helical magnetic order.

Helical structures are, however, easier to describe in momentum space. Being real, $\vec{M}(\vec{r})=\sum_{\vec{q}}\vec{m}_{\vec{q}}e^{i\vec{q}\cdot\vec{r}}\in\mathbb{R}$ implies that $\vec{m}_{-\vec{q}}=\vec{m}^*_{\vec{q}}$. This leads to the following representation of $F_2$ in momentum space

$$F_2=\sum_{\vec{q}}\left[(r_0+J\vec{q}^2)|m_{\vec{q}}|^2+2D\vec{m}^*_{\vec{q}}\cdot(i\vec{q}\times\vec{m}_{\vec{q}})\right],$$

or written in a matrix notation

$$F_2=\sum_{\vec{q}}m^a_{-\vec{q}}\Gamma^{ab}_{\vec{q}}\,m^b_{\vec{q}}$$

with

$$\Gamma^{ab}_q=\begin{pmatrix}r_0+J\vec{q}^2 & -2iDq_z & 2iDq_y\\ 2iDq_z & r_0+J\vec{q}^2 & -2iDq_x\\ -2iDq_y & 2iDq_x & r_0+J\vec{q}^2\end{pmatrix}.$$

A circularly polarized spiral mode minimizes the energy if $\nabla\times\vec{M}$ points in the direction of $-D\vec{M}$. For such modes

$$F_2=\sum_{\vec{q}}r(|\vec{q}|)|\vec{m}_{\vec{q}}|^2,$$

where $r(q)=r_0+Jq^2-2q|D|=r_0-JQ^2+J(q-Q)^2$ and $Q=|D|/J$. Here, we chose $D>0$ which selects a left-handed spiral.

Thus, the Gaussian theory determines the wavelength $\lambda=2\pi/Q=2\pi J/|D|$ and the chirality of the low-energy helical modes. As mentioned before, the prefactor $D$ is actually small. This means that the pitch of the helix is large in comparison with the crystallographic periods and, in general, it will be incommensurate with them.

However, since the Gaussian part of the free energy functional is rotational invariant, the direction of $\vec{q}$ relative to the crystallographic axes remains indeterminate. For a fixation of this direction, one has to include anisotropy terms. A more detailed description of terms that pin the helix is given in Sec. 6.4. Of course, also terms in higher order spin-orbit coupling are allowed by the crystal symmetry. In particular we count every derivative as one order of spin-orbit coupling. For example, cubic symmetry allows a term of the form [7]

$$\int d\vec{r}\,\frac{1}{2}\alpha'\left[\left(\frac{\partial M_x}{\partial x}\right)^2\left(\frac{\partial M_y}{\partial y}\right)^2\left(\frac{\partial M_z}{\partial z}\right)^2\right].$$

which is at least sixth order of spin-orbit coupling. However, we expect these terms to be small at all considered energy scales, and we may neglect them.

## 3.3 Stabilization of the A-Phase

To describe the A-phase, one first has to prove that the free energy of the A-phase is lower than that of the competing ground state, the conical phase. In Refs. [4, 14] this is shown within thermal Gaussian fluctuations on top of a mean field theory. Here, we will only summarize the main parts of it.

The basic idea is to use analogies of the A-phase to an ordinary crystal. The crystal formation of a solid out of a liquid state is often driven by cubic interactions of density waves [22]. In momentum space, they can be written as

$$\sum_{\vec{q}_1,\vec{q}_2,\vec{q}_3} \rho_{\vec{q}_1}\rho_{\vec{q}_2}\rho_{\vec{q}_3}\delta(\vec{q}_1+\vec{q}_2+\vec{q}_3)$$

The crystal can only gain energy from this term if the three momentum vectors $\vec{q}_1$, $\vec{q}_2$ and $\vec{q}_3$ lie in the same plane and add up to zero.

For MnSi, one gets a similar scenario for a part of the quartic interaction. The quartic interaction term $\int d\vec{r}\,(\vec{M}^2)^2$ of the free energy functional can be rewritten in momentum space as

$$\sum_{\vec{q}_0,\vec{q}_1,\vec{q}_2,\vec{q}_3} (\vec{m}_{\vec{q}_0}\cdot\vec{m}_{\vec{q}_1})(\vec{m}_{\vec{q}_2}\cdot\vec{m}_{\vec{q}_3})\delta(\vec{q}_0+\vec{q}_1+\vec{q}_2+\vec{q}_3),$$

where $\vec{m}_{\vec{q}}$ is the Fourier tranform of $\vec{M}(\vec{r})$, i.e. $\vec{M}(\vec{r}) = \sum_{\vec{q}}\vec{m}_{\vec{q}}\,e^{i\vec{q}\cdot\vec{r}}$. In the presence of a finite uniform component of the magnetization $\vec{M}_f$, one obtains terms which are effectively cubic in the modulated moment amplitudes

$$\sum_{\vec{q}_1,\vec{q}_2,\vec{q}_3} (\vec{M}_f\cdot m_{\vec{q}_1})(m_{\vec{q}_2}\cdot m_{\vec{q}_3})\delta(\vec{q}_1+\vec{q}_2+\vec{q}_3).$$

The three momentum vectors that add up to zero lie in the same plane. Hence, it is possible to characterize this plane by a normal vector $\hat{n}$. The modulus of the momentum vectors is fixed and can be determined by the interplay of the two gradient terms in the quadratic Ginzburg-Landau functional. As stated above, the modulus is given by $|\vec{q}| = |D|/J$. Consequently, the relative angles between the vectors are 120 ° (see Fig. 8). By symmetry, the energy change is proportional to $\vec{M}_f\cdot\hat{n}$, and therefore $\hat{n}$ aligns parallel to the magnetic field $\vec{B}$ indicating that all the three momentum vectors are perpendicular to $\vec{B}$.

These qualitative arguments explain the main experimental observations in the A-phase: For all orientations of the magnetic field with respect to the atomic lattice, six Bragg reflections are observed on a regular hexagon that is strictly perpendicular to the magnetic field. Therefore, it is a good ansatz to describe the magnetization in the A-phase by a superposition of three helices and a uniform magnetization. To minimize $F[\vec{M}]$ properly, one has to add higher-order Fourier components to

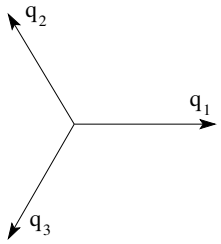


Figure 8: Three momentum vectors $\vec{q}_1$, $\vec{q}_2$ and $\vec{q}_3$ of the A-phase.

the magnetization, but these terms are small in the appropriate part of the phase diagram.

Accordingly, the A-phase is well described by

$$\vec{M}(\vec{r}) \approx \vec{M}_f + \sum_{j=1}^{3} \vec{M}^h_{\vec{q}^j}(\vec{r} + \Delta\vec{r}^j),$$

where $\vec{M}^h_{\vec{q}^j}(\vec{r}) = A(\hat{n}_1^j \cos(\vec{q}^j\vec{r}) + \hat{n}_2^j \sin(\vec{q}^j\vec{r}))$ is the magnetization of a single chiral helix with amplitude $A$. The wave vector $\vec{q}^j$ and the two unit vectors $\hat{n}_1^j$ and $\hat{n}_2^j$ are chosen such that the set $\{\vec{q}^j, \hat{n}_1{}^j, \hat{n}_2^j\}$ forms an orthonormal basis. All three helices have the same chiraliy, i.e. $\vec{q}^j \cdot (\hat{n}_1{}^j \times \hat{n}_2^j)$ has the same sign for all $j$. Finally, $\Delta\vec{r}^j$ is the relative shift of the helices. The right combination of these three phases, which emerge by minimizing the free energy functional, lead to a lattice of anti-Skyrmions.

However, whether the spin structure in the A-phase indeed represents a lattice of anti-Skyrmions, i.e. a crystalization of topologically stable knots of the spin structure [23], cannot be extracted from the neutron scattering data. Nevertheless, this phase relationship of the helices and, thus, the existence of a topologically nontrivial spin structure can be verified directly via the so-called topological Hall effect that is discussed in Sec. 8.

# 4 The Interplay of Magnetic Structures and Currents

So far we have examined different magnetic structures that occur in the phase diagramm of MnSi. Below we consider the influence of a current on these structures. To motivate the application of a current, we will comment on some basic ideas of spintronics: Electrons have a charge and a spin. In classical electronic applications, the charge degree of freedom is controlled by electric fields, but the spin degree of freedom is ignored. In other applications, i.e. magnetic recording, one benefits from the spin degree of freedom, but only because of its macroscopic accumulation, the total magnetization.

In general, spintronics describes spin transport electronics and is also known as magnetoelectronics. It is an emerging technology that exploits, in addition to the charge of an electron, its spin and its associated magnetic moment, in solid-state devices.

In 1988, the discovery of the giant magnetoresistance (GMR) effect paved the way to an efficient control of charge transport through the magnetization by acting on the spins of the electrons. This naturally leads to the idea to invert this effect, i.e. to control the magnetization by a current. Spin-transfer [24, 25, 26], i.e. the transfer of angular momentum produced by a flow of electrons through an inhomogeneous magnetization configuration, allows to manipulate the magnetization of a material using a current. This effect was theoretically proposed by Slonczewski and Berger [25, 26]. It has attracted a lot of attention due to its potential use in applications, where a magnetic state is altered by a current in contrast to conventional techniques involving magnetic fields.

The electrical control of the spin degree of freedom is a central part of spintronics, where one wants to use the electron spin for information processing and data storage. One of the long-term objective of spintronics is to combine semiconductor technology with magnetic materials to efficiently improve microelectronic devices.

Concerning MnSi, the work presented in the following is motivated by the the neutron scattering data obtained in the group of Pfleiderer, in particular for the A-phase. For the helical and the conical phase Pfleiderer *et al.* have, using neutron scattering experiments, not observed spin-torque effects under the influence of a current. However, in the A-phase the positions of the peaks change under the influence of a current. A more detailed description of this "position change" is given in Sec. 7.

One of the major challenges in the theoretical description of various spintronics phenomena, such as altering a magnetic state by a spin-polarized current, is their inherent nonequilibrium character. Therefore, to investigate the influence of a current on a magnetic structure, it is not possible to only minimize an energy functional.

Although one may use the Keldysh formalism for this situation, a probably simpler approach is to consider the equation of motion for the magnetization direction $\hat{\Omega}(\vec{x}, t)$ in the presence of a charge current $\vec{j}$. This equation is called Landau-Lifshitz-Gilbert equation [27], and will be introduced in the next section.

# 5 The Landau-Lifshitz-Gilbert Equation

The Landau-Lifshitz-Gilbert (LLG) equation is the equation of motion for the slow (up to first order in time derivative) and smooth (up to first order in space derivatives) varying magnetization direction $\hat{\Omega}(\vec{x},t) = \vec{M}(\vec{x},t)/|\vec{M}|$ with a constant amplitude $\vec{M}$. In the presence of a current $\vec{j}$, it is given by [27, 28, 29]:

$$\left(\frac{d}{dt} + \vec{v}_s \cdot \nabla\right) \hat{\Omega}(\vec{x},t) = -\hat{\Omega}(\vec{x},t) \times \vec{B}_{eff} - \alpha_G \hat{\Omega}(\vec{x},t) \times \left(\frac{d}{dt} + \frac{\beta}{\alpha_G}\vec{v}_s \cdot \nabla\right) \hat{\Omega}(\vec{x},t). \tag{4}$$

This equation is often derived phenomenologically, but it contains four parameters which can be determined only in terms of a microscopic theory:

- The effective magnetic field $\vec{B}_{\text{eff}} := -\frac{\delta F}{\delta \vec{M}} \approx -\frac{1}{|\vec{M}|}\frac{\delta F}{\delta \hat{\Omega}} = -\frac{1}{|\vec{M}|}\frac{\delta F}{\delta \vec{M}}\frac{\partial \vec{M}}{\partial \hat{\Omega}}$ including the external magnetic field and additional contributions due to magnetostatic interactions and magnetocrystalline anisotropy;
- the dimensionless Gilbert damping parameter $\alpha_G$;
- the dimensionless damping parameter $\beta$;
- the velocity $\vec{v}_s$ which is proportional to the spin-polarized current $\vec{v}_s \approx -\frac{a^3 P \vec{j}}{|e|}$ [30], where $\vec{j}$ is the charge current, $P$ the spin polarization and $e$ the electron charge. $a$ is the lattice constant, i.e. $a^{-3}$ is a measure of the magnetization density.

The term proportional to $\vec{v}_s$ on the l.h.s. is called the "reactive spin-transfer torque". The term proportional to $\beta\,\vec{v}_s$ on the r.h.s. is denoted as the "dissipative spin-transfer torque". The Landau-Lifshitz-Gilbert equation is valid if the direction of the magnetization changes slowly. Since the helical ground state of MnSi has a long wavelength, we are allowed to apply this equation for the magnetic phases of MnSi.

## 5.1 Motivation of the Landau-Lifshitz-Gilbert Equation

Let us consider a single, normalized magnetic moment $\vec{m}$ ($|\vec{m}| = 1$) in a magnetic field $\vec{H}$ without damping. For this scenario, the equation of motion is given by

$$\frac{d\vec{m}}{dt} = \left(\vec{m} \times \vec{B}\right) = \vec{T}$$

with the torque $\vec{T}$. The Larmor frequency is given by $\omega = -B$. Without damping, the magnetic moment only precesses around the magnetic field vector $\vec{B}$ and does not align parallel to $\vec{B}$ (see Fig. 9, left). Since the situation with $\vec{m} \parallel \vec{B}$ has the lowest energy, one needs a damping torque $\vec{T}_D$ which represents the rate at which

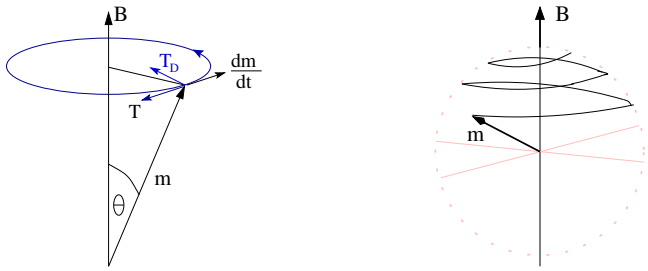


Figure 9: Sketch of a single magnetic moment in a magnetic field $B$. Left: Without damping, Right: With damping.

the magnetization relaxes to equilibrium (see Fig. 9, right). This damping torque $T_D$ should be orthogonal to $\vec{m}$ because $|\vec{m}| =$ constant, i.e. $\vec{m}$ remains on the unit sphere. Moreover, it shall be orthogonal to $\frac{d\vec{m}}{dt}$. Since $\vec{m} \perp \frac{d\vec{m}}{dt}$, $\vec{T}_D$ is well-defined by a constant times the cross product between these two vectors:

$$\vec{T}_D = -\alpha_G \left( \vec{m} \times \frac{d\vec{m}}{dt} \right).$$

Thus,

$$\frac{d\vec{m}}{dt} = \left( \vec{m} \times \vec{B} \right) - \alpha_G \left( \vec{m} \times \frac{d\vec{m}}{dt} \right).$$

Here, $\alpha_G > 0$ is the the Gilbert damping parameter which is a measure for the magnetization relaxation.

To motivate the term on the l.h.s. of Eq. (4) including $\vec{v}_s$, the so-called "reactive spin transfer torque term", we consider the following intuitive picture [28]: The spin of the electrons constituting the current rotates when it passes through the smoothly varying magnetic structure because it aligns with the local magnetization. Due to spin conservation, there is an opposite torque on the local magnetization which leads to a net displacement of the magnetic structure in the same direction as the electric current [31]. This "drift" can be described by substituting $\frac{\partial}{\partial t}$ by $\frac{\partial}{\partial t} + \vec{v}_s \cdot \nabla$ [32]: As the electrons traverse a solid, where the magnetization direction changes from $\hat{\Omega}(\vec{r}, t)$ to $\hat{\Omega}(\vec{r} + d\vec{r}, t)$, the conduction electrons experience a torque from the magnetization. Conversely, there is the reaction spin transfer-torque (sometimes referred to as the "adiabatic spin transfer torque") on the magnetization given by [25, 26, 33, 34]

$$\left. \frac{\partial \hat{\Omega}(\vec{r}, t)}{\partial t} \right|_{\text{current}} \propto \vec{v}_s \cdot \left( \hat{\Omega}(\vec{r} + d\vec{r}, t) - \hat{\Omega}(\vec{r}, t) \right) \propto (\vec{v}_s \cdot \nabla) \hat{\Omega}(\vec{r}, t).$$

Later, to explain some discrepancies with experiments, a so-called "dissipative spin transfer torque" (sometimes referred to as the "non-adiabatic spin transfer torque")

$$-\beta \hat{\Omega}(\vec{x}, t) \times \left( (\vec{v}_s \cdot \nabla) \hat{\Omega}(\vec{x}, t) \right)$$

was added to the Landau-Lifshitz-Gilbert equation [29, 35, 36, 37]. Physically, it is based on electron-spin relaxation and spin-flip scattering events [32]. The corresponding coefficient $\beta$ characterizes the degree to which spin is not conserved in the spin-transfer process.

Regarding the values of $\alpha_G$, $\beta$ and their ratio $\beta/\alpha_G$, it is generally accepted that $\beta$ is of the same order as $\alpha_G$. In general, however, they are not equal as indicated by recent experiments and microscopic theories [38]. Furthermore, neither $\beta$ nor $\alpha_G$ need to be constant. They depend on the properties of the material and are most likely also temperature dependent. Their typical magnitude range from $10^{-3}$ to $10^{-1}$ [39]. Microscopic derivations of Eq. (4) can be found, for example, in Refs. [27, 38, 40]. The approach used in Ref. [27] is based on a functional formulation of the Keldysh formalism. In another approach [38], the authors use imaginary-time methods to calculate $\alpha_G$ and $\beta$.

Spintronics in nanostructures is another field, where spin-transfer torques and the Landau-Lifshitz-Gilbert equation appear [40]. Here, one considers, for example, spin-torque driven domain wall dynamics. The current densities that are required for this are typically of the order of $10^{12}\,\mathrm{A/m^2}$ [41]. Compared to the current densities used in the experiments for MnSi, $|\vec{j}| \approx 10^6\,\mathrm{A/m^2}$, these differ by a factor of $10^6$. Typical experiments to detect these current-driven domain wall dynamics are performed by means of scanning electron microscopy (SEM) [42].

## 5.2 A Simple Example

To get a better understanding of Eq. (4), let us examine a simple case without damping $\alpha_G = \beta = 0$ and $F_2$ instead of the full free energy functional $F$. In this case, the LLG eq. (4) reduces to

$$\left(\frac{d}{dt} + \vec{v}_s \cdot \nabla\right) \hat{\Omega}(\vec{x}, t) = \hat{\Omega}(\vec{x}, t) \times \left(-\frac{\delta F_2[\vec{M}]}{\delta \vec{M}(\vec{x}, t)}\right). \tag{5}$$

In Sec. 3.2, we have seen that $F_2$ is minimized by a helical structure of the form

$$\vec{M}_0(\vec{x}) = |\vec{M}| \cdot \hat{\Omega}_0(\vec{x}) = |\vec{M}| \, \left[\cos(\hat{q} \cdot \vec{x})\hat{n}_1 + \sin(\hat{q} \cdot \vec{x})\hat{n}_2\right],$$

where the set $\{\hat{q}, \hat{n}_1, \hat{n}_2\}$ forms an orthonormal basis. This implies that

$$\frac{\delta F_2[\vec{M}]}{\delta \vec{M}(\vec{x}, t)}\Big|_{\vec{M}(\vec{x},t)=\vec{M}_0(\vec{x},t)} = 0.$$

Using this relation, it is easy to guess a solution of Eq. (5) since the right hand side vanishes. The remaining linear transport equation with transport velocity $\vec{v}_s$ is, for example, solved by:

$$\hat{\Omega}(\vec{r}, t) = \hat{\Omega}_0(\vec{r} - \vec{v}_s t) = \cos(\hat{q} \cdot (\vec{r} - \vec{v}_s t))\hat{n}_1 + \sin(\hat{q} \cdot (\vec{r} - \vec{v}_s t))\hat{n}_2. \tag{6}$$

It is, of course, possible to add a constant phase $\varphi_0$. From the above equation it is clear that the magnetization of the helix rotates with constant frequency

$$\omega = \hat{q} \cdot \vec{v}_s$$

around the helical spin-density wave vector $\hat{q}$ which corresponds to a translation or drift in the direction of $\hat{q}$. Another interpretation of this scenario, proposed by R. A. Duine, is to view the helical spin-density wave as a series of domain walls driven by the adiabatic spin-transfer torque. The corresponding domain wall velocity due to the spin current is then given by

$$V_{dw} = \frac{2\pi/|\hat{q}|}{2\pi\omega} = \frac{1}{|\vec{v}_s|}\,.$$

From this one can infer that a drift solution is inherent to Eq. (5) and therefore also to Eq. (4). Especially for the case $\frac{\beta}{\alpha_G} = 1$ this is easy to see. In this case, Eq. (6) is still a solution since the additional damping terms add up to zero. In the general case $\beta \neq \alpha_G$, we still expect a solution that drifts. Only the direction and the modulus of the drift, which were given by $\vec{v}_s$ for the special cases, should be modified. Thus, in an ansatz for the magnetization, one should include such a drift vector.

To solve Eq. (4) analytically is certainly too difficult. Therefore, we perform a different method which is motivated by a variation principle. In Sec. 9, we will see that the Landau-Lifshitz-Gilbert equation can, in principle, be derived from a variation principle which one may use to derive the equations of motion. However, the following strategy is more direct and does not contain problems such as surface terms.

## 5.3 Equations of Motion for Dynamical Variables

The main idea is to parameterize the direction of the magnetization by a few time-dependent variables $u_j$ $(j = 1, \ldots, n)$, i.e. $\hat{\Omega}(\vec{r}, t) = \hat{\Omega}(\vec{r}, u_1(t), \ldots, u_n(t))$. Starting from the LLG equation, we want to derive effective equations of motion for these variables. Multiplying Eq. (4) by $\left(\hat{\Omega} \times \frac{\partial \hat{\Omega}}{\partial u_j}\right)$, one has to calculate expressions like $(\hat{\Omega} \times \vec{Y}) \cdot (\hat{\Omega} \times \frac{\partial \hat{\Omega}}{\partial u_j})$. These can be simplified by realizing that $\hat{\Omega}$ is normalized, i.e. $|\hat{\Omega}| = 1$, thus $\hat{\Omega} \cdot \frac{\partial \hat{\Omega}}{\partial u_j} = 0$. This leads to

$$\begin{aligned}(\hat{\Omega} \times \vec{Y}) \cdot \left(\hat{\Omega} \times \frac{\partial \hat{\Omega}}{\partial u_j}\right) &= \epsilon_{klm}\, \hat{\Omega}_l Y_m \epsilon_{knp}\, \hat{\Omega}_n \left(\frac{\partial \hat{\Omega}}{\partial u_j}\right)_p \\ &= \left(\delta_{ln}\delta_{mp} - \delta_{lp}\delta_{mn}\right) \hat{\Omega}_l Y_m \hat{\Omega}_n \left(\frac{\partial \hat{\Omega}}{\partial u_j}\right)_p .\end{aligned}$$

We get

$$(\hat{\Omega} \times \vec{Y}) \cdot \left( \hat{\Omega} \times \frac{\partial \hat{\Omega}}{\partial u_j} \right) = Y_k \left( \frac{\partial \hat{\Omega}}{\partial u_j} \right)_k = \vec{Y} \cdot \frac{\partial \hat{\Omega}}{\partial u_j} \,. \tag{7}$$

Using this equation and integrating over the volume $V$ one obtains $n$ linear coupled differential equations of first order in time:

$$\begin{aligned} -\int_V d\vec{r} \left( \hat{\Omega} \times \frac{\partial \hat{\Omega}}{\partial u_j} \right) \cdot \left( \frac{d}{dt} + (\vec{v}_s \cdot \nabla) \right) \hat{\Omega} - \frac{1}{|\vec{M}|} \frac{\partial F}{\partial u_j} \\ = \int_V d\vec{r} \cdot \alpha_G \left( \frac{d}{dt} + \frac{\beta}{\alpha_G} (\vec{v}_s \cdot \nabla) \right) \hat{\Omega} \cdot \frac{\partial \hat{\Omega}}{\partial u_j}. \end{aligned} \tag{8}$$

# 6 The Helical Phase

Since the modulus of the momentum vector is fixed to the value $Q = |D|/J$ for the helix, we may perform our calculations in units of $Q$, i.e. we perform the calculation with a normalized momentum vector $\vec{q}$ and rescale the result at the end appropriately.

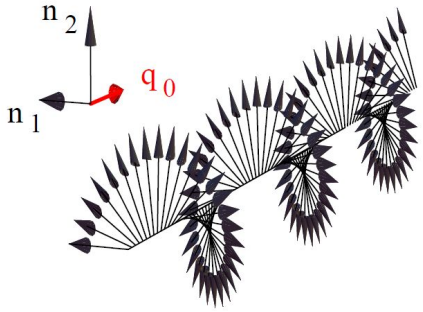


Figure 10: Picture of a helix. Figure taken from Ref. [43].

## 6.1 The Ansatz for the Helical Phase

A helical magnetic structure with constant amplitude $|\vec{M}| =: M$ is described by the ansatz [39]:

$$\begin{aligned}\vec{M}(\vec{r},t) &= M\,\hat{\Omega}(\vec{r},t) = M\,\hat{\Omega}\left(\hat{q}(t), \vec{r}-\vec{\varphi}(t), m(t)\right) \\ &= \frac{M}{\sqrt{1+m^2}}\Big(\cos(\vec{q}\cdot(\vec{r}-\vec{\varphi}))\hat{n}_1 + \sin(\vec{q}\cdot(\vec{r}-\vec{\varphi}))\hat{n}_2 + m\hat{q}\Big),\end{aligned} \tag{9}$$

where $\vec{q} = q \cdot \hat{q}$. Here $q = D/J$ as in Sec. 3.2, $\hat{q}$ is the direction vector of the helix, and $\hat{n}_1$ and $\hat{n}_2$ are choosen such that $\{\hat{q}, \hat{n}_1, \hat{n}_2\}$ forms an orthonormal basis. $\vec{\varphi}$ is the translation vector, and $m$ is a measure for the uniform magnetization in the direction of the helix. For $m = 0$ we have a helix, while for $m \neq 0$ we get a conical magnetic structure. Nevertheless, in the following we will denote this magnetic structure as a helix as well.

The purpose of this section is to calculate both sides of Eq. (8) for each of the dynamical variables $\vec{q}$, $\vec{\varphi}$ and $m$. To achieve this, we also need the free energy functional for the helix in terms of the dynamical variables.

## 6.2 Free Energy Functional

As a first approximation, we consider the free energy functional only in quadratic order in the magnetization $\vec{M}$:

$$F_2[\vec{M}] = \int_V d\vec{r}\left[r_0\,|\vec{M}|^2 + J\left(\nabla\vec{M}(\vec{x},t)\right)^2 + 2D\,\vec{M}(\vec{x},t)\cdot\left(\nabla\times\vec{M}(\vec{x},t)\right)\right].$$

For the helix described by the ansatz (9) we can calculate all terms. The first one is only a constant contribution $|\vec{M}|^2 = M^2$. The second one is given by $(\nabla\vec{M})^2 = M^2(\nabla\hat{\Omega})^2$ with

$$(\nabla\hat{\Omega})^2 = \left(\frac{d}{dx}\hat{\Omega}\right)^2 + \left(\frac{d}{dy}\hat{\Omega}\right)^2 + \left(\frac{d}{dz}\hat{\Omega}\right)^2 .$$

Using the relation

$$\frac{d}{dx}\hat{\Omega} = \frac{q_x}{\sqrt{1+m^2}}\left(-\sin(\vec{q}\cdot(\vec{r}-\vec{\varphi}))\hat{n}_1 + \cos(\vec{q}\cdot(\vec{r}-\vec{\varphi}))\hat{n}_2\right)$$

we get

$$\left(\frac{d}{dx}\hat{\Omega}\right)^2 = \frac{q_x^2}{1+m^2}$$

and thus

$$(\nabla\hat{\Omega})^2 = \frac{q_x^2+q_y^2+q_z^2}{1+m^2} = \frac{q^2}{1+m^2}$$

Similarly, starting from the relation

$$\vec{M}\cdot(\nabla\times\vec{M}) = M^2\,\hat{\Omega}\cdot(\nabla\times\hat{\Omega}) = M^2\,\hat{\Omega}_j\cdot(\nabla\times\hat{\Omega})_j$$

we may calculate

$$\begin{aligned}
\Big(\nabla\times\hat{\Omega}\Big)_x &= d_y\hat{\Omega}_z - d_z\hat{\Omega}_y \\
&= \frac{1}{\sqrt{1+m^2}}\Big(q_y\big(-\sin(\vec{q}\cdot(\vec{r}-\vec{\varphi}))n_{1_z} + \cos(\vec{q}\cdot(\vec{r}-\vec{\varphi}))n_{2_z}\big) \\
&\qquad - q_z\big(-\sin(\vec{q}\cdot(\vec{r}-\vec{\varphi}))n_{1_y} + \cos(\vec{q}\cdot(\vec{r}-\vec{\varphi}))n_{2_y}\big)\Big) \\
&= \frac{1}{\sqrt{1+m^2}}\Big(-\sin(\vec{q}\cdot(\vec{r}-\vec{\varphi}))\left(q_y n_{1_z} - q_z n_{1_y}\right) \\
&\qquad + \cos(\vec{q}\cdot(\vec{r}-\vec{\varphi}))\left(q_y n_{2_z} - q_z n_{2_y}\right)\Big) \\
&= -\frac{q}{\sqrt{1+m^2}}\Big(\sin(\vec{q}\cdot(\vec{r}-\vec{\varphi}))n_{2_x} + \cos(\vec{q}\cdot(\vec{r}-\vec{\varphi}))n_{1_x}\Big)
\end{aligned}$$

and thus we obtain

$$\hat{\Omega}\cdot(\nabla\times\hat{\Omega}) = -\frac{q}{1+m^2}\,.$$

For the quadratic free energy we get with $q = D/J$

$$F_2[\vec{M}] = \int_V d\vec{r}\,M^2\left(r_0 + \frac{Jq^2}{1+m^2} - \frac{2Dq}{1+m^2}\right) = \int_V d\vec{r}\,M^2\left(r_0 - \frac{D^2}{J}\frac{1}{1+m^2}\right).$$

Up to quadratic order, the free energy functional depends only on the uniform magnetic moment $m$. Therefore, $F_2$ contributes only to the equation of motion for $m$ with

$$\frac{\partial F_2}{\partial m} = \int_V d\vec{r}\;M^2\frac{D^2}{J}\,\frac{2m}{(1+m^2)^2}\,.$$

For simplicity let us choose units such that $|\vec{q}| = q = 1$, i.e. $J = D$. Then we have

$$\begin{aligned}\hat{\Omega}(\vec{r},t) &= \hat{\Omega}\left(\hat{q}(t), \vec{r} - \vec{\varphi}(t), m(t)\right) \\ &= \frac{1}{\sqrt{1+m^2}}\Big(\cos(\hat{q}\cdot(\vec{r}-\vec{\varphi}))\hat{n}_1 + \sin(\hat{q}\cdot(\vec{r}-\vec{\varphi}))\hat{n}_2 + m\hat{q}\Big),\end{aligned}$$

and

$$F_2[\vec{M}] = \int_V d\vec{r}\, M^2 \left(r_0 - J\frac{1}{1+m^2}\right).$$

respectively

$$\frac{\partial F_2}{\partial m} = \int_V d\vec{r}\; M^2 J\, \frac{2m}{(1+m^2)^2}.$$

## 6.3 The Equations of Motion

To calculate the equations of motion for all variables, we have to specify the direction vector $\hat{q}$. Being normalized, $\hat{q}$ depends on only two variables. Natural descriptions of $\hat{q}$ include:

1. Cartesian coordinates, $q_x, q_y$, i.e.

$$\hat{q} = \left(q_x, q_y, \sqrt{1-q_x^2-q_y^2}\right)^T. \tag{10}$$

2. Spherical coordinates in terms of two polar angles, $\theta, \phi$, i.e.

$$\hat{q} = (\cos\phi\sin\theta, \sin\phi\sin\theta, \cos\theta)^T.$$

3. A coordinate invariant manner by defining $\hat{q}$ by the directions of $\hat{n}_1$ and $\hat{n}_2$.

In the following, we will use the first method to describe $\hat{q}$ in terms of $q_x$ and $q_y$. Method 2 is infeasible as a lot of lenghty expressions will be generated. Finally, method 3 is, from a theoretical point of view, the best one, but so far we have not yet managed to write every term in a coordinate invariant form. Thus, in the following calculations $\hat{q}$ is given by Eq. (10). An orthonormal basis consists of the vectors $\hat{n}_1, \hat{n}_2$ and $\hat{q}$. Here, we define $\hat{n}_1$ and $\hat{n}_2$ by:

$$\begin{aligned}\hat{n}_1(q_x,q_y) &= \frac{1}{\sqrt{1-q_y}}\Big(\sqrt{1-q_x^2-q_y^2}, 0, -q_x\Big)^T, \\ \hat{n}_2(q_x,q_y) &= \frac{1}{\sqrt{1-q_y}}\Big(-q_xq_y, 1-q_y^2, -q_y\sqrt{1-q_x^2-q_y^2}\Big)^T.\end{aligned}$$

Note that $\vec{\varphi}$ is a vector, but only the component in the direction of $\vec{q}$ occurs in Eq. (9) for the helix. Therefore, the equations of motion for $\varphi_x$, $\varphi_y$ and $\varphi_z$ are effectively a single equation. This parametrization for the helix leads to four different equations of motion for the time-dependent variables $q_x(t)$, $q_y(t)$, $\vec{\varphi}(t)$ and $m(t)$. A derivation of these equations is given in App. A.

In the "static" case, where the $q$ vector and the uniform magnetic component $m$ are constant in time, i.e. $\dot{q}_x = \dot{q}_y = \dot{m} = 0$, the equations of motion reduce to:

$$\int_V d\vec{r} \left(\frac{1}{1+m^2}\right)^{3/2} \cdot \left(-\frac{m}{\sqrt{1+m^2}} \cdot 2\,J\,M + \hat{q} \cdot (\vec{v}_s - \dot{\vec{\varphi}})\right) = 0, \tag{11a}$$

and

$$0 = -\int_V d\vec{r}\, \frac{\alpha_G}{1+m^2}\, \hat{q} \cdot \left[\hat{q} \cdot \left(\frac{\beta}{\alpha_G}\vec{v}_s - \dot{\vec{\varphi}}\right)\right], \tag{11b}$$

$$0 = \int_V d\vec{r}\, \frac{\alpha_G}{1+m^2} \left[\left(\dot{\vec{\varphi}} - \frac{\beta}{\alpha_G}\,\vec{v}_s\right) \cdot \hat{q}\right] \cdot \left(\varphi_x - \frac{q_x \cdot \varphi_z}{\sqrt{1-q_x^2-q_y^2}}\right), \tag{11c}$$

$$0 = \int_V d\vec{r}\, \frac{\alpha_G}{1+m^2} \left\{ \left[\left(\dot{\vec{\varphi}} - \frac{\beta}{\alpha_G}\vec{v}_s\right) \cdot \hat{q}\right] \cdot \left(\varphi_y - \frac{q_y \cdot \varphi_z}{\sqrt{1-q_x^2-q_y^2}} - \frac{q_x q_y^2}{\sqrt{1-q_x^2-q_y^2}(1-q_y)}\right)\right\}. \tag{11d}$$

For an arbitrary volume $V$, Eq. (11b) is solved by

$$\hat{q} \cdot \left(\frac{\beta}{\alpha_G}\vec{v}_s - \dot{\vec{\varphi}}\right) = 0 \quad \Rightarrow \quad \dot{\vec{\varphi}} \cdot \hat{q} = \frac{\beta}{\alpha_G}\vec{v}_s \cdot \hat{q}.$$

As a result, the $q$-component of $\dot{\vec{\varphi}}$ and $\frac{\beta}{\alpha_G}\vec{v}_s$ should be equal in the basis $\{\hat{q}, \hat{n}_1, \hat{n}_2\}$. Likewise, equations (11c) and (11d) are fulfilled. Substituting $\dot{\vec{\varphi}} \cdot \hat{q}$ into Eq. (11a) we get for an arbitray volume $V$:

$$-\frac{m}{\sqrt{1+m^2}} \cdot 2\,J\,M + \hat{q} \cdot \vec{v}_s \left(1 - \frac{\beta}{\alpha_G}\right) = 0.$$

This equation can be solved for the uniform magnetic component in the direction of the $q$-vector by

$$\frac{m}{\sqrt{1+m^2}} = \frac{1-\beta/\alpha_G}{2\,J\,M}(\vec{v}_s \cdot \hat{q}).$$

Since only $q$-components occur in the solution, let us denote $\dot{\vec{\varphi}} \cdot \hat{q}$ by $\dot{\varphi}$ and $\vec{v}_s \cdot \hat{q}$ by $v_s$. To conclude, the solution of the equations of motion for $\hat{q}$, $\varphi$ and $m$ in the static limit ($\dot{\hat{q}} = 0$, $\dot{m} = 0$) is given by

$$\varphi(t) = \beta/\alpha_G\, v_s \cdot t, \quad \frac{m}{\sqrt{1+m^2}} = \frac{1-\beta/\alpha_G}{2\,J\,M}\, v_s.$$

Note that Goto *et al.* [39] obtain similar results from Eq. (4) for $\hat{q} = \vec{e}_x$ by solving the Landau-Lifshitz-Gilbert equation in one dimension.

This result implies that the spin current leads to a shift of the spiral pattern with a time-independent drift velocity $\dot{\varphi} = \beta/\alpha_G\, v_s$ in the direction of the helix. Moreover, it leads to the formation of a uniform magnetization $m/(1+m^2)^{1/2}$ in the direction of $\hat{q}$. The sign of $m$ is determined by $\alpha_G$ and $\beta$.

Furthermore, we find, that the spin current does not influence the direction of of the helix vector $\vec{q}$. This is consistent with the experimental data obtained from neutron scattering experiments, where no spin-torque effects in the helical and the conical phase are observed. However, Goto *et al.* [39] also performed numerical simulations on a two-dimensional square lattice. Starting from a random spin configuration, they have modeled the relaxation of the spins into the spiral state, first in the absence of a current. In this case, they observe, as expected, no ordering of the direction of the spiral wave vector. In the current applied case, they describe an annealing of the directional disorder of the spiral magnet. However since they analized a different problem (relaxation of spins into the spiral state instead of reorientating a helix), we can not directly compare both data. Nevertheless, in the special case of $\vec{j} \parallel \hat{q}$ all approaches coincide.

In this calculation, we considered the free energy functional only up to quadratic order, where $F_2$ is fully rotational invariant. In a real material, this rotation symmetry is spontaneously broken and the remaining global rotation symmetry of the entire spin structure is eliminated by weak crystaline anisotropies that pin the magnetic structure to the underlying atomic lattice. Therefore, the next step is to examine the effect of an anisotropy energy on the spiral by introducing higher order terms in the free energy fuctional.

## 6.4 The Helical Phase With a Pinning Term

Since the crystal anisotropy energy is small, we will consider it as a pertubation of the ground state that only influences the orientation of the helix. Higher order terms should, of course, respect the B20 crystal structure. In Ref. [44], the authors showed on symmetry grounds that the extrema of a crystal anisotropy function (as a function of the spiral direction) are in the $\langle 111 \rangle$ and $\langle 100 \rangle$ directions.

The simplest, lowest order term that produces such a pinning is of the form

$$F_p^{(1)}[\vec{M}(\vec{r})] = c_1 \int_V d\vec{r}\, \vec{M}(\vec{r}) \left(d_x^4 + d_y^4 + d_z^4\right) \vec{M}(\vec{r})$$

For a fixed amplitude of $\vec{M}$ and $\vec{q}$ we can simplify $F_p^{(1)}[\vec{M}(\vec{r})]$

$$\begin{aligned} F_p^{(1)}[\vec{M}(\vec{r})] &= c_1 M^2 \int_V d\vec{r}\, \hat{\Omega}(\vec{r}) \left(d_x^4 + d_y^4 + d_z^4\right) \hat{\Omega}(\vec{r}) \\ &= c_1 M^2 q^4 \sum_{\vec{q}} \left(q_x^4 + q_y^4 + (1 - q_x^2 - q_y^2)^2\right) |\vec{m}_{\vec{q}}|^2 \\ &=: \tilde{c}_1 \sum_{\vec{q}} f(q) |\vec{m}_{\vec{q}}|^2, \end{aligned}$$

where $\tilde{c}_1 = c_1 M^2 q^4$ and $f(q) = q_x^4 + q_y^4 + (1 - q_x^2 - q_y^2)^2$. Here $q_x^2 + q_y^2$ is restricted to be smaller or equal to one. Internal extrema of $f(q)$ are determined by the conditions

$\frac{\partial f}{\partial q_x} = \frac{\partial f}{\partial q_y} = 0$. Depending on the sign of the prefactor, $F_p^{(1)}$ has minima at $\langle 111\rangle$ or $\langle 100\rangle$. For example, for $\tilde{c}_1 > 0$ we get minima at $\langle 111\rangle$.

Since MnSi pins into the $\langle 111\rangle$ direction, we assume $\tilde{c}_1 > 0$, i.e. $q_x^2 = q_y^2 = 1/3$. For a helix given by Eq. (9) we get

$$F_p^{(1)}[\hat{\Omega}] = \tilde{c}_1 \int_V d\vec{r}\, \frac{q_x^4 + q_y^4 + (1 - q_x^2 - q_y^2)^2}{1 + m^2}\,.$$

With this extra term in the free energy functional,

$$F[\hat{\Omega}] = F_2[\hat{\Omega}] + F_p^{(1)}[\hat{\Omega}],$$

we get the following additional terms in the equations of motion:

$$\begin{aligned}
\frac{\partial F_p^{(1)}}{\partial m} &= -\tilde{c}_1 \int_V d\vec{r}\, \frac{2m}{1+m^2} \cdot \left(q_x^4 + q_y^4 + (1 - q_x^2 - q_y^2)^2\right), \\
\frac{\partial F_p^{(1)}}{\partial \vec{\varphi}} &= 0, \\
\frac{\partial F_p^{(1)}}{\partial q_x} &= -\tilde{c}_1 \int_V d\vec{r}\, \frac{4q_x \cdot (1 - q_x^2 - q_y^2 - q_x^2)}{(1+m^2)^2}\,, \\
\frac{\partial F_p^{(1)}}{\partial q_y} &= -\tilde{c}_1 \int_V d\vec{r}\, \frac{4q_y \cdot (1 - q_x^2 - q_y^2 - q_y^2)}{(1+m^2)^2}\,.
\end{aligned}$$

In the static case with pinning term $F_p^{(1)}$ we obtain the following equations of motion:

$$\int_V d\vec{r}\left(\frac{1}{1+m^2}\right)^{3/2}\left[-\frac{2m}{\sqrt{1+m^2}}\frac{D}{q}M + c_1 q^4 M(q_x^4 + q_y^4 + (1 - q_x^2 - q_y^2)^2)) + \hat{q}\cdot(\vec{v}_s - \dot{\vec{\varphi}})\right] = 0 \tag{12a}$$

and

$$0 = -\int_V d\vec{r}\, \frac{\alpha_G}{1+m^2}\hat{q}\cdot\left[\hat{q}\cdot\left(\frac{\beta}{\alpha_G}\vec{v}_s - \dot{\vec{\varphi}}\right)\right], \tag{12b}$$

$$\begin{aligned}
0 = \int_V d\vec{r}\Bigg\{ &\frac{\alpha_G}{1+m^2}\left[\left(\dot{\vec{\varphi}} - \frac{\beta}{\alpha_G}\vec{v}_s\right)\cdot\hat{q}\right]\cdot\left(\varphi_x - \frac{q_x\cdot\varphi_z}{\sqrt{1 - q_x^2 - q_y^2}}\right) \\
&- \frac{\tilde{c}_1}{M}\frac{4q_x\cdot(1 - q_x^2 - q_y^2 - q_x^2)}{(1+m^2)^2}\Bigg\},
\end{aligned} \tag{12c}$$

$$\begin{aligned}
0 = \int_V d\vec{r}\Bigg\{ &\frac{\alpha_G}{1+m^2}\left[\left(\dot{\vec{\varphi}} - \frac{\beta}{\alpha_G}\vec{v}_s\right)\cdot\hat{q}\right]\cdot\left(\varphi_y - \frac{q_y\cdot\varphi_z}{\sqrt{1 - q_x^2 - q_y^2}}\right. \\
&\left. - \frac{q_x q_y^2}{\sqrt{1 - q_x^2 - q_y^2}(1 - q_y)}\right)\Bigg] - \frac{\tilde{c}_1}{M}\frac{4q_x\cdot(1 - q_x^2 - q_y^2 - q_x^2)}{(1+m^2)^2}\Bigg\}.
\end{aligned} \tag{12d}$$

Eq. (12b) remains unchanged compared to Eq. (11b). For an arbitrary volume $V$ it is solved by

$$\hat{q}\cdot\left(\frac{\beta}{\alpha_G}\vec{v}_s - \dot{\vec{\varphi}}\right) = 0 \quad \Rightarrow \quad \dot{\vec{\varphi}}\cdot\hat{q} = \frac{\beta}{\alpha_G}\vec{v}_s\cdot\hat{q},$$

again implying that in the basis $\{\hat{q}, \hat{n}_1, \hat{n}_2\}$ the $q$-component of $\dot{\vec{\varphi}}$ and $\frac{\beta}{\alpha_G}\vec{v}_s$ have to be equal. Likewise, in Eqs. (12c) and (12d), the first term vanishes. Therefore, a solution of the equations of motion has to fulfill

$$\frac{\delta F_p^{(1)}}{\delta q_x} = \frac{\delta F_p^{(1)}}{\delta q_y} = 0.$$

However, this condition is already met by requiring a minimization of the pinning term $\frac{\partial f}{\partial q_x} = \frac{\partial f}{\partial q_x} = 0$. In particular, for MnSi we have

$$q_x^2 = q_y^2 = 1/3 \quad \Rightarrow \quad 1 - q_x^2 - q_y^2 - q_x^2 = 1 - q_x^2 - q_y^2 - q_y^2 = 0.$$

The additional term in Eq. (12a), using $q_x^2 = q_y^2 = 1/3$ for MnSi, is given by $-c_1 q^4 M \int_V d\vec{r}\, \frac{1}{3} \cdot \frac{2m}{1+m^2}$. Thus, it only adds a constant to $D/q$. Using the results obtained above, we get for an arbitrary volume $V$ the relation

$$\frac{m}{\sqrt{1+m^2}} = \frac{1 - \beta/\alpha_G}{2M(D/q + 1/3\, c_1 q^4)} (\vec{v}_s \cdot \hat{q}).$$

Since only $q$-components occur in the solution, we choose the same notation as before.

To sum up, the solution of the equations of motion including the pinning term $F_p^{(1)}$ for $\hat{q}$, $\varphi$ and $m$ in the static limit ($\dot{\hat{q}} = 0$, $\dot{m} = 0$) is given by

$$\varphi(t) = \beta/\alpha_G\, v_s \cdot t, \quad \frac{m}{\sqrt{1+m^2}} = \frac{1 - \beta/\alpha_G}{2M(D/q + 1/3\, c_1 q^4)}\, v_s.$$

Hence, this pinning term does not reorientate the helix, and the direction of the drift is unchanged. For example, other rotationally non-invariant terms of fourth order spin-orbit coupling that are allowed by the crystal symmetry are [21, 45]

$$F_p^{(2)} = \tilde{c}_2 \int_V d\vec{r} \left[ (\partial_x \vec{M}_x)^2 + (\partial_y \vec{M}_y)^2 + (\partial_z \vec{M}_z)^2 \right],$$
$$F_p^{(3)} = \tilde{c}_3 \int_V d\vec{r} \left( \vec{M}_x^4 + \vec{M}_y^4 + \vec{M}_z^4 \right).$$

Of course, one can also examine higher order terms in spin-orbit coupling, but these will have an even more smaller prefactor such that the effect of these terms is insignificant. In this analysis, we have neglected the amplitude degree of freedom of the helix since we expected it to remain constant. Moreover, we have not included the influence of an external magnetic field, noise terms and disorder.

# 7 A-Phase

While the application of a current does not alter the direction of the $q$-vector in the helical phase, the situation is different for the A-phase. In the experiments one clearly observes a change of the A-phase under a current as can be seen in Fig. 11. This picture is produced in the following way. One has to perform two measurements in the temperature and magnetic field range of the A-phase. For example, the first one is done with a current into the $\hat{x}$ direction. The second measurement should then be performed with an applied current in the opposite direction, here the $-\hat{x}$ direction. In the final step, one subtracts the data of the measurements, which leads to the shown data. Obviously, the position change of the $q$-vectors is an odd effect in the current. One possible interpretation of the experimental data is that under the influence of a current the $q$-vectors of the A-phase rotate around the axis of the magnetic field which determines the plane of the $q$-vectors. The purpose of this Section is to develop a theoretical understanding of the experimental data and, in particular, to explain the spin-torque effects in the A-phase.

As shown in Sec. 3.3, it is a good approximation to describe the magnetization in the A-phase by a superposition of three helices and a uniform magnetization. Hence, the ansatz for the A-phase is much more complex than for a single helix. Certainly, the full dynamical equations of motions will be too complicated to allow for a closed solution. Therefore, we restrict ourselves from the beginnig to the "static" limit, defined analog to the helical case. Moreover, not everything can be computed analytically for the A-phase.

However, as argued in Sec. 5.2 the magnetic structure will drift under the influence of a current. In the following, we will derive analytically this drift velocity in the static limit.

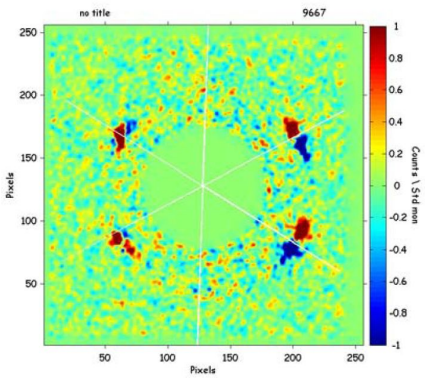


Figure 11: Experimental data for plus and minus current subtracted.

## 7.1 Analytical Determination of the Drift Velocity in the Static Limit

By claiming that the magnetization direction $\hat{\Omega}$ only depends on the drift vector $\vec{\varphi}$ in the combined the structure $(\vec{r}-\vec{\varphi})$, i.e.

$$\hat{\Omega}(\vec{r},t) = \hat{\Omega}(\vec{r}-\vec{\varphi}(t), u_1(t), \ldots, u_m(t)),$$

where $u_j(t)$ are the other dynamical variables, the structure $(\vec{r}-\vec{\varphi})$ leads to

$$\int_V d\vec{r}\left(\hat{\Omega}\times\frac{\partial\hat{\Omega}}{\partial\varphi_j}\right)\cdot\left(\frac{d}{dt}\hat{\Omega}+(\vec{v}_s\cdot\nabla)\hat{\Omega}\right) = \int_V d\vec{r}\,4\pi\left(\vec{\Phi}\times(\vec{v}_s-\dot{\vec{\varphi}})\right)_j. \tag{13}$$

Here, the Skyrmion density $\vec{\Phi}$ is given by [46]

$$\Phi_j = \frac{1}{8\pi}\,\epsilon_{jkl}\,\hat{\Omega}\cdot\left(\frac{\partial\hat{\Omega}}{\partial x_k}\times\frac{\partial\hat{\Omega}}{\partial x_l}\right). \tag{14}$$

Note that a derivation of Eq. (13) is given below. Let us consider without loss of generality the case, where the magnetic field is parallel to the $z$-direction $\vec{B}=B\cdot\hat{z}$ and where the plane of the three $q$-vectors is the $xy$-plane. For this ansatz we get

$$\dot{\vec{\varphi}} = \frac{\beta}{\alpha_G}\vec{v}_s + \left(1-\frac{\beta}{\alpha_G}\right)\frac{Y^2}{\alpha_G^2X^2+Y^2}\vec{v}_s - \left(1-\frac{\beta}{\alpha_G}\right)\frac{\alpha_G X}{\alpha_G^2X^2+Y^2}\cdot Y(\hat{z}\times\vec{v}_s), \tag{15}$$

where $X\equiv\int_V d\vec{r}\,\frac{1}{2}\,(\nabla\hat{\Omega})^2$ and $Y\equiv\int_V d\vec{r}\,4\pi\,\Phi_z$. A derivation of this formula is also given below.

Thus, $\dot{\vec{\varphi}}$ is a time-independent vector that lies in the $xy$-plane. Without a Skyrmion density, $\Phi=0$, we reproduce the result for the helix as $\dot{\vec{\varphi}}=(\beta/\alpha_G)\vec{v}_s$. In the Galilei invariant case, $\beta/\alpha_G=1$, we obtain $\dot{\vec{\varphi}}=\vec{v}_s$ as expected. More explicitely, in the limit $\frac{\beta}{\alpha_G}\approx 1+\epsilon$ and $\epsilon,\alpha_G\ll 1$, i.e. small damping, we get

$$\dot{\vec{\varphi}} = (1+\epsilon)\vec{v}_s - \epsilon\frac{Y^2}{\alpha_G^2X^2+Y^2}\vec{v}_s + \epsilon\frac{\alpha_G X}{\alpha_G^2X^2+Y^2}\cdot Y(\hat{z}\times\vec{v}_s) \xrightarrow{\alpha_G\to 0} \vec{v}_s.$$

For the A-phase we may simplify Eq. (15) by integrating over a magnetic unit cell with volume $V_0$ and using $Y=4\pi\int_{V_0}d\vec{r}\,\Phi_z=-4\pi$. This leads to

$$\dot{\vec{\varphi}} = \frac{\beta}{\alpha_G}\vec{v}_s + \left(1-\frac{\beta}{\alpha_G}\right)\frac{1}{\alpha_G^2X^2+1}\vec{v}_s + \left(1-\frac{\beta}{\alpha_G}\right)\frac{\alpha_G X}{\alpha_G^2X^2+1}\,\hat{z}\times\vec{v}_s$$

Note that in Subsection 7.3, we will give a different, but equivalent derivation for $\dot{\vec{\varphi}}$.

### Derivation of Eqs. (13) and (15)

Since the magnetic structure in the A-phase is translational invariant in the direction of the magnetic field, we get $\frac{\partial\hat{\Omega}}{\partial z}=-\frac{\partial\hat{\Omega}}{\partial\varphi_z}=0$ for $\vec{B}\parallel\hat{z}$. Thus, $\Phi_x=\Phi_y=0$ and

$$\begin{aligned}\Phi_z &= \frac{1}{8\pi}\hat{\Omega}\cdot\left(\frac{\partial\hat{\Omega}}{\partial x}\times\frac{\partial\hat{\Omega}}{\partial y}\right) - \frac{1}{8\pi}\hat{\Omega}\cdot\left(\frac{\partial\hat{\Omega}}{\partial y}\times\frac{\partial\hat{\Omega}}{\partial x}\right)\\ &= \frac{1}{4\pi}\hat{\Omega}\cdot\left(\frac{\partial\hat{\Omega}}{\partial x}\times\frac{\partial\hat{\Omega}}{\partial y}\right).\end{aligned}$$

Moreover, in the "static limit", where $\dot{u}_j = 0$ for all variables except $\vec{\varphi}$, we get

$$\frac{d}{dt}\hat{\Omega} = \frac{\partial\hat{\Omega}}{\partial\varphi_j}\cdot\dot{\varphi}_j = -\frac{\partial\hat{\Omega}}{\partial r_j}\cdot\dot{\varphi}_j = -(\dot{\vec{\varphi}}\cdot\nabla)\,\hat{\Omega}$$

This implies

$$\left(\frac{d}{dt} + (\vec{v}_s\cdot\nabla)\right)\hat{\Omega} = \left((\vec{v}_s - \dot{\vec{\varphi}})\cdot\nabla\right)\hat{\Omega} =: (\vec{w}\cdot\nabla)\,\hat{\Omega}$$

with the modified velocity $\vec{w} = \vec{v}_s - \dot{\vec{\varphi}}$. Therefore, for $j = x$ we obtain:

$$\begin{aligned}
&\int_V d\vec{r}\left(\hat{\Omega}\times\frac{\partial\hat{\Omega}}{\partial\varphi_x}\right)\cdot\left(\frac{d}{dt} + (\vec{v}_s\cdot\nabla)\right)\hat{\Omega} = -\int_V d\vec{r}\left(\hat{\Omega}\times\frac{\partial\hat{\Omega}}{\partial x}\right)\cdot(\vec{w}\cdot\nabla)\,\hat{\Omega}\\
&= \int_V d\vec{r}\,\hat{\Omega}\cdot\left((\vec{w}\cdot\nabla)\hat{\Omega}\times\frac{\partial\hat{\Omega}}{\partial x}\right) = \int_V d\vec{r}\,w_y\,\hat{\Omega}\cdot\left(\frac{\partial\hat{\Omega}}{\partial y}\times\frac{\partial\hat{\Omega}}{\partial x}\right)\\
&= \int_V d\vec{r}\,(-4\pi)\,w_y\cdot\frac{1}{4\pi}\,\hat{\Omega}\cdot\left(\frac{\partial\hat{\Omega}}{\partial x}\times\frac{\partial\hat{\Omega}}{\partial y}\right) = \int_V d\vec{r}\,4\pi\,(-w_y\cdot\Phi_z + w_z\cdot\Phi_y)\\
&= \int_V d\vec{r}\,4\pi\left(\vec{\Phi}\times\vec{w}\right)_x = \int_V d\vec{r}\,4\pi\left(\vec{\Phi}\times(\vec{v}_s - \dot{\vec{\varphi}})\right)_x,
\end{aligned}$$

where the penultimate line follows from $\Phi_y = 0$. The analog result is obtained for $j = y$.

To derive Eq. (15) one has to calculate both sides of Eq. (8) in the case of $u_j = \varphi_j$. Assuming that the free energy functional does not depend on $\vec{\varphi}$, i.e. $\frac{\partial F}{\partial\varphi_j} = 0$, one has already calculated the l.h.s. of Eq. (8) by using Eq. (13). To calculate the r.h.s. of Eq. (8), we use the following relations that are valid in the static limit:

$$\frac{\partial d_t\hat{\Omega}}{\partial\dot{\varphi}_j} = \frac{\partial\hat{\Omega}}{\partial\varphi_j} \quad\text{and}\quad \left(\frac{d}{dt} + \frac{\beta}{\alpha_G}(\vec{v}_s\cdot\nabla)\right)\hat{\Omega} = \left[\left(\frac{\beta}{\alpha_G}\,\vec{v}_s - \dot{\vec{\varphi}}\right)\cdot\nabla\right]\hat{\Omega} =: (\vec{w}_{\alpha_G\beta}\cdot\nabla)\,\hat{\Omega}$$

with the modified velocity $\vec{w}_{\alpha_G\beta} = \frac{\beta}{\alpha_G}\,\vec{v}_s - \dot{\vec{\varphi}}$. Thus we get

$$\begin{aligned}
&\int_V d\vec{r}\,\alpha_G\left(\frac{d}{dt} + \frac{\beta}{\alpha_G}(\vec{v}_s\cdot\nabla)\right)\hat{\Omega}\cdot\frac{\partial d_t\hat{\Omega}}{\partial\dot{\varphi}_j}\\
&= \int_V d\vec{r}\,\alpha_G\left((\vec{w}_{\alpha_G\beta}\cdot\nabla)\,\hat{\Omega}\right)\cdot\frac{\partial\hat{\Omega}}{\partial\varphi_j}\\
&= -\int_V d\vec{r}\cdot\alpha_G\,(\vec{w}_{\alpha_G\beta})_k\,\frac{\partial\hat{\Omega}}{\partial r_k}\cdot\frac{\partial\hat{\Omega}}{\partial r_j}\\
&=: -\alpha_G\,\mathcal{D}_{jk}\cdot(\vec{w}_{\alpha_G\beta})_k = -\alpha_G\,\mathcal{D}_{jk}\cdot\left(\frac{\beta}{\alpha_G}\,\vec{v}_s - \dot{\vec{\varphi}}\right)_k
\end{aligned}$$

with the entries of the matrix $\mathcal{D}$ given by

$$\mathcal{D}_{jk} = \int_V d\vec{r}\,\frac{\partial\hat{\Omega}}{\partial r_j}\cdot\frac{\partial\hat{\Omega}}{\partial r_k}\,.$$

Because of the translational invariance in the $z$ direction, derivatives with respect to $z$ vanish. Numerical calculations lead to

$$\int_V d\vec{r}\left(\frac{\partial\hat{\Omega}}{\partial x}\right)^2 = \int_V d\vec{r}\left(\frac{\partial\hat{\Omega}}{\partial y}\right)^2 \quad \text{and} \quad \int_V d\vec{r}\,\frac{\partial\hat{\Omega}}{\partial x}\cdot\frac{\partial\hat{\Omega}}{\partial y} = 0.$$

This can be explained in the following way. In the absence of a current and without anisotropy terms, neither the $x$ nor the $y$ direction is preferred. Besides, both directions are "independent" of each other. Therefore, the matrix $\mathcal{D}$ is given by

$$\mathcal{D} = X \cdot \begin{pmatrix} 1 & 0 & 0 \\ 0 & 1 & 0 \\ 0 & 0 & 0 \end{pmatrix}$$

with

$$X = \int_V d\vec{r}\left(\frac{\partial\hat{\Omega}}{\partial x}\right)^2 = \int_V d\vec{r}\left(\frac{\partial\hat{\Omega}}{\partial y}\right)^2 = \frac{1}{2}\int_V d\vec{r}\,(\nabla\hat{\Omega})^2.$$

Here, $X$ can be interpreted as a kinetic energy. It is the same term that appears in the Ginzburg-Landau free energy functional. Therefore, we have

$$\int_V d\vec{r}\cdot\alpha_G\left(\frac{d}{dt} + \frac{\beta}{\alpha_G}(\vec{v}_s\cdot\nabla)\right)\hat{\Omega}\cdot\frac{\partial d_t\hat{\Omega}}{\partial\dot{\vec{\varphi}}} = -\alpha_G\,\mathcal{D}\cdot\vec{w}_{\alpha_G\beta} \quad \text{and}$$
$$-\int_V d\vec{r}\left(\hat{\Omega}\times\frac{\partial\hat{\Omega}}{\partial\vec{\varphi}}\right)\cdot\left(\frac{d}{dt}\hat{\Omega} + (\vec{v}_s\cdot\nabla)\hat{\Omega}\right) = -\int_V d\vec{r}\,4\pi\left(\vec{\Phi}\times\vec{w}\right).$$

The second equation may be written in a matrix notation as well:

$$\int_V d\vec{r}\,4\pi\left(\vec{\Phi}\times\vec{w}\right) = \int_V d\vec{r}\,4\pi\begin{pmatrix} 0 & -\Phi_z & 0 \\ \Phi_z & 0 & 0 \\ 0 & 0 & 0 \end{pmatrix}\cdot\vec{w} =: \begin{pmatrix} 0 & -Y & 0 \\ Y & 0 & 0 \\ 0 & 0 & 0 \end{pmatrix}\cdot\vec{w} =: \mathcal{T}\cdot\vec{w}$$

with $Y = \int_V d\vec{r}\,4\pi\,\Phi_z$.

Since the $z$-component of Eq. (8) vanishes, the above relation reduces to an effective $2\times 2$ matrix equation:

$$\begin{pmatrix} 0 & -Y \\ Y & 0 \end{pmatrix}\cdot(\vec{v}_s - \dot{\vec{\varphi}}) = \alpha_G\begin{pmatrix} X & 0 \\ 0 & X \end{pmatrix}\cdot\left(\frac{\beta}{\alpha_G}\,\vec{v}_s - \dot{\vec{\varphi}}\right)$$
$$\Rightarrow \quad \begin{pmatrix} \beta X & Y \\ -Y & \beta X \end{pmatrix}\cdot\vec{v}_s = \begin{pmatrix} \alpha_G X & Y \\ -Y & \alpha_G X \end{pmatrix}\cdot\dot{\vec{\varphi}}. \tag{16}$$

Note that in the $2\times 2$ matrix equation $\vec{v}_s$ and $\dot{\vec{\varphi}}$ denote the reduced two component vectors which include only the $x$ and $y$ components. Since

$$\det\begin{pmatrix} \alpha_G X & Y \\ -Y & \alpha_G X \end{pmatrix} = \alpha_G^2 X^2 + Y^2 \neq 0,$$

it is always possible to invert the matrix on the r.h.s. of Eq. (16) and to find a solution for $\dot{\vec{\varphi}}$:

$$\begin{aligned}\dot{\vec{\varphi}} &= \begin{pmatrix} \alpha_G X & Y \\ -Y & \alpha_G X \end{pmatrix}^{-1} \cdot \begin{pmatrix} \beta X & Y \\ -Y & \beta X \end{pmatrix} \cdot \vec{v}_s \\ &= \frac{1}{\alpha_G^2 X^2 + Y^2} \cdot \begin{pmatrix} \alpha_G \beta X^2 + Y^2 & XY(\alpha_G - \beta) \\ XY(\beta - \alpha_G) & \alpha_G \beta X^2 + Y^2 \end{pmatrix} \cdot \vec{v}_s.\end{aligned}$$

Rewriting this solution in a three-dimensional notation one gets

$$\dot{\vec{\varphi}} = \frac{\beta}{\alpha_G}\vec{v}_s + \left(1 - \frac{\beta}{\alpha_G}\right) \frac{Y^2}{\alpha_G^2 X^2 + Y^2}\vec{v}_s - \left(1 - \frac{\beta}{\alpha_G}\right) \frac{\alpha_G X}{\alpha_G^2 X^2 + Y^2} \cdot Y(\hat{z} \times \vec{v}_s),$$

where

$$\begin{aligned} X &= \int_V d\vec{r} \left(\frac{\partial \hat{\Omega}}{\partial x}\right)^2 = \int_V d\vec{r} \left(\frac{\partial \hat{\Omega}}{\partial y}\right)^2 = \int_V d\vec{r} \, \frac{1}{2} \left(\nabla \hat{\Omega}\right)^2 \quad \text{and} \\ Y &= \int_V d\vec{r} \, 4\pi \, \Phi_z = 4\pi \int_V d\vec{r} \, \Phi_z \end{aligned}$$

which reproduces Eq. (15).

## 7.2 The Ansatz for the A-Phase

To get further results, we have to characterize the magnetic structure in the A-phase by some time-dependent parameters. As variational parameters we choose

- Two helical vectors $\vec{q}_1, \vec{q}_2$ in an arbitrary direction, $[3 + 3]$
  while the third vector $\vec{q}_3$ is given by $\vec{q}_3 = -\vec{q}_1 - \vec{q}_2$.
- The corresponding complex Fourier components

  $$\vec{m}_{q_j} = \vec{m}^{(r)}_{q_j} + i \, \vec{m}^{(i)}_{q_j}, \quad j = 1, 2, 3. \qquad [2 * 3 * 3]$$

  with the real $\vec{m}^{(r)}_{q_j}$ and imaginary part $\vec{m}^{(i)}_{q_j}$.
- The uniform magnetization $\vec{m}_h$ in an arbitrary direction. $[3]$

Consequently, our ansatz consists of $6 + 18 + 3 = 27$ parameters $u_j$ $(j = 1, \ldots, 27)$:

$$\vec{u} = \left\{ \vec{q}_1, \, \vec{q}_2, \, \vec{m}_h, \, \vec{m}^{(r)}_{q_1}, \, \vec{m}^{(r)}_{q_2}, \, \vec{m}^{(r)}_{-q_1-q_2}, \, \vec{m}^{(i)}_{q_1}, \vec{m}^{(i)}_{q_2}, \, \vec{m}^{(i)}_{-q_1-q_2} \right\}.$$

To simplify calculations and to minimize computing time, we neglect amplitude fluctuations by normalizing the magnetic structure only globally and not locally, i.e. we assume the normalization factor $\mathcal{N}$ to be constant in space and time. In principle, the qualitative results should be the same, although the quantitative results will differ slightly.

Therefore, our ansatz for the magnetization in the A-phase is given by

$$\begin{aligned}\vec{M}_A(\vec{r},t) &= \frac{1}{\mathcal{N}}\left[\vec{m}_h + \sum_{j=1}^{3}\left(\vec{m}_{\vec{q}_j}e^{i\vec{q}_j\vec{r}} + \vec{m}^*_{\vec{q}_j}e^{-i\vec{q}_j\vec{r}}\right)\right] \\ &= \frac{1}{\mathcal{N}}\left[\vec{m}_h + \sum_{j=1}^{6}\vec{m}_{\vec{q}_j}e^{i\vec{q}_j\vec{r}}\right].\end{aligned}$$

In the second line, $\vec{q}_4$ is given by $-\vec{q}_1$, $\vec{q}_5 = -\vec{q}_2$, and $\vec{q}_6 = -\vec{q}_3$. We determine the normalization $\mathcal{N}$ such that the integrated Skyrmion density is equal to $-1$.

## 7.3 The Calculation Scheme

The calculation scheme is as follows:

1. Calculate the approximative ground state solutions $u_j^0$ by minimizing the free energy

   $$G \approx F[\vec{M}_0]$$

   with respect to the variational parameters. In the following, we will denote $u_j^0$ as ground state values or ground state solutions and the fluctuation matrix by $\mathcal{M}$, where

   $$\mathcal{M}_{jk} = \frac{\delta^2 F}{\delta M_j \delta M_k}\,.$$

2. We expect that a small spin-polarized current will change the ground state values smoothly. Therefore, we perform a pertubation ansatz for the dynamical variables $u_j$ up to linear order in the spin-polarized current:

   $$u_j = u_j^0 + \Delta u_j + \mathcal{O}(|\vec{v}_s|^2)$$

   with $\Delta u_j \propto |\vec{v}_s|$.

3. Calculate the equations of motions for $u_j$ up to linear order in $|\vec{v}_s|$:

   - The dissipation and the Berry phase term are linear in $\vec{v}_s$. Therefore, it suffices to plug in the ground state solution. These two terms will add up to a vector, independent of $\Delta u_j$, which we multiply by the magnetization amplitude $M$ and denote the result as $\vec{c}$.
   - $\frac{\partial F}{\partial u_j}$ is, to linear order in $|\vec{v}_s|$, given by

     $$\begin{aligned}&\frac{\partial F}{\partial u_j}\Big|_{u_j=u_j^0+\Delta u_j} = \frac{\partial F}{\partial u_j}\Big|_{u_j^0} + \frac{\partial^2 F}{\partial u_j \partial u_k}\cdot\Delta u_k + \mathcal{O}(|\vec{v}_s|^2) \\ \Rightarrow\ &\frac{\partial F}{\partial u_j}\Big|_{u_j=u_j^0+\Delta u_j} = \mathcal{M}_{jk}\Delta u_k + \mathcal{O}(|\vec{v}_s|^2).\end{aligned}$$

- Combining these two observations, this leads to the equation

$$\mathcal{M}_{jk}\Delta u_k = c_j. \tag{17}$$

4. To find solutions for $\Delta u_k$ we have to, in principle, invert the matrix $\mathcal{M}$. However, $\mathcal{M}$ has zero eigenvalues originating from Goldstone modes. Therefore, we have to

   - first identify the zero eigenvalues,
   - and then check that $\vec{c}$ is orthogonal the corresponding eigenmodes. Physically, this means that the two contributions to $\vec{c}$, the Berry phase and dissipation term, do not couple to the Goldstone modes.
   - If so, we can define $\widetilde{\mathcal{M}} := \mathcal{M} + |0\rangle\, d\, \langle 0|$, where we project out the zero modes $|0\rangle$ with an arbitrary prefactor $d \neq 0$. Since $\vec{c}$ is orthogonal to the eigenmodes, the result does not dependent on $d$.
   - $\widetilde{\mathcal{M}}$ may now be inverted, and we finally get

$$\vec{\Delta u} = \left(\widetilde{\mathcal{M}}\right)^{-1} \vec{c}.$$

We may apply this scheme to the case, where we consider a rotational invariant free energy functional $F$, and to the case, where we add anisotropy terms to $F$. Before we pursue this procedure, we will concern ourselves with issues that are relevant for both cases.

In the first step, we calculate the fluctuation matrix $\mathcal{M}$, where

$$\mathcal{M}_{jk} = \frac{\delta^2 F}{\delta u_j \delta u_k}\,.$$

It is a hermitian $27 \times 27$ matrix, i.e. $\mathcal{M}^\dagger = (\mathcal{M}^*)^T = \mathcal{M}$. Hence, it has only real eigenvalues as expected. Moreover, $\mathcal{M}$ may be diagonalized, and the normalized eigenvectors can be chosen such that they form an orthonormal basis.

In the third step, we calculate the integrals over the volume $V$ with the same calculation rules as before for the helix (see App. A).

In the fourth and last step, we identify the eigenmodes. $\mathcal{M}$ has two translational eigenmodes $\vec{t}_1$ and $\vec{t}_2$, which are 27-components vectors. These are useful to determine $\dot{\vec{\varphi}}$ by demanding that

$$\vec{t}_1 \cdot \vec{c} = 0 \quad \wedge \quad \vec{t}_2 \cdot \vec{c} = 0 \quad \wedge \quad \dot{\vec{\varphi}} \cdot (\hat{q}_1 \times \hat{q}_2) = 0.$$

The third condition ensures that the structure drifts only in the plane of the three momentum vectors since the magnetic structure is translational invariant in the normal direction of this plane. To demonstrate that these conditions are equivalent

to the method used above for determining $\dot{\vec{\varphi}}$, we consider the Berry phase term and the dissipation term for $\varphi_x$. Using the abbrevations defined in App. A, i.e.

$$B_{u_j} := \int_V d\vec{r}\left(\hat{\Omega} \times \frac{\partial \hat{\Omega}}{\partial u_j}\right) \cdot \left(\frac{d}{dt} + (\vec{v}_s \cdot \nabla)\right) \hat{\Omega},$$
$$D_{u_j} := \int_V d\vec{r}\, \alpha_G \frac{\partial \hat{\Omega}}{\partial u_j} \cdot \left(\frac{d}{dt} + \frac{\beta}{\alpha_G}(\vec{v}_s \cdot \nabla)\right) \hat{\Omega},$$

we get in the static limit:

$$0 \stackrel{!}{=} B_{\varphi_x} + D_{\varphi_x} = \int_V d\vec{r}\left(-\hat{\Omega} \times (\vec{w} \cdot \nabla)\hat{\Omega} + \alpha_G(\vec{w}_{\alpha_G \beta} \cdot \nabla)\hat{\Omega}\right) \cdot \frac{\partial \hat{\Omega}}{\partial \varphi_x},$$
$$\frac{\partial \hat{\Omega}}{\partial \varphi_x} = -\frac{\partial \hat{\Omega}}{\partial x}.$$

To take the derivative with respect to $x$ for the ansatz of the A-phase

$$\vec{M}_A(\vec{r}, t) = \frac{1}{\mathcal{N}}\left[\vec{m}_h + \sum_{j=1}^{6} \vec{m}_{\vec{q}_j} e^{i\vec{q}_j \vec{r}}\right],$$

is equivalent to calculating

$$\frac{\partial \vec{M}_A(\vec{r}, t)}{\partial x} = \frac{1}{\mathcal{N}} \sum_{j=1}^{6} i\, q_x\, \vec{m}_{\vec{q}_j} e^{i\vec{q}_j \vec{r}} = \sum_{j=1}^{6} \frac{\partial \vec{M}_A(\vec{r}, t)}{\partial \vec{m}_{\vec{q}_j}} \cdot \left(i\, q_x\, \vec{m}_{\vec{q}_j}\right).$$

The last expression can be interpreted as scalar product of the two 27-component vectors $\frac{\partial \vec{M}_A}{\partial u_j} \cdot \vec{t}_{x_j}$, where the translation mode in $x$ direction $\vec{t}_x$ is given by

$$\vec{t}_x = \Big\{\vec{0},\, \vec{0},\, \vec{0},\, -q_{1_x}\vec{m}^{(i)}_{q_1},\, -q_{2_x}\vec{m}^{(i)}_{q_2}, -(q_{1_x} + q_{2_x})\vec{m}^{(i)}_{-q_1-q_2},$$
$$q_{1_x}\vec{m}^{(r)}_{q_1},\, q_{2_x}\vec{m}^{(r)}_{q_2}, (q_{1_x} + q_{2_x})\vec{m}^{(r)}_{-q_1-q_2}\Big\}^T$$

with $\vec{0} = \{0, 0, 0\}^T$. Using this result, we obtain for the A-phase:

$$0 \stackrel{!}{=} B_{\varphi_x} + D_{\varphi_x} = \int_V d\vec{r}\left(-\vec{M}_A \times (\vec{w} \cdot \nabla)\vec{M}_A + \alpha_G(\vec{w}_{\alpha_G \beta} \cdot \nabla)\vec{M}_A\right) \cdot \frac{\partial \vec{M}_A}{\partial u_j} \cdot \vec{t}_{x_j}$$
$$= \left(B_{u_j} + D_{u_j}\right) \cdot \vec{t}_{x_j} = \vec{c} \cdot \vec{t}_x.$$

We obtain similar results for $\varphi_y$ and $\varphi_z$. Considering $\vec{t}_1$ and $\vec{t}_2$ as a linear combination of $\vec{t}_x$, $\vec{t}_y$ and $\vec{t}_z$ we may infer that $\vec{t}_1 \cdot \vec{c} = 0$ and $\vec{t}_2 \cdot \vec{c} = 0$.

This implies that the drift velocity is adjusted such that the overlap of the translation modes and $\vec{c}$ vanishes. Therefore, in the second part of the last step we only have to check this condition for other potential Goldstone modes. If there are no other Goldstone modes present, then the conditions for $\dot{\vec{\varphi}}$ ensure that the equation $\mathcal{M}_{jk}\Delta u_k = c_j$ is solvable.

At the end of the last step, we get the current-induced distortion of the ground state variables. To explain the position changes of the neutron peaks, we are particularly interested in the change of the momentum vectors, i.e. the first six components of $\vec{u}$. Without an explicit calculation one knows that the three momentum vectors should add up to zero. For this reason, there are only the following possibilities or a superposition thereof to change the momentum vectors:

- The plane of the $q$-vectors tilts, but the 120° symmetry remains.
- The three momentum vectors rotate slightly in the plane, but the 120° symmetry remains.
- The 120° symmetry does not remain. The three $q$-vectors change their angles *and* their lengths.

In the following, we consider two different cases, the first one without anisotropy terms, and the second one including some anisotropy terms. Below, we report only the basic results of the numerical calculations. Some explicit numerical results are summarized in App. D.

## 7.4 The Rotational Invariant Case: No Anisotropy Terms

In the rotational invariant case, the fluctuation matrix $\mathcal{M}$ has an additional Goldstone mode, a rotation mode denoted by $\overrightarrow{\text{rot}}$ in the following. However, neither the Berry phase nor the dissipation term couple to $\overrightarrow{\text{rot}}$, i.e. $\vec{c} \cdot \overrightarrow{\text{rot}} = 0$. Obeying the calculation rules of the fourth step we get the current-induced distortions of the ground state variables. Obviously, the lengths of the $q$-vectors is almost constant under the influence of the current, thus the threefold rotation symmetry basically remains. However, the plane of the three $q$-vectors changes as it tilts slightly, i.e. it obtains a component in the direction of the magnetic field. Below we repeat the calculation with a weak anisotropy term included.

## 7.5 The A-Phase Including Anisotropy Terms

In this part, we will add terms to the free energy functional that break the rotational symmetry. Therefore, the rotation mode (still denoted by $\overrightarrow{\text{rot}}$) is no longer a Goldstone mode of the fluctuation matrix. Nevertheless, the modulus of the corresponding eigenvalue is small, since these anisotropy terms are small. The basic idea is that in the anisotropic case $\vec{c}$ couples to the eigenmode of this small eigenvalue which, by inverting the matrix, may lead to a huge prefactor and therefore to a measureable effect.

First, let us consider the rotational invariant free energy functional. To leading order, it is given by

$$F[\vec{M}] = \int_V d\vec{r} \left( r_0 \vec{M}^2 + J(\nabla \vec{M})^2 + 2D\vec{M} \cdot (\nabla \times \vec{M}) + U(\vec{M}^2)^2 - \vec{B} \cdot \vec{M} \right).$$

To simplify the following calculations, we rescale the free energy functional in the following way:

$$\begin{aligned} \tilde{\vec{r}} &= Q\vec{r} & \Rightarrow \qquad & \vec{r} = 1/Q\, \tilde{\vec{r}}, \quad \nabla = Q\tilde{\nabla} \\ \tilde{\vec{M}} &= [U/(JQ^2)]^{1/2} \vec{M} & \Rightarrow \qquad & \vec{M} = [(JQ^2)/U]^{1/2}\, \tilde{\vec{M}} \\ \tilde{\vec{B}} &= [U/(JQ^2)^3]^{1/2}\, \vec{B} \end{aligned}$$

such that $|\vec{q}_j| \approx 1$ $(j = 1, 2, 3)$. Applying this scaling transformation to the Ginzburg-Landau free energy functional ($U, J, D > 0$ $Q = |\vec{Q}| = D/J$) we get

$$F[\tilde{\vec{M}}] = \frac{J^2 Q}{U} \int_V d\vec{r} \left( (1+t)\tilde{\vec{M}}^2 + (\tilde{\nabla}\tilde{\vec{M}})^2 + 2\tilde{\vec{M}} \cdot (\tilde{\nabla} \times \tilde{\vec{M}}) + (\tilde{\vec{M}}^2)^2 - \tilde{\vec{B}} \cdot \tilde{\vec{M}} \right),$$

where $t = r_0/(JQ^2) - 1$. This rescaling has the additional advantage that the rescaled free energy functional depends only on one parameter $t$ and on a global prefactor. We observe that the free energy functional scales linear in $Q$. To simplify the notation, we omit the tildes in the following and keep in mind that we are using rescaled units.

To this free energy functional we add the following two anisotropy terms:

$$\begin{aligned} F_{\text{ani}}^{(1)} &= \delta_1 \cdot \int_V d\vec{r} \left\{ [\partial_x M_y]^2 + [\partial_y M_z]^2 + [\partial_z M_x]^2 \right\} \\ &= \delta_1 \cdot \sum_{j=1}^{3} \left\{ [(\vec{q}_j)_x]^2 \left| (\vec{m}_{\vec{q}_j})_y \right|^2 + [(\vec{q}_j)_y]^2 \left| (\vec{m}_{\vec{q}_j})_z \right|^2 + [(\vec{q}_j)_z]^2 \left| (\vec{m}_{\vec{q}_j})_x \right|^2 \right\} \end{aligned}$$

and

$$\begin{aligned} F_{\text{ani}}^{(2)} &= \delta_2 \cdot \int_V d\vec{r} \left\{ \vec{M}(\partial_x^6 + \partial_y^6 + \partial_z^6)\vec{M} \right\} \\ &= \delta_2 \cdot \sum_{j=1}^{3} \left\{ [(\vec{q}_j)_x]^6 + [(\vec{q}_j)_y]^6 + [(\vec{q}_j)_z]^6 \right\} \left| \vec{m}_{\vec{q}_j} \right|^2 \end{aligned}$$

with the prefactors $\delta_1$ and $\delta_2$ determining their relative strength. The first prefactor, $\delta_1$, is quadratic in spin-orbit coupling. It provides an overlap of $\vec{c}$ and the rotation mode $\overrightarrow{\text{rot}}$ to lowest order spin-orbit coupling. This overlap is linear in $\delta_1$ and $|\vec{v}_s|$, but depends only barely on $\delta_2$. The second prefactor is of higher order in spin orbit coupling, and pins the A-phase to liner order. It provides the "mass" of the rotation mode such that for $\delta_2 \neq 0$ we do not have a Goldstone mode. Thus, $F$ is given by

$$F = \gamma \cdot \left( F_2 + F_4 + F_{\text{ani}}^{(1)} + F_{\text{ani}}^{(2)} + F_B \right)$$

with

$$F_2 = \int d\vec{r} \left[ (1+t)\vec{M}^2 + (\nabla \vec{M})^2 + 2\vec{M} \cdot (\nabla \times \vec{M}) \right],$$
$$F_4 = \int d\vec{r} (\vec{M}^2)^2,$$
$$F_B = -\int d\vec{r}\, \vec{B} \cdot \vec{M}.$$

Repeating the calculation with these weak anisotropies, we get the current-induced distortions of the ground state variables. Some explicit numerical results are summarized in App. D.

We again observe that the lengths of the $q$-vectors are almost constant under the influence of the current so that the threefold rotation symmetry basically remains. As before, the plane of the three $q$-vectors tilts. However, we also observe a rotation of the $q$-vectors, where the magnitude of the rotation depends strongly on the directions of $\vec{B}$ and $\vec{v}_s$ with respect to the crystal. For example, there is no rotation for the magnetic field applied in the $\langle 001 \rangle$ direction. In this special case, there is an additional rotation symmetry of 180° around the $\hat{z}$ axis such that the contribution from the Berry phase term to the rotation angle does not provide a term linear in $|\vec{v}_s|$. On the other hand, for a magnetic field in the $\langle 110 \rangle$ direction, this rotation symmetry does not exist.

Let us rewrite the rotation angle $\theta$ between the ground state wave vectors and the current-distorted wave vectors by

$$\cos(\theta) = \frac{\hat{q}_2^0 \cdot \hat{q}_2}{|\hat{q}_2^0| \cdot |\hat{q}_2|}.$$

For small angles $\theta$ we may expand the cosine such that

$$\theta \approx \pm \sqrt{2 \left( 1 - \frac{\hat{q}_2^0 \cdot \hat{q}_2}{|\hat{q}_2^0| \cdot |\hat{q}_2|} \right)}. \tag{18}$$

For a magnetic field applied in the $\langle 110 \rangle$ direction, we find $\theta$ to be proportional to

$$\theta \sim |\vec{v}_s| \cdot \frac{\delta_1}{\delta_2} \left( \frac{\beta}{\alpha_G} - 1 \right) \alpha_G \cdot \hbar \cdot \sqrt{\frac{JQ^2}{U}} \frac{U}{J^2 Q^3}. \tag{19}$$

Here, we also applied the current in the $\langle 110 \rangle$ direction, which is a ground state direction of one of the three helices and perpendicular to the magnetic field.

Some of these factors are easy to understand. By construction, we get a term that is linear in the strength of the current $|\vec{v}_s|$. The rotation angle should be proportional to $\delta_1$ since the first anisotropy term provides an overlap with the rotation mode. $\delta_2$ is a measure of the eigenvalue that corresponds to the rotation mode. By inverting the matrix one therefore obtains mainly $1/\delta_2$. This huge prefactor $1/\delta_2$ compensates

the other small prefactors and leads to an appreciable effect. In the Galilei-invariant case, $\beta = \alpha_G$, we also do not expect a rotation of the A-phase since then $\dot{\vec{\varphi}} = \vec{v}_s$, and the Skrymion density does not enter. Unless the rotation angle is proportional to $\alpha_G$, the main contribution for the rotation comes from the Berry phase term, because in the limit of small $\alpha_G$ the difference $\dot{\vec{\varphi}} - \vec{v}_s$ vanishes for the A-phase. Therefore, the Berry phase term is proportional to $\alpha_G$. For a single helix the situation is different as $\dot{\vec{\varphi}}$ depends only on $\beta/\alpha_G$ and not on $\alpha_G$ alone. The remaining factors $\hbar \cdot \sqrt{\frac{JQ^2}{U}} \frac{U}{J^2Q^3}$ are due to physical rescaling. For further details on this subject see App. D.

## 7.6 Results for the A-Phase

Concluding this Section we will summarize the results we have obtained. We have shown that the magnetic pattern of the A-phase drifts, with the drift velocity

$$\dot{\vec{\varphi}} = \frac{\beta}{\alpha_G}\vec{v}_s + \left(1 - \frac{\beta}{\alpha_G}\right)\frac{1}{\alpha_G^2 X^2 + 1}\vec{v}_s + \left(1 - \frac{\beta}{\alpha_G}\right)\frac{\alpha_G X}{\alpha_G^2 X^2 + 1}\,\hat{z} \times \vec{v}_s,$$

where $X \equiv \int_V d\vec{r}\,\frac{1}{2}\,(\nabla\hat{\Omega})^2$. Moreover, originating in a non-zero Skyrmion density and slight crystal anisotropies, the three momentum vectors, constituting the A-phase tilt and rotate, in general. The rotation angle between the ground state wave vectors and the current-distorted wave vectors is proportional to

$$\theta \sim |\vec{v}_s| \cdot \frac{\delta_1}{\delta_2}\left(\frac{\beta}{\alpha_G} - 1\right)\alpha_G \cdot \hbar \cdot \sqrt{\frac{JQ^2}{U}}\frac{U}{J^2Q^3}\,.$$

A related phenomenon, that also only occurs because of a non-zero Skyrmion density is the topological Hall effect, that is described in the following Section.

# 8 Topological Hall Effect in the A-Phase

Applying an electric current flows through a conductor in a magnetic field, the magnetic field exerts a transverse force on the moving charge carriers leading to a potential difference transverse to the current. The presence of this measurable transverse voltage is called the Hall effect. The Hall resistivity $\rho_{xy}$ is the proportionality factor between the current and the Hall voltage. In nonmagnetic materials, $\rho_{xy}$ is proportional to the magnetic field $B$.

However, in many ferromagnetic materials there is an additional contribution to the Hall resistivity, denoted as the anomalous Hall effect (AHE). It is proportional to the magnetization of the material, $\rho_{xy} = R_0 B + \mu_0 R_s M$. Here, $R_0$ and $R_S$ are the normal and anomalous Hall coefficients, respectively.

However, in Ref. [47] the authors present another contribution to the Hall resistivity that occurs in chiral spin textures, the so-called "topological Hall effect". The origin of this extra Hall contribution is a Berry phase that can produce an additional effective magnetic field $B_\Phi$ via the spin degrees of freedom. The basic idea behind the topological Hall effect is as follows. A conduction electron that moves through a chiral metal may acquire a Berry phase $\Phi_B$ when following adiabatically the spin polarization of topological objects [46, 48]. This Berry phase can be viewed as an Aharonov-Bohm phase resulting from an effective magnetic field $\vec{B}_{\text{eff}} = \Phi_0 \vec{\Phi}$ with opposite sign for majority and minority spins. Here, $\Phi_0 = h/e$ is the flux quantum for a single electron, and $\vec{\Phi}$ is the Skyrmion density, given by Eq. (14). Thus, $B_\Phi$ produces a Hall conductivity $\sigma_{\text{top}}$ that is proportional to $\vec{\Phi}$. The Berry phase reflects the integrated Skyrmion density per unit cell, which is a measure for a winding number of the topological spin structur and therefore quantized as an integer number.

Experimentally, this topological Hall contribution can be well distinguished from both conventional Hall effect contributions. Therefore Hall experiments are a means to detect topological spin structures in helical magnets [13, 46, 47, 49].

As mentioned in Ref. [46], a helical state with a single wavevector does not have a Skrymion density, i.e. it vanishes. Hence, there is no topological Hall effect in the helical or conical phase. This was also confirmed by experiments [13]. Only a proper superposition of spiral states lead to a finite Skyrmion density. Skyrmion textures naturally leads to a non-zero chirality. Theoretically, it is predicted that $\sigma_{\text{top}}$ is proportional to the Skyrmion number or to the Skyrmion density, respectively [47].

Neubauer *et al.* used the properties of the topological Hall effect to substantiate the anti-Skyrmion lattice in the A-Phase [13]. They used the direct measurement of the Skyrmion density via the topological Hall effect of the quantized Berry phase. Most of the following work in this Section has been published in Ref. [13].

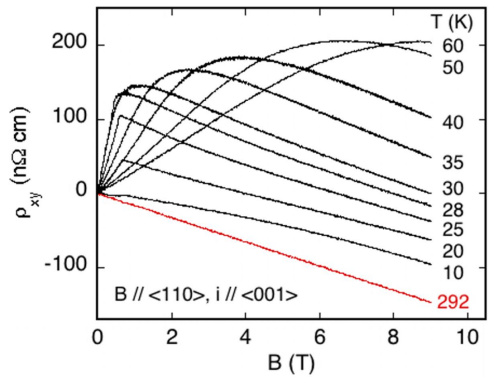


Figure 12: Hall resistivity of MnSi. Figure taken from Ref. [13].

Fig. 12 shows a typical measurement for the Hall resistivity $\rho_{xy}$ of MnSi for $\vec{B} \parallel \langle 110 \rangle$ and the current in the $\langle 001 \rangle$ direction. At room temperature, the behavior is dominated by the normal Hall effect. For low temperatures, however, the behaviour is more complicated.

Since the topological Hall effect is predicted to occur only in the A-phase, a detailed measurement of the Hall resistivity in the temperature and field range of the A-phase was performed. This is shown in the left part of Fig. 13.

To better see the additional topological contribution, the authors approximated the Hall signal linearly from below to above the A-phase and subtracted this part of the total signal. The resulting contribution $\Delta\rho_{xy}$ is shown on the right part of Fig. 13. The curves have been shifted vertically for better visibility.

The main results of $\Delta\rho_{xy}$ are the following:

- The sign of the signal is opposite to the normal Hall effect.
- The magnitude of $\Delta\rho_{xy}$ is approximately given by $\Delta\rho_{xy} \approx 4.5 \pm 1\,\mathrm{n\Omega\,cm}$.
- The signal is roughly the same for the two different orientations of the magnetic field $\vec{B} \parallel \langle 110 \rangle$ and $\vec{B} \parallel \langle 111 \rangle$.

A simple formula for $\Delta\rho_{xy}$ can be given in the "adiabatic limit":

$$\Delta\rho_{xy} \approx P R_0 \, B^z_{\mathrm{eff}}. \tag{20}$$

In this limit, the lifetime of the conduction electrons is taken to be infinite, and when passing through the solid the spin polarization of the electrons follow smoothly the magnetic structure. In Eq. (20), the applied magnetic field is in the $\hat{z}$ direction, $R_0$ is the normal Hall constant, and $P$ is the local spin polarization of the conduction electrons. Within this simplified formula, some of the main features observed may be explained. Since the A-phase of MnSi forms a lattice of anti-Skyrmions, the

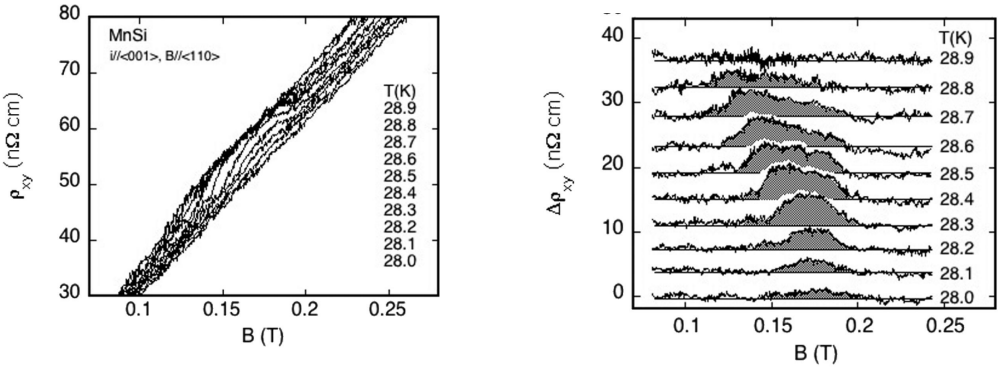


Figure 13: Hall resistivity of MnSi in the A-phase; Left: Total Hall resistivity; Right: Topological part of the Hall resistivity. Figures taken from Ref. [13].

Skyrmion density integrated over each two-dimensional magnetic unit cell is $-1$. This implies that the effective field is quantized and oriented opposite to the applied field. Moreover, this formula allows a theoretical estimate of the size of $\Delta\rho_{xy}$ that is in good argeement with the experiment.

Although the Skyrmion density already appears in the equations of motion for the A-Phase, in particular in the equation for the drift velocity, the emergence of a Berry phase can be seen more explicitly by deriving the Landau-Lifshitz-Gilbert equation from a variational principle. We will discuss this derivation in the following Section.

# 9 Derivation of the Landau-Lifshitz-Gilbert Equation From a Variation Principle

The Landau-Lifshitz-Gilbert equation

$$\left(\frac{d}{dt} + \vec{v}_s \cdot \nabla\right) \hat{\Omega}(\vec{x}, t) = \\ \hat{\Omega}(\vec{x}, t) \times \left(-\frac{1}{M} \frac{\delta F[\hat{\Omega}]}{\delta \hat{\Omega}(\vec{x}, t)}\right) - \alpha_G \, \hat{\Omega}(\vec{x}, t) \times \left(\frac{d}{dt} + \frac{\beta}{\alpha_G} \vec{v}_s \cdot \nabla\right) \hat{\Omega}(\vec{x}, t)$$

for a constant magnetization amplitude $M$ may be derived from the variational principle [28] at least up to a surface term discussed below:

$$\frac{\delta \mathcal{A}[\hat{\Omega}]}{\delta \hat{\Omega}(\vec{x}, t)} = \frac{\delta \mathcal{R}[\hat{\Omega}]}{\delta d_t \hat{\Omega}(\vec{x}, t)} \,. \tag{21}$$

In this formula, the dissipation functional $\mathcal{R}$ is given by

$$\mathcal{R}[\hat{\Omega}] = \frac{\alpha_G}{2} \int dt \int_V d\vec{x} \left[\left(\frac{d}{dt} + \frac{\beta}{\alpha_G} (\vec{v}_s \cdot \nabla)\right) \hat{\Omega}(\vec{x}, t)\right]^2 ,$$

and $\mathcal{A}$ is the action functional

$$\mathcal{A}[\hat{\Omega}] = -\int dt \left\{ \int_V d\vec{x} \cdot \vec{A}(\hat{\Omega}(\vec{x}, t)) \cdot \left(\frac{d}{dt} + \vec{v}_s \cdot \nabla\right) \hat{\Omega}(\vec{x}, t) + \frac{1}{M} F[\hat{\Omega}(\vec{x}, t)] \right\} .$$

Here, $\vec{A}(\hat{\Omega}(\vec{x}, t))$ is the vector potential associated with the topological Berry phase term according to a magnetic field of a monopole. In spherical coordinates, i.e. $\hat{\Omega}(r, \theta, \phi) = r(\sin\theta\cos\phi, \sin\theta\sin\phi, \cos\theta)^T$, a possible parametrization is given by

$$\vec{A}(r, \theta, \phi) = \frac{1 - \cos\theta}{r \sin\theta} \hat{e}_\phi \quad \text{with} \quad \hat{e}_\phi = (-\sin\phi, \cos\phi, 0)^T .$$

A derivation of this formula, which is singular for $\theta = \pi$, may be found in App. B. Thus, on the unit sphere, $|\hat{\Omega}| = r = 1$, one gets

$$\vec{A}(\theta, \phi) = \frac{1 - \cos\theta}{\sin\theta} \hat{e}_\phi .$$

Moreover, in spherical coordinates $\mathcal{A}$ is given by

$$\mathcal{A}[\theta, \phi] = -\int dt \left\{ \left[ \int_V d\vec{x} \, (1 - \cos\theta(\vec{x}, t)) \left(\frac{d}{dt} + (\vec{v}_s \cdot \nabla)\right) \phi(\vec{x}, t) \right] + \frac{1}{M} F[\theta, \phi] \right\} , \tag{22}$$

because ($r = 1$)

$$\hat{\Omega}(\vec{x}, t) = \hat{\Omega}(\theta(\vec{x}, t), \phi(\vec{x}, t)) = \begin{pmatrix} \sin\theta\cos\phi \\ \sin\theta\sin\phi \\ \cos\theta \end{pmatrix} , \tag{23}$$

and

$$(\vec{v}_s \cdot \nabla)\hat{\Omega} = \hat{e}_\theta \left((\vec{v}_s \cdot \nabla)\theta\right) + \hat{e}_\phi \left((\vec{v}_s \cdot \nabla)\phi\right)) \sin\theta.$$

Thus,

$$\begin{aligned} A[\hat{\Omega}] \cdot (\vec{j} \cdot \nabla)\hat{\Omega} &= \frac{1-\cos\theta}{\sin\theta}\hat{e}_\phi \cdot \left(\hat{e}_\theta \left((\vec{j} \cdot \nabla)\theta\right) + \hat{e}_\phi \left((\vec{j} \cdot \nabla)\phi\right) \sin\theta\right) \\ &= (1-\cos\theta) \cdot (\vec{j} \cdot \nabla)\phi. \end{aligned}$$

Performing a similar calculation for the time derivative of $\hat{\Omega}$ we obtain Eq. (22).

To derive the Landau-Lifshitz-Gilbert equation from the variational principle, one has first to calulate both variations of Eq. (21). In a second step one has to take the cross product on both sides of Eq. (21).

Let us start with the fist step: The action functional contains the Ginburg-Landau energy functional and two Berry-phase terms. Therefore, we divide it into three parts:

$$\begin{aligned} \mathcal{A}[\hat{\Omega}] &= -\int dt \left\{ \int_V d\vec{x} \cdot \vec{A}(\hat{\Omega}(\vec{x},t)) \cdot \left(\frac{d}{dt} + \vec{v}_s \cdot \nabla\right) \hat{\Omega}(\vec{x},t) + \frac{1}{M} F[\hat{\Omega}(\vec{x},t)] \right\} \\ &=: -\left(\mathcal{A}^{(t)}[\hat{\Omega}(\vec{x},t)] + \mathcal{A}^{(\nabla)}[\hat{\Omega}(\vec{x},t)] + \mathcal{A}^{(F)}[\hat{\Omega}(\vec{x},t)]\right) \end{aligned} \tag{24}$$

with

$$\begin{aligned} \mathcal{A}^{(t)}[\hat{\Omega}(\vec{x},t)] &= \int dt \int_V d\vec{x} \cdot \vec{A}(\hat{\Omega}(\vec{x},t)) \cdot \frac{d}{dt}\hat{\Omega}(\vec{x},t), \\ \mathcal{A}^{(\nabla)}[\hat{\Omega}(\vec{x},t)] &= \int dt \int_V d\vec{x} \cdot \vec{A}(\hat{\Omega}(\vec{x},t)) \cdot (\vec{v}_s \cdot \nabla)\,\hat{\Omega}(\vec{x},t), \\ \mathcal{A}^{(F)}[\hat{\Omega}(\vec{x},t)] &= \int dt\, \frac{1}{M} F[\hat{\Omega}(\vec{x},t)]. \end{aligned}$$

For these three terms we get

$$\begin{aligned} \frac{\delta\mathcal{A}^{(t)}[\hat{\Omega}(\vec{x},t)]}{\delta\Omega_j(\vec{y},t')} &= \left(\frac{d\hat{\Omega}(\vec{y},t')}{dt'} \times \hat{\Omega}(\vec{y},t')\right)_j \\ \frac{\delta\mathcal{A}^{(\nabla)}[\hat{\Omega}(\vec{x},t)]}{\delta\Omega_j(\vec{y},t')} &= \left(\left[(\vec{v}_s \cdot \nabla)\hat{\Omega}(\vec{y},t')\right] \times \hat{\Omega}(\vec{y},t')\right)_j \\ &\quad + \int_{S(V)} d\sigma^{(x)}\, \delta(\vec{x}-\vec{y}) A_j[\hat{\Omega}(\vec{x},t')](\vec{v}_s \cdot \vec{\nu}) \\ \frac{\delta\mathcal{A}^{(F)}[\hat{\Omega}(\vec{x},t)]}{\delta\Omega_j(\vec{y},t')} &=: \frac{1}{M}\frac{\delta F[\hat{\Omega}(\vec{x},t')]}{\delta\hat{\Omega}(\vec{y},t')}\,. \end{aligned} \tag{25}$$

A detailed calculation of the first two terms is summarized in App. C. In the last equation, we consider the functional $F[\hat{\Omega}]$ at a fixed time $t'$ to eliminate the time integral. Exchanging $\vec{x}, \vec{y}$ and $t, t'$ we get

$$\begin{aligned} \frac{\delta\mathcal{A}[\hat{\Omega}]}{\delta\hat{\Omega}(\vec{x},t)} &= \hat{\Omega}(\vec{x},t) \times \left(\frac{d}{dt} + \vec{v}_s \cdot \nabla\right) \hat{\Omega}(\vec{x},t) - \frac{1}{M}\frac{\delta F[\hat{\Omega}]}{\delta\hat{\Omega}(\vec{x},t)} \\ &\quad - \int_{S(V)} d\sigma^{(y)}\, \delta(\vec{y}-\vec{x}) A_j[\hat{\Omega}(\vec{y},t)](\vec{v}_s \cdot \vec{\nu}). \end{aligned} \tag{26}$$

The variation of the dissipation functional with respect to $d_t\hat{\Omega}(\vec{x},t)$ is then given by

$$\frac{\delta\mathcal{R}[\hat{\Omega}]}{\delta d_t\hat{\Omega}(\vec{x},t)} = \alpha_G\left(\frac{d}{dt}+\frac{\beta}{\alpha_G}\vec{v}_s\cdot\nabla\right)\hat{\Omega}(\vec{x},t). \tag{27}$$

In the second step, we have to take the cross product with $\hat{\Omega}$ on both sides of Eq. (21). Therefore, we consider the relation

$$\hat{\Omega}(\vec{x},t)\times\frac{\delta\mathcal{R}[\hat{\Omega}]}{\delta d_t\hat{\Omega}(\vec{x},t)} = \alpha_G\hat{\Omega}(\vec{x},t)\times\left(\frac{d}{dt}+\frac{\beta}{\alpha_G}\vec{v}_s\cdot\nabla\right)\hat{\Omega}(\vec{x},t).$$

Neglecting the boundary term and using that $\hat{\Omega}$ is a unit vector similiar to Eq. (7) we get for the action functional

$$\begin{aligned}\hat{\Omega}(\vec{x},t)\times\frac{\delta\mathcal{A}[\hat{\Omega}]}{\delta\hat{\Omega}(\vec{x},t)} &= \hat{\Omega}(\vec{x},t)\times\left[\hat{\Omega}(\vec{x},t)\times\left(\frac{d}{dt}+(\vec{v}_s\cdot\nabla)\right)\hat{\Omega}(\vec{x},t)\right]\\ &\quad+\hat{\Omega}(\vec{x},t)\times\left(-\frac{1}{M}\frac{\delta F[\hat{\Omega}]}{\delta\hat{\Omega}(\vec{x},t)}\right)\\ &= -\left(\frac{d}{dt}+(\vec{v}_s\cdot\nabla)\right)\hat{\Omega}(\vec{x},t)+\hat{\Omega}(\vec{x},t)\times\left(-\frac{1}{M}\frac{\delta F[\hat{\Omega}]}{\delta\hat{\Omega}(\vec{x},t)}\right).\end{aligned}$$

Combining the two formulas we obtain the Landau-Lifshitz-Gilbert equation.

## 9.1 Derivation of the Equations of Motion for Dynamical Variables from a Variation Principle

In principle, it is possible to derive the effective equations of motion (cf. Eq. (8)) from a variation principle under the condition that one neglects the boundary term which occurs in Eq. (25). However, including this term we get an additional contribution that is not necessarily a surface term. To demonstrate this, we will use the following lemma: Let $F(t)$ be a sufficiently smooth function that depends on $t$. If $F$ depends on a parameter $u = u(t)$, such that $F(t) = F(u(t))$, then

$$\frac{\delta F(t')}{\delta u(t)} = \frac{\partial F(u)}{\partial u}\delta(t'-t).$$

Let the magnetization direction $\hat{\Omega}$ be parameterized by a few time-dependent variables $u_j$ $(j = 1,\ldots,n)$, i.e. $\hat{\Omega}(\vec{r},t) = \hat{\Omega}(\vec{x},u_1(t),\ldots,u_n(t))$ as in Sec. 5.3. If $u_j$ solves the variational equation

$$\frac{\delta\mathcal{A}[\hat{\Omega}]}{\delta u_j(s)} = \frac{\delta\mathcal{R}[\hat{\Omega},d_t\hat{\Omega}]}{\delta d_t u_j(s)} \tag{28}$$

and if one neglects the boundary term occuring in Eq. (25) then $u_j$ solves Eq. (8).

To show this assertion, we assume without loss of generality $n = 1$ and set $u_1(t) = u(t)$. We start from the variation principle (cf. Eq. (21)) and show that if $\hat{\Omega}$ solves Eq. (21), then $u_j$ solves Eq. (28). By chain rule we get

$$\frac{d}{dt}\hat{\Omega}(\vec{x},u) = \frac{\partial\hat{\Omega}(\vec{x},u)}{\partial u}\,\dot{u}$$

which implies that

$$\left.\frac{\partial(d_t\hat{\Omega}(\vec{x},u,\dot{u}))}{\partial\dot{u}}\right|_u = \frac{\partial\hat{\Omega}(\vec{x},u)}{\partial u} \quad \text{because} \quad \frac{\partial\hat{\Omega}(\vec{x},u)}{\partial\dot{u}} = 0.$$

Applying above lemma we get

$$\frac{\delta\hat{\Omega}(\vec{y},t')}{\delta u(t)} = \frac{\partial\hat{\Omega}(\vec{y},u)}{\partial u}\delta(t'-t) \quad \text{and} \quad \left.\frac{\delta(d_t\hat{\Omega}(\vec{y},t'))}{\delta\dot{u}(t)}\right|_u = \left.\frac{\partial(d_t\hat{\Omega}(\vec{y},u,\dot{u}))}{\partial\dot{u}}\right|_u \cdot \delta(t'-t).$$

This implies

$$\begin{aligned}
0 &= \int_V d\vec{y}\int dt\frac{\delta\mathcal{A}[\hat{\Omega}(\vec{x},t)]}{\delta\hat{\Omega}(\vec{y},t')}\,\delta(t-t')\overbrace{\left(\frac{\partial\hat{\Omega}(\vec{y},t)}{\partial u} - \left.\frac{\partial(d_t\hat{\Omega}(\vec{y},t))}{\partial\dot{u}}\right|_u\right)}^{=0} \\
&= \int_V d\vec{y}\int dt\frac{\delta\mathcal{A}[\hat{\Omega}(\vec{x},t)]}{\delta\hat{\Omega}(\vec{y},t')}\left(\frac{\delta\hat{\Omega}(\vec{y},t')}{\delta u(t)} - \left.\frac{\delta(d_t\hat{\Omega}(\vec{y},t'))}{\delta\dot{u}(t)}\right|_u\right) \\
&= \int_V d\vec{y}\int dt\frac{\delta\mathcal{A}[\hat{\Omega}(\vec{x},t)]}{\delta\hat{\Omega}(\vec{y},t')}\frac{\delta\hat{\Omega}(\vec{y},t')}{\delta u(t)} - \int_V d\vec{y}\int dt\frac{\delta\mathcal{R}[\hat{\Omega}(\vec{y},t),d_t\hat{\Omega}(\vec{x},t)]}{\delta(d_t\hat{\Omega}(\vec{y},t))}\left.\frac{\delta(d_t\hat{\Omega}(\vec{y},t'))}{\delta\dot{u}(t)}\right|_u \\
&= \frac{\delta\mathcal{A}[\hat{\Omega}(\vec{x},t)]}{\delta u(t)} - \frac{\delta\mathcal{R}[\hat{\Omega}(\vec{x},t),d_t\hat{\Omega}(\vec{x},t)]}{\delta\dot{u}(t)}\,,
\end{aligned}$$

where in the penultimate line we applied Eq. (21). Neglecting the boundary term which appears in Eq. (25) we obtain the assertion.

In principle, this proof is sufficient, but one does not see clearly the influence of the boundary term. To get a better understanding of this additional term we will perform a second proof: Applying chain rule we get

$$\frac{\delta\mathcal{A}[\hat{\Omega}(\vec{x},t)]}{\delta u_j(s)} = \int_V d\vec{y}\int dt'\left.\frac{\delta\mathcal{A}[\hat{\Omega}(\vec{x},t)]}{\delta\hat{\Omega}_j(\vec{y},t')}\right|_{\hat{\Omega}=\hat{\Omega}(u)}\cdot\frac{\delta\hat{\Omega}_j(\vec{y},t')}{\delta u(s)}\,. \tag{29}$$

Using above lemma we obtain

$$\frac{\delta\Omega_j(\vec{y},t')}{\delta u(s)} = \frac{\partial\Omega_j(\vec{y},u)}{\partial u}\delta(s-t')$$

and inserting the result of App. C, Eq. (38) we get

$$\begin{aligned}
\frac{\delta\mathcal{A}[\hat{\Omega}(\vec{x},t)]}{\delta u(s)} &= \int_V d\vec{y}\int dt'\left[\left(\hat{\Omega}(\vec{y},t')\times\left(\frac{d}{dt}+\vec{v}_s\cdot\nabla\right)\hat{\Omega}(\vec{y},t')\right)_j - \frac{1}{M}\frac{\delta F[\hat{\Omega}]}{\delta\hat{\Omega}_j(\vec{y},t')}\right. \\
&\qquad \left. - \int_{S(V)} d\sigma^{(y')}\,\delta(\vec{y}\,'-\vec{y})A_j[\hat{\Omega}(\vec{y}\,',t')](\vec{v}_s\cdot\vec{\nu})\right]\cdot\frac{\partial\Omega_j(\vec{y},t')}{\partial u}\delta(s-t')\Big|_{\hat{\Omega}=\hat{\Omega}(\vec{y},u)} \\
&= \int_V d\vec{y}\left(\hat{\Omega}(\vec{y},s)\times\left(\frac{d}{dt}+\vec{v}_s\cdot\nabla\right)\hat{\Omega}(\vec{y},s)\right)\cdot\frac{\partial\Omega_j(\vec{y},s)}{\partial u} - \frac{1}{M}\frac{\partial F[\hat{\Omega}]}{\partial u} \\
&\qquad - \int_V d\vec{y}\left(\int_{S(V)} d\sigma^{(y')}\,\delta(\vec{y}\,'-\vec{y})A_j[\hat{\Omega}(\vec{y}\,',s)](\vec{v}_s\cdot\vec{\nu})\right)\cdot\left.\frac{\partial\Omega_j(\vec{y},s)}{\partial u}\right|_{\hat{\Omega}=\hat{\Omega}(\vec{y},u)}
\end{aligned}$$

The boundary term may be simplified further:

$$\begin{aligned}&\int_{S(V)} d\sigma^{(y')} \int_V d\vec{y}\, \frac{\partial \Omega_j(\vec{y},s)}{\partial u} \delta(\vec{y}\,' - \vec{y}) A_j[\hat{\Omega}(\vec{y}\,',s)](\vec{v}_s \cdot \vec{\nu}) \\ &= \int_{S(V)} d\sigma^{(y')} \frac{\partial \Omega_j(\vec{y},s)}{\partial u} A_j[\hat{\Omega}(\vec{y}\,',s)] \underbrace{(\vec{v}_s \cdot \vec{\nu})}_{=v_{s_i}\hat{e}_i\cdot\vec{\nu}}\end{aligned}$$

applying Gauss theorem yields

$$= \int_V d\vec{y}\,'\, v_{s_i} \frac{d}{dy_i'} \left( \frac{\partial \Omega_j(\vec{y}\,',s)}{\partial u} A_j[\hat{\Omega}(\vec{x},s)] \right)$$

and a renaming of variables leads to

$$= \int_V d\vec{x}\, (\vec{v}_s \cdot \nabla) \left( \frac{\partial \Omega_j(\vec{x},s)}{\partial u} A_j[\hat{\Omega}(\vec{x},s)] \right).$$

A technical problem to calculate this term is the explicit appearance of the vector potential $A[\hat{\Omega}(\vec{x},s)]$ which cannot be written in a coordinate invariant form (see App. B).

For the dissipation functional we may perform the same steps. Because of $\frac{\partial \hat{\Omega}}{\partial \dot{u}} = 0$ we get

$$\frac{\delta \mathcal{R}[\hat{\Omega}(\vec{x},t), d_t\hat{\Omega}(\vec{x},t)]}{\delta \dot{u}(s)} = \int_V d\vec{y} \int dt' \frac{\delta \mathcal{R}[\hat{\Omega}(\vec{x},t), d_t\hat{\Omega}(\vec{x},t)]}{\delta(d_t\hat{\Omega}_j(\vec{y},t'))}\bigg|_{\hat{\Omega}=\hat{\Omega}(\vec{y},u)} \cdot \frac{\delta(d_t\hat{\Omega}_j(\vec{y},t'))}{\delta \dot{u}(s)}. \tag{30}$$

Using the above lemma again with

$$\frac{\delta(d_t\Omega_j(\vec{y},t'))}{\delta \dot{u}(s)} = \frac{\partial(d_t\Omega_j(\vec{y},u))}{\partial \dot{u}} \delta(s-t')$$

and the result of Eq. (27) we may simplify Eq. (30). To sum up we get

$$\begin{aligned}\frac{\delta \mathcal{A}[\hat{\Omega}(\vec{x},t)]}{\delta u_j(s)} &= -\int_V d\vec{y} \left( \hat{\Omega}(\vec{y},s) \times \frac{\partial \hat{\Omega}(\vec{y},s)}{\partial u_j} \right) - \frac{1}{M} \frac{\partial F[\hat{\Omega}(\vec{x},s)]}{\partial u_j} \\ &\quad - \int_V d\vec{y}\, (\vec{v}_s \cdot \nabla) \left( \frac{\partial \Omega_k(\vec{y},s)}{\partial u_j} A_k[\hat{\Omega}(\vec{y},s)] \right), \\ \frac{\delta \mathcal{R}[\hat{\Omega}(\vec{x},t), d_t\hat{\Omega}(\vec{x},t)]}{\delta \dot{u}_j(t)} &= \alpha_G \int_V d\vec{x} \left[ \left( \frac{d}{dt} + \frac{\beta}{\alpha_G} (\vec{v}_s \cdot \nabla) \right) \hat{\Omega}(\vec{x},t) \right] \cdot \frac{\partial(d_t\hat{\Omega})}{\partial \dot{u}_j}.\end{aligned}$$

In the absence of the last term in $\delta \mathcal{A}[\hat{\Omega}(\vec{x},t)]/\delta u_j(s)$, this reproduces the equations of motion. Thus, it arises the question of the meaning of the third term.

## 9.2 Discussion of the Boundary Term

As one may derive the equations of motion directly from of Eq. (4), we claim that this is just an artefact of the choice of the action functional. At first glance, it seems

that the additional term is only a boundary term and will not influence the main part. However, if one first calculates the action functional and then, in a second step, takes the derivative with respect to the dynamical variables, this may produce some errors, as we will show in the following example.

Let us consider the simplest case of a helix with no applied magnetic field, $\vec{B} = 0$, and in the abscence of Gilbert damping, $\alpha_G = \beta = 0$, and without pinning terms. In this case, a helix in an arbitrary direction solves the Landau-Lifshitz-Gilbert equation, for example in the $z$-direction:

$$\hat{\Omega}(\vec{x}, t) = \cos\left[q(z + \varphi_z(t))\right] \hat{x} + \sin\left[q(z + \varphi_z(t))\right] \hat{y}, \tag{31}$$

where $\varphi_z = \vec{v}_{s_z} \cdot t$. For a normalized $q$-vector we have $q = 1$, but for clarity we write here $q$ instead of 1.

Let us now consider the representation of $\mathcal{A}^{(\nabla)}[\hat{\Omega}(\vec{x}, t)]$ in spherical coordinates. With $\hat{\Omega}(\vec{x}, t) = \hat{e}_r(\theta(\vec{x}, t), \phi(\vec{x}, t))$ we get

$$\begin{aligned}
\mathcal{A}^{(\nabla)}[\hat{\Omega}(\vec{x}, t)] &= \int dt \int_V d\vec{x}\, \vec{A}(\hat{\Omega}(\vec{x}, t)) \cdot (\vec{v}_s \cdot \nabla)\hat{\Omega}(\vec{x}, t) \\
&= \int dt \int_V d\vec{x}\, (1 - \cos(\theta))(\vec{v}_s \cdot \nabla)\, \phi \\
&=: \int dt\, E_{\mathrm{SST}}.
\end{aligned}$$

A comparison of Eq. (31) and $\hat{\Omega}(\vec{x}, t) = \hat{e}_r(\theta, \phi)$ yields

$$\begin{aligned}
&\cos(\theta) \stackrel{!}{=} 0 && \Rightarrow \quad \theta = \frac{\pi}{2} + n\pi, \quad n \in \mathbb{Z} \\
&\sin(\theta)\cos(\phi) \stackrel{!}{=} \cos(qz + \varphi_z(t)) && \Rightarrow \quad \phi = qz + \varphi_z(t) + 2\pi m, \quad m \in \mathbb{Z} \\
&&& \quad \wedge \quad \sin(\theta) = 1 \quad \Rightarrow \quad \theta = \frac{\pi}{2} + 2\pi n, \quad n \in \mathbb{Z} \\
&\sin(\theta)\sin(\phi) \stackrel{!}{=} \sin(qz + \varphi_z(t)) && \Rightarrow \quad \phi = qz + \varphi_z(t) + 2\pi m, \quad m \in \mathbb{Z} \\
&&& \quad \wedge \quad \sin(\theta) = 1 \quad \Rightarrow \quad \theta = \frac{\pi}{2} + 2\pi n, \quad n \in \mathbb{Z}
\end{aligned}$$

Thus,

$$\begin{aligned}
E_{\mathrm{STT}}[\hat{\Omega}] &= \int_V d\vec{x}\, \frac{\hbar}{e} \left(\vec{j} \cdot \nabla\right) (qz + \varphi_z(t)) \\
&= \int_V d\vec{x}\, \frac{\hbar}{e} j_z\, q = \int_V d\vec{x}\, \frac{\hbar}{e} \vec{j} \cdot \hat{q} \quad \text{with} \quad \hat{q} = (0, 0, 1)^T.
\end{aligned} \tag{32}$$

Therefore, one is tempted to believe that $E_{\mathrm{STT}}$ for a helix is given by

$$E_{\mathrm{STT}}[\hat{\Omega}] = \int_V d\vec{x} \frac{\hbar}{e} \vec{j} \cdot \vec{q}, \tag{33}$$

and that this term produces a contribution to the derivative of the action functional with respect to the $q$-vector.

However, we have not proven so far that the last step taken in Eq. (32) is correct for all helical directions, but at least we found one helical direction where $E_{\mathrm{STT}}$ is given by Eq. (33). In the following, we will argue that such a term is rather non-physical. To see this, let us consider the helix described above and perform a rotation of 180° around the $x$-axis. Under this rotation $\hat{q}, \hat{x}, \hat{y}$ change as

$$\hat{q} \to -\hat{q} \quad \wedge \quad \hat{x} \to \hat{x} \quad \wedge \quad \hat{y} \to -\hat{y}$$

and we get

$$\hat{\Omega}_{\mathrm{rotated}}(\vec{x}, t) = \cos\left[-q(z + \varphi_z(t))\right] \hat{x} + \sin\left[-q(z + \varphi_z(t))\right] (-\hat{y}) = \hat{\Omega}_(\vec{x}, t),$$

while the helix remains unaffected. Hence, every term which describes the physical properties of the helix should be invariant under this rotation. However the "energy" $E_{\mathrm{STT}}$ changes the sign under this rotation.

This simple and straightforward example shows that first calculating the action and then taking the derivative with respect to the variables may lead to errors in the equation of motion. The origin of these additional terms is somehow the choice of the action, viz. by taking the derivative with respect to $u_j$ we get the additional term

$$-\int_V d\vec{y}\, (\vec{v}_s \cdot \nabla) \left( \frac{\partial \Omega_k(\vec{y}, s)}{\partial u_j} A_k[\hat{\Omega}(\vec{y}, s)] \right)$$

which we first denoted a as boundary term. However, from this example we may infer that this term produces bulk contributions, too. To see this, one only has to choose for $u_j$ a component of the $q$ vector. Then $\partial \Omega_k(\vec{y}, s)/\partial q_j$ produces a term linear in $r_j$ on which the derivative can act.

Thus, the correct way of deriving the equations of motion is the way described in Sec. 5.3.

## Summary

In this thesis, we have investigated the influence of an electric current on the different magnetic phases of manganese silicide (MnSi). In the appropriate temperature and magnetic field ranges, MnSi develops helical or conical order. Moreover, it exhibits a topologically nontrivial phase, the so-called "A-phase", which is well described by a superposition of three helices and a uniform magnetic component. The existence of this phase is detected by neutron scattering and may be explained within the Ginzburg-Landau framework of the free energy.

To describe the dynamic evolution of the local magnetic moments of MnSi, we have focused on the Landau-Lifshitz-Gilbert equation. Using this equation as an ansatz for a general magnetic structure, we have obtained the equations of motion for a finite number of variables describing this structure.

By applying this method to the helical phase and the A-phase we have shown that a current leads to a drift of the magnetic configuration. While the magnetic texture is not altered by the current in the helical phase, it leads to a rotation and a tilting of the magnetic structure in the A-phase. Both modifications of the magnetic texture in the A-phase are linear in the strength of the current. To explain this rotation, we have considered Gaussian fluctuations around the minimum to stabilize the A-phase. Moreover, we have taken different anisotropy terms into account which distort the crystal lattice under the influence of a current.

Altogether, we have proposed a theory that is able to explain the current-induced distortion of the A-phase observed in neutron scattering experiments. Furthermore, by means of the topological Hall effect the A-phase has been identified as a lattice of anti-Skyrmions.

Apart from MnSi, there exists a large number of materials that share the same crystal structure B20 and similar physical properties like chiral itinerant magnetism with MnSi, e.g. CrSi, FeGe, FeSi and CoSi. Although FeSi is a semiconductor and CoSi is a diamagnetic semimetal, the doped material $Fe_xCo_{1-x}Si$ is a metal that possesses not only helical order (observed in the concentration range $0.2 < x < 0.95$), but also the A-phase which has been detected experimentally in $Fe_xCo_{1-x}Si$ for $x = 0.2$ and $x = 0.25$.

Finally, it seems that the A-phase of MnSi is not only a special feature which is unique to this compound, but that a lot of the displayed formalism is also applicable to other chiral magnetic materials as well.

# Appendix

## A Calculation of the Equations of Motion for the Helix

As shown in Sec. 6, a parametrization of the helix is given by

$$\hat{\Omega}(\vec{r},t) = \hat{\Omega}(\hat{q}(t), \vec{r}-\vec{\varphi}(t), m(t)) = \frac{1}{\sqrt{1+m^2}}\Big(\cos(\hat{q}\cdot(\vec{r}-\vec{\varphi}))\hat{n}_1 + \sin(\hat{q}\cdot(\vec{r}-\vec{\varphi}))\hat{n}_2 + m\hat{q}\Big)$$

with $q_x$, $q_y$, $m$ and $\vec{\varphi}$ as dynamical variables. Here, we want to calculate the equations of motion for the helix, i.e.

$$-\int_V d\vec{r}\left(\hat{\Omega}\times\frac{\partial\hat{\Omega}}{\partial u_j}\right)\cdot\left(\frac{d}{dt}+(\vec{v}_s\cdot\nabla)\right)\hat{\Omega} - \frac{1}{M}\frac{\partial F}{\partial u_j} = \int_V d\vec{r}\cdot\alpha_G\left(\frac{d}{dt}+\frac{\beta}{\alpha_G}(\vec{v}_s\cdot\nabla)\right)\hat{\Omega}\cdot\frac{\partial\hat{\Omega}}{\partial u_j}$$

with $u_1 = m$, $u_2 = \vec{\varphi}$, $u_3 = q_x$ and $u_4 = q_y$. The explicit choice of the $q$-vector, of the perpendicular vectors $\hat{n}_1$ and $\hat{n}_2$ and their derivatives are shown on the next page. Furthermore, we introduce the following abbrevations:

$$\begin{aligned}
B_{u_j} &:= \int_V d\vec{r}\left(\hat{\Omega}\times\frac{\partial\hat{\Omega}}{\partial u_j}\right)\cdot\left(\frac{d}{dt}+(\vec{v}_s\cdot\nabla)\right)\hat{\Omega},\\
D_{u_j} &:= \int_V d\vec{r}\cdot\alpha_G\left(\frac{d}{dt}+\frac{\beta}{\alpha_G}(\vec{v}_s\cdot\nabla)\right)\hat{\Omega}\cdot\frac{\partial\hat{\Omega}}{\partial u_j},\\
\epsilon &:= \hat{q}\cdot(\vec{r}-\vec{\varphi}) = q_x(r_x-\varphi_x) + q_y(r_y-\varphi_y) + \sqrt{1-q_x^2-q_y^2}\,(r_z-\varphi_z).
\end{aligned}$$

The motivation for $B$ and $D$ are taken from Sec. 9, where "$B$" denotes the Berry phase term and "$D$" the dissipation term.

Substitutuing the ansatz into $B$ and $D$ for different $u_j$, one obtains terms, amongst others, that are linear in $x, y$ or $z$. These occur by taking a derivative with respect to $q_x$ or $q_y$. Moreover, one gets terms that contains a remaining $\cos(\epsilon)$ or $\sin(\epsilon)$. Assuming a large volume $V$ centered in the origin, such terms cancel for a soft boundary. This can be seen from the following examples:

$$\begin{aligned}
&\int_{-\infty}^{\infty} dx\,(c+ax)\cdot e^{-(x/L)^2} = cL\sqrt{\pi}\\
&\int_{-\infty}^{\infty} dx\,\cos(kx+p)\cdot(c+ax)\cdot e^{-(x/L)^2}\\
&\quad = -\frac{1}{2}e^{-1/4\,k^2L^2}\cdot\left[L\sqrt{\pi}\left(-2c\cos(p)+akL^2\sin(p)\right)\right] \underset{L\to\infty}{\longrightarrow} 0\\
&\int_{-\infty}^{\infty} dx\,\cos^2(kx+p)\cdot(c+ax)\cdot e^{-(x/L)^2}\\
&\quad = \frac{1}{2}\sqrt{\pi}c\,L + \frac{1}{4}\sqrt{\pi}\,e^{-k^2L^2-2ip}\,L\left(c(1+e^{4ip}) + i\,akL^2(-1+e^{4ip})\right) \underset{L\to\infty}{\longrightarrow} \frac{1}{2}\sqrt{\pi}cL.
\end{aligned}$$

In the representation of $D_{q_x}$ and $D_{q_y}$ there exist terms that are quadratic in the components of $\vec{r}$. In these terms, the integrals over cosine and sine are effectively averaged to 1/2. Moreover, we profit from $\hat{q}$, $\hat{n}_1$ and $\hat{n}_2$ being unit vectors as, for example, $|q| = 1$ implies

$$0 = \frac{d}{dt}(\hat{q} \cdot \hat{q}) = 2\hat{q} \cdot \dot{\hat{q}} \quad \Rightarrow \quad \hat{q} \cdot \dot{\hat{q}} = 0.$$

Using these simplifications we obtain the following relations for $B_{u_j}$ and $D_{u_j}$ (see the next page).

Here, $C_1$ and $C_2$ are defined by

$$C_1(m, \vec{\varphi}, q_x, q_y) = \frac{-(1-q_y^2)^2 + 2m^2(-1+q_x^2)(1-q_y^2)^2 - q_x^2(-1+2q_y^2+q_y^4)}{2(1-q_y^2)^2(-1+q_x^2+q_y^2)},$$

$$C_2(m, \vec{\varphi}, q_x, q_y) = -\frac{q_x q_y^2}{\sqrt{1-q_x^2-q_y^2}(1-q_y^2)} \cdot \left(\varphi_x - \frac{q_x \varphi_z}{\sqrt{1-q_x^2-q_y^2}}\right) + \frac{q_x q_y (1+q_y^2+2m^2(1-q_y^2))}{2(1-q_y^2)(1-q_x^2-q_y^2)}.$$

$$B_m = \int_V d\vec{r} \left(\frac{1}{1+m^2}\right)^{3/2} \cdot \left\{ \left( \hat{q} \cdot (\dot{\vec{\varphi}} - \vec{v}_s) \right) - \dot{q}_x \left( \frac{-\sqrt{1-q_y^2}\,(\hat{n}_1 \cdot \vec{\varphi}) + q_y}{\sqrt{1-q_x^2-q_y^2}} \right) + \dot{q}_y \left( \varphi_y - \frac{q_y \varphi_z}{\sqrt{1-q_x^2-q_y^2}} - \frac{q_x q_y^2}{\sqrt{1-q_x^2-q_y^2}(1-q_y^2)} \right) \right\},$$

$$B_{\vec{\varphi}} = -\int_V d\vec{r} \left(\frac{1}{1+m^2}\right)^{3/2} \dot{m} \cdot \hat{q},$$

$$B_{q_x} = -\int_V d\vec{r} \left\{ \left(\frac{1}{1+m^2}\right)^{3/2} \dot{m} \cdot \left( \varphi_x - \frac{q_x \cdot \varphi_z}{\sqrt{1-q_x^2-q_y^2}} - \frac{q_y}{\sqrt{1-q_x^2-q_y^2}} \right) - \frac{m}{\sqrt{1+m^2}} \cdot \frac{\dot{q}_y}{\sqrt{1-q_x^2-q_y^2}} \right\},$$

$$B_{q_y} = -\int_V d\vec{r} \left\{ \left(\frac{1}{1+m^2}\right)^{3/2} \dot{m} \cdot \left( \varphi_y - \frac{q_y \cdot \varphi_z}{\sqrt{1-q_x^2-q_y^2}} - \frac{q_x q_y^2}{\sqrt{1-q_x^2-q_y^2}(1-q_y^2)} \right) + \frac{m}{\sqrt{1+m^2}} \cdot \frac{\dot{q}_x}{\sqrt{1-q_x^2-q_y^2}} \right\},$$

$$D_m = \int_V d\vec{r}\, \alpha_G \frac{\dot{m}}{(1+m^2)^2},$$

$$D_{\vec{\varphi}} = \int_V d\vec{r} \left\{ -\frac{\alpha_G}{1+m^2} \hat{q} \left( -\dot{\hat{q}} \cdot \vec{\varphi} - \hat{q} \cdot \dot{\vec{\varphi}} + \frac{\beta}{\alpha} \vec{v}_s \cdot \hat{q} + \frac{q_y}{\sqrt{1-q_x^2+q_y^2}} \dot{q}_x - \frac{q_x q_y^2}{\sqrt{1-q_x^2+q_y^2}(1-q_y^2)} \dot{q}_y \right) \right\},$$

$$\begin{aligned} D_{q_x} = \int_V d\vec{r} \frac{\alpha_G}{1+m^2} \Bigg\{ & \dot{q}_x r_x^2 + \frac{q_x \cdot (q_x \dot{q}_x + q_y \dot{q}_y)}{1-q_x^2-q_y^2} r_z^2 + \dot{q}_y r_x r_y - \frac{(2q_x \dot{q}_x + q_y \dot{q}_y) r_x r_z}{\sqrt{1-q_x^2-q_y^2}} - \frac{q_x \dot{q}_y r_y r_z}{\sqrt{1-q_x^2-q_y^2}} \\ & + \left[ \dot{\hat{q}} \cdot \vec{\varphi} + \left( \dot{\vec{\varphi}} - \frac{\beta}{\alpha} \vec{v}_s \right) \cdot \hat{q} - \frac{q_y}{\sqrt{1-q_x^2-q_y^2}} \cdot \left( \frac{q_x q_y}{1-q_y^2}\, \dot{q}_y + \dot{q}_x \right) \right] \cdot \left( \varphi_x - \frac{q_x \cdot \varphi_z}{\sqrt{1-q_x^2-q_y^2}} \right) \Bigg\}, \end{aligned}$$

$$\begin{aligned} D_{q_y} = \int_V d\vec{r} \frac{\alpha_G}{1+m^2} \Bigg\{ & \dot{q}_y r_y^2 + \frac{q_y (q_x \dot{q}_x + q_y \dot{q}_y)}{1-q_x^2-q_y^2} r_z^2 + \dot{q}_x r_x r_y - \frac{\dot{q}_x q_y r_x r_z}{\sqrt{1-q_x^2-q_y^2}} - \frac{q_x \dot{q}_x + 2 q_y \dot{q}_y}{\sqrt{1-q_x^2-q_y^2}} r_y r_z - \frac{q_x q_y^2}{\sqrt{1-q_x^2-q_y^2}(1-q_y)} \left( \dot{\vec{\varphi}} - \frac{\beta}{\alpha} \vec{v}_s \right) \cdot \hat{q} \\ & + \left[ \dot{\hat{q}} \cdot \vec{\varphi} + \left( \dot{\vec{\varphi}} - \frac{\beta}{\alpha} \vec{v}_s \right) \cdot \hat{q} - \frac{q_y}{\sqrt{1-q_x^2-q_y^2}} \cdot \left( \frac{2 q_x q_y}{1-q_y^2} \dot{q}_y + \dot{q}_x \right) \right] \cdot \left( \varphi_y - \varphi_z \frac{q_y}{\sqrt{1-q_x^2-q_y^2}} \right) + C_1(m, \vec{\varphi}, q_x, q_y) \dot{q}_y + C_2(m, \vec{\varphi}, q_x, q_y) \dot{q}_x \Bigg\}. \end{aligned}$$

For the free energy functional up to quadratic order we get in units in which $|\vec{q}| = q = 1$, i.e. $J = D$

$$F_2[\vec{M}] = \int_V d\vec{r}\, M^2 \left( r_0 - J \frac{1}{1+m^2} \right)$$

with the following derivatives:

$$\frac{\partial F_2}{\partial \vec{\varphi}} = 0, \quad \frac{\partial F_2}{\partial q_x} = \frac{\partial F_2}{\partial q_y} = 0 \quad \text{and}$$
$$\frac{\partial F_2}{\partial m} = \int_V d\vec{r}\, M^2 J \frac{2m}{(1+m^2)^2}.$$

This leads to the following four equations of motion:

$$-B_m - \frac{\partial F}{\partial m} = D_m, \tag{34a}$$
$$-B_{\vec{\varphi}} - \frac{\partial F}{\partial \vec{\varphi}} = D_{\vec{\varphi}}, \tag{34b}$$
$$-B_{q_x} - \frac{\partial F}{\partial q_x} = D_{q_x}, \tag{34c}$$
$$-B_{q_y} - \frac{\partial F}{\partial q_y} = D_{q_y}. \tag{34d}$$

These are four linear, coupled differential equations of first order in time. However, they are too complicated to solve them analytically.

To estimate if the current influences the direction vector of the helix, it suffices to consider the "static" case, where the $q$-vector and the uniform magnetic component are constant in time, i.e. $\dot{q}_x = \dot{q}_y = \dot{m} = 0$. The above complicated terms reduce to:

$$B_m = \int_V d\vec{r} \left( \frac{1}{1+m^2} \right)^{3/2} \cdot \left( \hat{q} \cdot (\dot{\vec{\varphi}} - \vec{v}_s) \right),$$
$$B_{\vec{\varphi}} = 0, \quad B_{q_x} = 0, \quad B_{q_y} = 0,$$

and

$$D_m = 0,$$
$$D_{\vec{\varphi}} = -\int_V d\vec{r}\, \frac{\alpha_G}{1+m^2}\, \hat{q} \cdot \left[ \hat{q} \cdot \left( \frac{\beta}{\alpha} \vec{v}_s - \dot{\vec{\varphi}} \right) \right],$$
$$D_{q_x} = \int_V d\vec{r}\, \frac{\alpha_G}{1+m^2} \left[ \left( \dot{\vec{\varphi}} - \frac{\beta}{\alpha} \vec{v}_s \right) \cdot \hat{q} \right] \cdot \left( \varphi_x - \frac{q_x \cdot \varphi_z}{\sqrt{1 - q_x^2 - q_y^2}} \right),$$
$$D_{q_y} = \int_V d\vec{r}\, \frac{\alpha_G}{1+m^2} \left[ \left( \dot{\vec{\varphi}} - \frac{\beta}{\alpha} \vec{v}_s \right) \cdot \hat{q} \right] \cdot \left( \varphi_y - \frac{\varphi_z q_y}{\sqrt{1 - q_x^2 - q_y^2}} - \frac{q_x q_y^2}{\sqrt{1 - q_x^2 - q_y^2}(1 - q_y)} \right).$$

Obviously, the Berry phase terms $B_{q_x}$ and $B_{q_y}$ vanish and therefore do not contribute to the corresponding equation of motion. Finally, these are given by

$$\int_V d\vec{r} \left( \frac{1}{1+m^2} \right)^{3/2} \cdot \left( -\frac{m}{\sqrt{1+m^2}} \cdot 2JM + \hat{q} \cdot (\vec{v}_s - \dot{\vec{\varphi}}) \right) = 0 \tag{35a}$$

and

$$0 = -\int_V d\vec{r}\,\frac{\alpha_G}{1+m^2}\,\hat{q}\cdot\left[\hat{q}\cdot\left(\frac{\beta}{\alpha}\vec{v}_s - \dot{\vec{\varphi}}\right)\right], \tag{35b}$$

$$0 = \int_V d\vec{r}\,\frac{\alpha_G}{1+m^2}\left[\left(\dot{\vec{\varphi}} - \frac{\beta}{\alpha}\vec{v}_s\right)\cdot\hat{q}\right]\cdot\left(\varphi_x - \frac{q_x\cdot\varphi_z}{\sqrt{1-q_x^2-q_y^2}}\right), \tag{35c}$$

$$0 = \int_V d\vec{r}\,\frac{\alpha_G}{1+m^2}\left[\left(\dot{\vec{\varphi}} - \frac{\beta}{\alpha}\vec{v}_s\right)\cdot\hat{q}\right]\cdot\left(\varphi_y - \frac{\varphi_z q_y}{\sqrt{1-q_x^2-q_y^2}} - \frac{q_x q_y^2}{\sqrt{1-q_x^2-q_y^2}(1-q_y)}\right). \tag{35d}$$

leading to Eqs. (11a) – (11d) in Sec. 6.3 of the main text.

# B Derivation of the Vector Potential

A possible parametrization of the vector potential $\vec{A}$ is given by (see e.g. [50])

$$\vec{A}(r,\theta,\phi) = \frac{1-\cos\theta}{r\sin\theta}\hat{e}_\phi \quad \text{with} \quad \hat{e}_\phi = (-\sin\phi, \cos\phi, 0)^T.$$

To substantiate this, we have to consider the vector potential $\vec{A}$ corresponding to $\hat{\Omega}$. It is implicitly defined by the relation

$$\nabla_{\hat{\Omega}} \times \vec{A} = \hat{\Omega}, \tag{36}$$

where $\nabla_{\hat{\Omega}} = \left(\frac{\partial}{\partial\Omega_x}, \frac{\partial}{\partial\Omega_y}, \frac{\partial}{\partial\Omega_z}\right)^T$. Such a vector potential cannot be defined in $\mathbb{R}^3$ without singularities. This can be seen by integrating Eq. (36) over the surface $\partial V$ of a volume $V$ yielding:

$$4\pi = \int_{\partial V} \hat{\Omega}\, d\vec{\sigma} = \int_{\partial V} \nabla_{\hat{\Omega}} \times \vec{A}\, d\vec{\sigma} = \int_V \operatorname{div} \nabla_{\hat{\Omega}} \times \vec{A}\, d\vec{x}.$$

If $\vec{A}$ does not have singularities, then $\operatorname{div}(\operatorname{rot}\vec{A})$ is zero. A technical problem to use Eq. (36) is that $\hat{\Omega}$ is normalized. To calculate the derivative properly, one has to implement this condition into the derivative. A simpler way is to use the more general equation for a magnetic monopole which is not normalized:

$$\nabla \times \vec{A} = \frac{1}{r^2}\hat{e}_r,$$

and then to apply the result for the normalized case. In spherical coordinates, this gives

$$\begin{aligned}\nabla_{\hat{\Omega}} \times \vec{A} = &\left[\frac{1}{r\sin\theta}\left(\frac{\partial}{\partial\theta}(A_\theta \sin\theta) - \frac{\partial A_\theta}{\partial\phi}\right)\right]\hat{e}_r \\ &+ \left[\frac{1}{r\sin\theta}\frac{\partial A_r}{\partial\phi} - \frac{1}{r}\frac{\partial}{\partial r}(rA_\phi)\right]\hat{e}_\theta + \left[\frac{1}{r}\left(\frac{\partial}{\partial r}(rA_\theta) - \frac{\partial A_r}{\partial\theta}\right)\right]\hat{e}_\phi.\end{aligned}$$

Thus, we have three partial differential equations for the variables $r$, $\theta$ and $\phi$:

$$\frac{1}{r^2} = \frac{1}{r\sin\theta}\left(\frac{\partial}{\partial\theta}(A_\theta\sin\theta) - \frac{\partial A_\theta}{\partial\phi}\right), \tag{37a}$$

$$0 = \frac{1}{r\sin\theta}\frac{\partial A_r}{\partial\phi} - \frac{1}{r}\frac{\partial}{\partial r}(rA_\phi), \tag{37b}$$

$$0 = \frac{1}{r}\left(\frac{\partial}{\partial r}(rA_\theta) - \frac{\partial A_r}{\partial\theta}\right). \tag{37c}$$

Because of the gauge freedom of electrodynamics we may require $\vec{A} \perp \hat{e}_r$ such that $A_r$ is zero. From Eqs. (37b) and (37c) it follows that $\partial A_\phi/\partial r = -1/r\, A_\phi$ and that $\partial A_\theta/\partial r = -1/r\, A_\theta$. These equations are solved by $A_\phi, A_\theta \propto 1/r$ or 0, but $A_\phi$ and $A_\theta$ are still coupled via Eq. (37a). In the case, where $A_\theta = 0$, then $A_\phi$ has to fulfill

$$\begin{aligned}\frac{1}{r}\sin\theta &= \frac{\partial}{\partial\theta}(A_\phi\sin\theta), \\ \frac{\partial}{\partial\theta}A_\phi &= \frac{1}{r} - A_\theta\frac{\cos\theta}{\sin\theta}.\end{aligned}$$

The solution to this inhomogeneous differential equation reads

$$\vec{A} = \frac{C - \cos\theta}{r \sin\theta}\, \hat{e}_\phi,$$

where $C$ is an integration constant that corresponds to the choice of the particular gauge. For $C = 1$ and $r = |\hat{\Omega}|$ we finally obtain above formula.

# C Explicit Calculation of $\delta\mathcal{A}[\hat{\Omega}(\vec{x},t)]/\delta\Omega_j(\vec{y},t')$

The action functional $\mathcal{A}[\hat{\Omega}]$ separates into three terms $\mathcal{A}^{(t)}[\hat{\Omega}]$, $\mathcal{A}^{(\nabla)}[\hat{\Omega}]$ and $\mathcal{A}^{(F)}[\hat{\Omega}]$ as defined in Eq. (24). To calculate the variation $\delta\mathcal{A}[\hat{\Omega}(\vec{x},t)]/\delta\Omega_j(\vec{y},t')$, we will calculate the terms explicitly.

Let us start by considering $\mathcal{A}^{(t)}[\hat{\Omega}(\vec{x},t)]$. Its variational derivative is by definition given by

$$\frac{\delta\mathcal{A}^{(t)}[\hat{\Omega}(\vec{x},t)]}{\delta\Omega_j(\vec{y},t')} = \lim_{\epsilon\to 0}\frac{1}{\epsilon}\left(\mathcal{A}^{(t)}[\hat{\Omega}(\vec{x},t)+\epsilon\,\hat{e}_j\delta(\vec{x}-\vec{y},t-t')] - \mathcal{A}^{(t)}[\hat{\Omega}(\vec{x},t)]\right)$$

with a variation in the direction of $\hat{e}_j$. To ensure that $\hat{\Omega}(\vec{x},t)+\epsilon\,\hat{e}_j\delta(\vec{x}-\vec{y},t-t')$ is to linear order in $\epsilon$ normalized, one has to choose $\hat{e}_j \perp \hat{\Omega}$. We thus get:

$$\begin{aligned}
&\frac{\delta\mathcal{A}^{(t)}[\hat{\Omega}(\vec{x},t)]}{\delta\hat{\Omega}_j(\vec{y},t')}\\
&= \lim_{\epsilon\to 0}\frac{1}{\epsilon}\left[\int_V d\vec{x}\int dt\left(\frac{d}{dt}\left(\hat{\Omega}(\vec{x},t)+\epsilon\,\hat{e}_j\delta(\vec{x}-\vec{y},t-t')\right)_k\right.\right.\\
&\qquad\left.\left.\cdot A_k\left[\hat{\Omega}(\vec{x},t)+\epsilon\,\hat{e}_j\delta(\vec{x}-\vec{y},t-t')\right] - \frac{d\Omega_k(\vec{x},t)}{dt}\cdot A_k[\hat{\Omega}(\vec{x},t)]\right)\right]\\
&= \lim_{\epsilon\to 0}\frac{1}{\epsilon}\left[\int_V d\vec{x}\int dt\left(\frac{d\Omega_k(\vec{x},t)}{dt}\left(A_k\left[\hat{\Omega}(\vec{x},t)+\epsilon\,\hat{e}_j\delta(\vec{x}-\vec{y},t-t')\right] - A_k[\hat{\Omega}(\vec{x},t)]\right)\right.\right.\\
&\qquad\left.\left.+\epsilon\,\delta_{jk}\frac{d\delta(\vec{x}-\vec{y},t-t')}{dt}A_k\left[\hat{\Omega}(\vec{x},t)+\epsilon\,\hat{e}_j\delta(\vec{x}-\vec{y},t-t')\right]\right)\right]\\
&= \int_V d\vec{x}\int dt\,\frac{d\Omega_k(\vec{x},t)}{dt}\lim_{\epsilon\to 0}\frac{1}{\epsilon}\left(A_k\left[\hat{\Omega}(\vec{x},t)+\epsilon\,\hat{e}_j\delta(\vec{x}-\vec{y},t-t')\right] - A_k[\hat{\Omega}(\vec{x},t)]\right)\\
&\qquad+\lim_{\epsilon\to 0}\int_V d\vec{x}\int dt\left(\frac{d\delta(\vec{x}-\vec{y},t-t')}{dt}A_j\left[\hat{\Omega}(\vec{x},t)+\epsilon\,\hat{e}_j\delta(\vec{x}-\vec{y},t-t')\right]\right)\\
&= \int_V d\vec{x}\int dt\,\frac{d\Omega_k(\vec{x},t)}{dt}\delta(\vec{x}-\vec{y},t-t')\cdot\frac{\partial A_k[\hat{\Omega}(\vec{x},t)]}{\partial\Omega_j} + \frac{d\delta(\vec{x}-\vec{y},t-t')}{dt}A_j[\hat{\Omega}(\vec{x},t)]\\
&\overset{\text{p.i.}}{=}\left(\frac{d\Omega_k(\vec{x},t)}{dt}\cdot\frac{\partial A_k[\hat{\Omega}(\vec{x},t)]}{\partial\Omega_j}\bigg|_{\vec{x}=\vec{y},t=t'} - \int_V d\vec{x}\int dt\delta(\vec{x}-\vec{y},t-t')\frac{dA_j[\hat{\Omega}(\vec{x},t)]}{dt}\right)\\
&\qquad+\Big(A_j[\hat{\Omega}(\vec{y},t_2)]\delta(t_2-t') - A_j[\hat{\Omega}(\vec{y},t_1)]\delta(t_1-t')\Big)\\
&=: \mathrm{MT}_j^{(t)} + \mathrm{BT}_j^{(t)}.
\end{aligned}$$

Here, $t_1$ and $t_2$ are the limits of the time integral. The abbrevation p.i. denotes partial integration, "MT" denotes the main term, while "BT" denotes the boundary term. $\mathrm{BT}_j^{(t)}$ is zero because of the usual Lagrange formalism. We only allow for variations which leave the initial and final time configurations fixed. The main term

$\mathrm{MT}_j^{(t)}$ can be simplified further as follows:

$$\begin{aligned}
\mathrm{MT}_j^{(t)} &= \frac{d\Omega_k(\vec{x},t)}{dt}\cdot\frac{\partial A_k[\hat{\Omega}(\vec{x},t)]}{\partial\Omega_j}\bigg|_{\vec{x}=\vec{y},t=t'} - \int_V d\vec{x}\int dt\,\delta(\vec{x}-\vec{y},t-t')\frac{dA_j[\hat{\Omega}(\vec{x},t)]}{dt} \\
&= \left(\frac{d\Omega_k(\vec{x},t)}{dt}\cdot\frac{\partial A_k[\hat{\Omega}(\vec{x},t)]}{\partial\Omega_j} - \frac{dA_j[\hat{\Omega}(\vec{x},t)]}{dt}\right)\bigg|_{\vec{x}=\vec{y},t=t'} \\
&= \frac{d\Omega_k(\vec{x},t)}{dt}\cdot\left(\frac{\partial A_k[\hat{\Omega}(\vec{x},t)]}{\partial\Omega_j} - \frac{\partial A_j[\hat{\Omega}(\vec{x},t)]}{\partial\Omega_k}\right)\bigg|_{\vec{x}=\vec{y},t=t'} \\
&= \frac{d\Omega_k(\vec{x},t)}{dt}\cdot(\delta_{ja}\delta_{kb}-\delta_{jb}\delta_{ka})\frac{\partial A_b[\hat{\Omega}(\vec{x},t)]}{\partial\hat{\Omega}_a}\bigg|_{\vec{x}=\vec{y},t=t'} \\
&=: \frac{d\Omega_k(\vec{x},t)}{dt}\epsilon_{jkm}\epsilon_{mab}\frac{\partial A_b[\hat{\Omega}(\vec{x},t)]}{\partial\hat{\Omega}_a}\bigg|_{\vec{x}=\vec{y},t=t'} \\
&= \frac{d\Omega_k(\vec{x},t)}{dt}\epsilon_{jkm}\left(\nabla_{\hat{\Omega}}\times\vec{A}[\hat{\Omega}(\vec{x},t)]\right)_m\bigg|_{\vec{x}=\vec{y},t=t'} \\
&= \epsilon_{jkm}\frac{d\Omega_k(\vec{x},t)}{dt}\Omega(\vec{x},t)_m\bigg|_{\vec{x}=\vec{y},t=t'} \\
&= \left(\frac{d\hat{\Omega}(\vec{y},t')}{dt'}\times\hat{\Omega}(\vec{y},t')\right)_j,
\end{aligned}$$

where $\nabla_{\hat{\Omega}} := \left(\frac{\partial}{\partial\hat{\Omega}_x},\frac{\partial}{\partial\hat{\Omega}_y},\frac{\partial}{\partial\hat{\Omega}_z}\right)^T$, and we have used the relation $\nabla_{\hat{\Omega}}\times\vec{A}=\hat{\Omega}$. Finally,

$$\frac{\delta\mathcal{A}^{(t)}[\hat{\Omega}(\vec{x},t)]}{\delta\hat{\Omega}_j(\vec{y},t')} = \left(\frac{d\hat{\Omega}(\vec{y},t')}{dt'}\times\hat{\Omega}(\vec{y},t')\right)_j.$$

Now let us focus on $\mathcal{A}^{(\nabla)}[\hat{\Omega}(\vec{x},t)]$. By definition we obtain:

$$\frac{\delta\mathcal{A}^{(\nabla)}[\hat{\Omega}(\vec{x},t)]}{\delta\hat{\Omega}_j(\vec{y},t')} = \lim_{\epsilon\to0}\frac{1}{\epsilon}\left(\mathcal{A}^{(\nabla)}[\hat{\Omega}(\vec{x},t)+\epsilon\,\hat{e}_j\delta(\vec{x}-\vec{y},t-t')] - \mathcal{A}^{(\nabla)}[\hat{\Omega}(\vec{x},t)]\right)$$

with $\hat{e}_j\perp\hat{\Omega}$ as in the case of $\mathcal{A}^{(t)}$. From this follows:

$$\begin{aligned}
&\frac{\delta\mathcal{A}^{(\nabla)}[\hat{\Omega}(\vec{x},t)]}{\delta\hat{\Omega}_j(\vec{y},t')} \\
&= \lim_{\epsilon\to0}\frac{1}{\epsilon}\left[\int_V d\vec{x}\int dt\left((\vec{v}_s\cdot\nabla)\left(\hat{\Omega}(\vec{x},t)+\epsilon\,\hat{e}_j\delta(\vec{x}-\vec{y},t-t')\right)\right.\right. \\
&\qquad\left.\left.\cdot A_k[\hat{\Omega}(\vec{x},t)+\epsilon\,\hat{e}_j\delta(\vec{x}-\vec{y},t-t')] - (\vec{v}_s\cdot\nabla)\Omega_k(\vec{x},t)\cdot A_k[\hat{\Omega}(\vec{x},t)]\right)\right] \\
&= \lim_{\epsilon\to0}\frac{1}{\epsilon}\left[\int_V d\vec{x}\int dt\left((\vec{v}_s\cdot\nabla)\Omega_k(\vec{x},t)\left(A_k[\hat{\Omega}(\vec{x},t)+\epsilon\,\hat{e}_j\delta(\vec{x}-\vec{y},t-t')] - A_k[\hat{\Omega}(\vec{x},t)]\right)\right.\right. \\
&\qquad\left.\left.+\epsilon\,\delta_{jk}(\vec{v}_s\cdot\nabla)\delta(\vec{x}-\vec{y},t-t')A_k[\hat{\Omega}(\vec{x},t)+\epsilon\,\hat{e}_j\delta(\vec{x}-\vec{y},t-t')]\right)\right] \\
&= \int_V d\vec{x}\int dt\,(\vec{v}_s\cdot\nabla)\Omega_k(\vec{x},t)\lim_{\epsilon\to0}\frac{1}{\epsilon}\left(A_k[\hat{\Omega}(\vec{x},t)+\epsilon\,\hat{e}_j\delta(\vec{x}-\vec{y},t-t')] - A_k[\hat{\Omega}(\vec{x},t)]\right) \\
&\qquad + \lim_{\epsilon\to0}\int_V d\vec{x}\int dt\left((\vec{v}_s\cdot\nabla)\delta(\vec{x}-\vec{y},t-t')A_j[\hat{\Omega}(\vec{x},t)+\epsilon\,\hat{e}_j\delta(\vec{x}-\vec{y},t-t')]\right)
\end{aligned}$$

$$
\begin{aligned}
&= \int_V d\vec{x} \int dt\, (\vec{v}_s \cdot \nabla)\Omega_k(\vec{x},t)\delta(\vec{x}-\vec{y},t-t') \cdot \frac{\partial A_k[\hat{\Omega}(\vec{x},t)]}{\partial \Omega_j} \\
&\qquad + \int_V d\vec{x} \int dt\, (\vec{v}_s \cdot \nabla)\delta(\vec{x}-\vec{y},t-t') A_j[\hat{\Omega}(\vec{x},t)] \\
&\overset{\text{p.i.}}{=} \left[ (\vec{v}_s \cdot \nabla)\Omega_k(\vec{x},t) \cdot \frac{\partial A_k[\hat{\Omega}(\vec{x},t)]}{\partial \Omega_j}\bigg|_{\vec{x}=\vec{y},t=t'} \right. \\
&\qquad \left. - \int_V d\vec{x} \int dt\, \delta(\vec{x}-\vec{y},t-t')(\vec{v}_s \cdot \nabla) A_j[\hat{\Omega}(\vec{x},t)] \right] \\
&\qquad + \int dt \int_{S(V)} d\sigma^{(x)}\, \delta(\vec{x}-\vec{y},t-t') A_j[\hat{\Omega}(\vec{x},t)](\vec{v}_s \cdot \vec{\nu}) \\
&=: \mathrm{MT}_j^{(\nabla)} + \mathrm{BT}_j^{(\nabla)}.
\end{aligned}
$$

Here, $d\sigma^{(x)}$ is the area element, and $\vec{\nu}$ is the outer normal unit vector on the surface $S(V)$ of the volume $V$, i.e. $d\vec{\sigma}^{(x)} = \vec{\nu} d\sigma^{(x)}$. Note that the superscript $x$ implies the integration over $\vec{x}$, but not $\vec{y}$.

Similar to the calculation for $\mathcal{A}^{(t)}$ we get:

$$
\begin{aligned}
\mathrm{MT}_j^{(\nabla)} &= [(\vec{v}_s \cdot \nabla)\Omega_k(\vec{x},t)] \cdot \frac{\partial A_k[\hat{\Omega}(\vec{x},t)]}{\partial \Omega_j}\bigg|_{\vec{x}=\vec{y},t=t'} \\
&\qquad - \int_V d\vec{x} \int dt\, \delta(\vec{x}-\vec{y},t-t')(\vec{v}_s\ cdot\nabla) A_j[\hat{\Omega}(\vec{x},t)] \\
&= \left( [(\vec{v}_s \cdot \nabla)\Omega_k(\vec{x},t)] \cdot \frac{\partial A_k[\hat{\Omega}(\vec{x},t)]}{\partial \Omega_j} - (\vec{v}_s \cdot \nabla) A_j[\hat{\Omega}(\vec{x},t)] \right)\bigg|_{\vec{x}=\vec{y},t=t'} \\
&= [(\vec{v}_s \cdot \nabla)\Omega_k(\vec{x},t)] \cdot \left( \frac{\partial A_k[\hat{\Omega}(\vec{x},t)]}{\partial \Omega_j} - \frac{\partial A_j[\hat{\Omega}(\vec{x},t)]}{\partial \Omega_k} \right)\bigg|_{\vec{x}=\vec{y},t=t'} \\
&= [(\vec{v}_s \cdot \nabla)\Omega_k(\vec{x},t)] \cdot (\delta_{ja}\delta_{kb} - \delta_{jb}\delta_{ka}) \frac{\partial A_b[\hat{\Omega}(\vec{x},t)]}{\partial \hat{\Omega}_a}\bigg|_{\vec{x}=\vec{y},t=t'} \\
&= [(\vec{v}_s \cdot \nabla)\Omega_k(\vec{x},t)] \cdot \epsilon_{jkm}\epsilon_{mab} \frac{\partial A_b[\hat{\Omega}(\vec{x},t)]}{\partial \hat{\Omega}_a}\bigg|_{\vec{x}=\vec{y},t=t'} \\
&= [(\vec{v}_s \cdot \nabla)\Omega_k(\vec{x},t)] \cdot \epsilon_{jkm} \left( \nabla_{\hat{\Omega}} \times \vec{A}[\hat{\Omega}(\vec{x},t)] \right)_m \Big|_{\vec{x}=\vec{y},t=t'} \\
&= \epsilon_{jkm} \left[ (\vec{v}_s \cdot \nabla)\Omega_k(\vec{x},t) \right] \Omega(\vec{x},t)_m \Big|_{\vec{x}=\vec{y},t=t'} \\
&= \left( \left[ (\vec{v}_s \cdot \nabla)\hat{\Omega}(\vec{y},t') \right] \times \hat{\Omega}(\vec{y},t') \right)_j .
\end{aligned}
$$

In the boundary term, we can perform the time integration, and we are left with

$$
\begin{aligned}
\mathrm{BT}_j^{(\nabla)} &= \int dt \int_{S(V)} d\sigma^{(x)}\, \delta(\vec{x}-\vec{y},t-t') A_j[\hat{\Omega}(\vec{x},t)](\vec{v}_s \cdot \vec{\nu}) \\
&= \int_{S(V)} d\sigma^{(x)}\, \delta(\vec{x}-\vec{y}) A_j[\hat{\Omega}(\vec{x},t')](\vec{v}_s \cdot \vec{\nu}).
\end{aligned}
$$

Finally we get:

$$\frac{\delta\mathcal{A}^{(\nabla)}[\hat{\Omega}(\vec{x},t)]}{\delta\Omega_j(\vec{y},t')} = \Big(\Big[(\vec{v}_s\cdot\nabla)\hat{\Omega}(\vec{y},t')\Big]\times\hat{\Omega}(\vec{y},t')\Big)_j + \int_{S(V)} d\sigma^{(x)}\,\delta(\vec{x}-\vec{y})A_j[\hat{\Omega}(\vec{x},t')](\vec{v}_s\cdot\vec{\nu}). \quad (38)$$

Now we can insert the results obtained above into Eq. (29) of Sec. 9.1 of the main text.

# D Numerical Results of the Calculations for the A-Phase

We have performed the numerical calculations with $t = -0.8$ that describes the distance to the phase transition. For the magnetic field parallel to $\langle 110 \rangle$ we set $\vec{B} = \frac{1}{\sqrt{2}} \left\{ \frac{1}{2}\sqrt{-2t}, \frac{1}{2}\sqrt{-2t}, 0 \right\}^T$. For the magnetic field parallel to $\langle 110 \rangle$ we set $\vec{B} = \left\{ 0, 0, \frac{1}{2}\sqrt{-2t} \right\}^T$. In the anisotropic case, we have chosen $\delta_1 = 0.012$ and $\delta_2 = 0.001$, while in the isotropic case we set $\delta_1 = \delta_2 = 0$. Moreover, we set $\alpha_G = 1$ and $\beta = 2$.

In the abscence of a current, we find the ground state solutions for the different cases which are given in Table 1 on the next page.

The numerical data for the case with applied current is given in Table 2 on the next page. In the case $|\vec{v}_s| = v = 0$, we get the ground state values. Thus, we only present the changes linear in the prefactor $v$, i.e. $\Delta u_j / v$. However, we have to keep in mind that we have calculated the data using rescaled units, such that the scalar $v$ is not the physical spin-polarized velocity. It rather contains additional factors of $Q$, $J$ and $U$. Finally, note that $\vec{v}_s \parallel \vec{q}_2$ implies that the current is applied in the direction of the corresponding $\vec{q}_2$ vector that adjusts without a current.

To analyze how the first $q$ vector changes, we define the angle $\Delta\phi$ between $\vec{q}_1$ and $\vec{q}_1 + \Delta\vec{q}_1$ as

$$\cos(\Delta\phi) = \frac{\vec{q}_1 \cdot (\vec{q}_1 + \Delta\vec{q}_1)}{|\vec{q}_1|\,|\vec{q}_1 + \Delta\vec{q}_1|}$$

To be consistent we consider $\Delta\phi$ only up to linear oder in $v$. These data are given in Table 3. At first glance it seems, that all three configurations leads to a similar result, but this is not the case. In the isotropic case, the momentum vectors only get a component in the direction of the magnetic field, i.e. in this case $\Delta\phi$ only describes a tilt of the plane of the momentum vectors. In the second column, the situation is, however, different. We still observe a tilt, but additionally a rotation of the momentum vectors, which is shown in Fig. 14. Here, we have plotted the different momentum vectors and their corresponding planes for $v = 0.02$. The black lines and the corresponding yellow triangle belong to the ground state values, whereas the blue lines with the red triangle to the current distorted values.

The case $\vec{B} \parallel \langle 100 \rangle$ is similar to the isotropic case, i.e. there is no real rotation, but only a tilt.

| | isotropic<br>$\vec{B} \parallel \langle 110 \rangle$ | anisotropic<br>$\vec{B} \parallel \langle 110 \rangle$ | anisotropic<br>$\vec{B} \parallel \langle 001 \rangle$ |
|---|---|---|---|
| $\vec{q}_1$ | $\{-0.0025, 0.0025, -0.9992\}^T$ | $\{-0.3530, 0.3524, -0.8618\}^T$ | $\{0.4980, 0.8621, 0.0000\}^T$ |
| $\vec{q}_2$ | $\{-0.6107, 0.6107, 0.5026\}^T$ | $\{-0.3530, 0.3524, 0.8618\}^T$ | $\{-0.9959, 0.0000, 0.0000\}^T$ |
| $\vec{q}_3$ | $\{0.6131, -0.6131, 0.4966\}^T$ | $\{0.7059, -0.7049, 0.0000\}^T$ | $\{0.4980, -0.8621, 0.0000\}^T$ |
| $\vec{m}_h$ | $\{0.2050, 0.2050, -0.0000\}^T$ | $\{0.2052, 0.2052, 0.0000\}^T$ | $\{0.0000, 0.0000, 0.2903\}^T$ |

Table 1: The momentum vectors and the uniform magnetization in the abscence of a current.

| | isotropic $\delta_1 = \delta_2 = 0$<br>$\vec{B} \parallel \langle 110 \rangle$<br>$\vec{v}_s \parallel \vec{q}_2$ | anisotropic<br>$\vec{B} \parallel \langle 110 \rangle$<br>$\vec{v}_s \parallel \vec{q}_2$ | anisotropic<br>$\vec{B} \parallel \langle 001 \rangle$<br>$\vec{v}_s \parallel \vec{q}_2$ |
|---|---|---|---|
| $\Delta\vec{q}_1/v$ | $\{-0.0928, -0.0928, 0.0000\}^T$ | $\{-0.1640, 0.0309, 0.0796\}^T$ | $\{-0.0097, 0.0056, -0.1322\}^T$ |
| $\Delta\vec{q}_2/v$ | $\{-1.1384, -1.1384, 0.0000\}^T$ | $\{-1.023, -1.2193, 0.0794\}^T$ | $\{0.0000, -0.0112, -1.6570\}^T$ |
| $\Delta\vec{q}_3/v$ | $\{1.2312, 1.2312, 0.0000\}^T$ | $\{1.1817, 1.1884, -0.1590\}^T$ | $\{0.0097, 0.0056, 1.7892\}^T$ |
| $\Delta\vec{m}_h/v$ | $\{-0.1572, 0.1572, -0.0143\}^T$ | $\{-0.1390, 0.1390, 0.0979\}^T$ | $\{-0.1865, 0.1251, 0.0000\}^T$ |

Table 2: The current induced modification of the momentum vectors and the uniform magnetization.

| | isotropic $\delta_1 = \delta_2 = 0$<br>$\vec{B} \parallel \langle 110 \rangle$<br>$\vec{v}_s \parallel \vec{q}_2$ | anisotropic<br>$\vec{B} \parallel \langle 110 \rangle$<br>$\vec{v}_s \parallel \vec{q}_2$ | anisotropic<br>$\vec{B} \parallel \langle 001 \rangle$<br>$\vec{v}_s \parallel \vec{q}_2$ |
|---|---|---|---|
| $\Delta\phi/v$ | 0.1313 | 0.1856 | 0.1332 |

Table 3: Angle between $\vec{q}_1$ and $\vec{q}_1 + \Delta\vec{q}_1$.

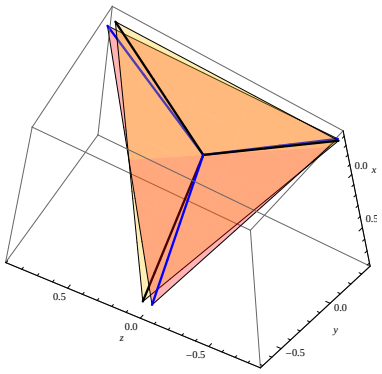


Figure 14: Different planes of the $q$-vectors for $v = 0.08$; black lines are the ground state values of the $q$-vectors that lie in the yellow area, and the blue lines represent the current distorted values that lie in the red area.

To determine how the prefactors depend on $J$, $U$ and $Q$ we have to consider the rescaling. Note, that we have rescaled the free energy in the following way:

$$\begin{aligned} \tilde{\vec{r}} &= Q\vec{r} && \Rightarrow && \vec{r} = 1/Q\,\tilde{\vec{r}}, \quad \nabla = Q\tilde{\nabla} \\ \tilde{\vec{M}} &= [U/(JQ^2)]^{1/2}\vec{M} && \Rightarrow && \vec{M} = [(JQ^2)/U]^{1/2}\,\tilde{\vec{M}} \\ \tilde{\vec{B}} &= [U/(JQ^2)^3]^{1/2}\,\vec{B} \end{aligned}$$

The same scaling should be applied to the Berry phase and the dissipation term in the LLG equation

$$\begin{aligned} \int_V d\vec{r}\left(\hat{\Omega}\times\frac{\partial\hat{\Omega}}{\partial u_j}\right)\cdot\left(\frac{d}{dt}+(\vec{v}_s\cdot\nabla)\right)\hat{\Omega}+\frac{1}{|\vec{M}|}\frac{\partial F}{\partial u_j} \\ = -\int_V d\vec{r}\cdot\alpha_G\left(\frac{d}{dt}+\frac{\beta}{\alpha_G}(\vec{v}_s\cdot\nabla)\right)\hat{\Omega}\cdot\frac{\partial\hat{\Omega}}{\partial u_j}. \end{aligned} \tag{39}$$

Let us define again

$$\begin{aligned} B &:= \int d\vec{r}\left(\hat{\Omega}\times\frac{\partial\hat{\Omega}}{\partial u_j}\right)\cdot\left(\frac{d}{dt}+\vec{v}_s\cdot\nabla\right)\hat{\Omega} \\ &= \frac{1}{Q^3}\int d\tilde{\vec{r}}\left(\hat{\Omega}\times\frac{\partial\hat{\Omega}}{\partial u_j}\right)\cdot\left(\frac{d}{dt}+Q\vec{v}_s\cdot\tilde{\nabla}\right)\hat{\Omega} =: \frac{1}{Q^3}\tilde{B}(Q\vec{v}_s), \end{aligned}$$

and

$$\begin{aligned} D &:= \int d\vec{r}\,\alpha_G\,\frac{\partial\hat{\Omega}}{\partial u_j}\cdot\left(\frac{d}{dt}+\frac{\beta}{\alpha_G}\vec{v}_s\cdot\nabla\right)\hat{\Omega} \\ &= \frac{1}{Q^3}\,\alpha_G\int d\tilde{\vec{r}}\,\frac{\partial\hat{\Omega}}{\partial u_j}\cdot\left(\frac{d}{dt}+\frac{\beta}{\alpha_G}Q\vec{v}_s\cdot\tilde{\nabla}\right)\hat{\Omega} =: \frac{1}{Q^3}\tilde{D}(Q\vec{v}_s). \end{aligned}$$

Since the prefactor of the free energy functional is $J^2Q/U$, and $|\vec{M}|$ scales like $[(JQ^2)/U]^{1/2}$, the fluctuation matrix $\mathcal{M}$ scales like $J^2Q/U \cdot [(JQ^2)/U]^{-1/2} = [J^3/U]^{1/2}$. Thus, $\mathcal{M}^{-1} = [U/J^3]^{1/2}\widetilde{\mathcal{M}}^{-1}$, and

$$\Delta u = \sqrt{\frac{U}{J^3}} \cdot \frac{1}{Q^3} \left(\widetilde{\mathcal{M}}\right)^{-1} \cdot \left(\tilde{B}(Q\vec{v}_s) + \tilde{D}(Q\vec{v}_s)\right).$$

Since

$$\left(\widetilde{\mathcal{M}}\right)^{-1} \cdot \left(\tilde{B}(Q\vec{v}_s) + \tilde{D}(Q\vec{v}_s)\right) \sim (Q \cdot |\vec{v}_s|) \cdot \alpha_G \left(1 - \frac{\beta}{\alpha_G}\right) \frac{\delta_1}{\delta_2}$$

we finally get

$$\Delta u = \sqrt{\frac{U}{J^3}} \cdot \frac{1}{Q^3} |\vec{v}_s| \cdot \alpha_G \left(1 - \frac{\beta}{\alpha_G}\right) \frac{\delta_1}{\delta_2} \cdot f(t, \hat{B}, \hat{v}_s).$$

The function $f$ depends on the distance to the phase transition, and the direction of the magnetic field, as well as the direction of the current. For the values chosen above $f$ is of the order of $10^{-2}$.

# List of Figures



# List of Tables

## References


[1] W. Münzer, A. Neubauer, S. Mühlbauer, C. Franz, T. Adams, F. Jonietz, R. Georgii, P. Boni, B. Pedersen, M. Schmidt, A. Rosch, and C. Pfleiderer. Skyrmion lattice in a doped semiconductor. *arXiv:0903.2587*, 2009.

[2] Y. Ishikawa, G. Shirane, J.A. Tarvin, and M. Kohgi. Magnetic excitations in the weak itinerant ferromagnet MnSi. *Physical Review B*, 16(11):4956–4970, 1977.

[3] N. Doiron-Leyraud, I. R. Walker1, L. Taillefer, M. J. Steiner, S. R. Julian, and G. G. Lonzarich. Fermi-liquid breakdown in the paramagnetic phase of a pure metal. *Nature*, 425:595–599, 2003.

[4] S. Mühlbauer, B. Binz, F. Jonietz, C. Pfleiderer, A. Rosch, A. Neubauer, R. Georgii, and P. Boni. Skyrmion lattice in a chiral magnet. *arXiv:0902.1968*, 2009.

[5] O. Wessely, B. Skubic, and L. Nordstrom. Spin-transfer torque in helical spin-density waves. *arXiv:0812.2509*, 2008.

[6] J. M. Hopkinson and H.-Y. Kee. Origin and consequence of an unpinned helical magnet: application to partial order in MnSi under pressure. *arXiv:0808.0712*, 2008.

[7] L. D. Landau and E. M. Lifshitz. *Electrodynamics of continuous media.* Pergamon Press, Oxford, 1884.

[8] Y. Ishikawa, K. Tajima, D. Bloch, and M.Roth. Helical spin structure in manganese silicide MnSi. *Solid State Commun.*, 19:525, 1976.

[9] P. Bak and M. H. Jensen. Theory of helical magnetic structures and phase transitions in MnSi and FeGe. *J. Phys. C: Solid State Physics*, 13:L881–5, 1980.

[10] A. Hasegawat 0. Nakanishi, A. Yanase and M. Kataoka. The origin of the helical spin density wave in MnSi. *Solid State Communications*, 35:995–998, 1980.

[11] M.L. Plumer and M. B. Walker. Wavevector and spin reorientation in MnSi. *J. Phys. C: Solid State Physics*, 14:4689, 1981.

[12] M. Kataoka and O. Nakanishi. Helical spin density wave due to antisymmetric exchange interaction. *J. Phys. Soc. Japan*, 12:3888– 3896, 1981.

[13] A. Neubauer, C. Pfleiderer, B. Binz, A. Rosch, R. Ritz, P. G. Niklowitz, and P. Boni. Topological hall effect in the A-phase of MnSi. *Physical Review Letters*, 102:186602, 2009.

[14] S. Mühlbauer, B. Binz, F. Jonietz, C. Pfleiderer, A. Rosch, A. Neubauer, R. Georgii, and P. Boni. Skyrmion lattice in a chiral magnet (supporting material). *arXiv:0902.1968*, 2009.

[15] G. Shirane Y. Ishikawa and J.A. Tarvin. Magnetic excitations in the weak itinerant ferromagnet MnSi. *Physical Review B*, 16(11), 1977.

[16] B. Lebech *et al.* Magnetic phase diagram of MnSi. *Journal of Magnetism and Magnetic Materials*, 140-144:119–120, 1995.

[17] S. V. Grigoriev *et al.* Magnetic structure of MnSi under an applied field probed by polarized small-angle neutron scattering. *Physical Review B*, 74(214414), 2006.

[18] J. W. Negele and H. Orland. *Quantum Many-Particle Systems*. Westview Press, 1998.

[19] I. Dzyaloshinskii. A thermodynamic theory of "weak" ferromagnetism of antiferromagnetics. *Journal of Physics and Chemistry of Solids*, 4:241, 1958.

[20] T. Moriya. Anisotropic superexchange interaction and weak ferromagnetism. *Physical Review*, 120(1):91–98, 1960.

[21] P. Bak and M. Hogh. Theory of helical magnetic structures and phase transitions in MnSi and FeGe. *Journal of Physics C*, 13(L881), 1980.

[22] P. M. Chaikin and T. C. Lubensky. *Principles of Condensed Matter Physics*. Cambridge University Press, Cambridge, 1995.

[23] D.A. Yablonskii A.N. Bogdanov. *Sov. Phys. JETP*, 68(101), 1989.

[24] D. C. Ralph and M. D. Stiles. Spin transfer torques. *Journal of Magnetism and Magnetic Materials*, 320:1190, 2008.

[25] J. C. Slonczewski. Current-driven excitation of magnetic multilayers. *Journal of Magnetims and Magnetic Materials*, 159, 1996.

[26] L. Berger. Emission of spin waves by a magnetic multilayer traversed by a current. *Physical Review B*, 54(13), 1996.

[27] R. A. Duine, A. S. Nunez, Jairo Sinova, and A. H. MacDonald. Functional keldysh theory of spin torques. *Physical Review B*, 75:214420, 2007.

[28] M. E. Lucassen, H. J. van Driel, C. Morais Smith, and R. A. Duine. Current-driven and field-driven domain walls at nonzero temperature, 2009.

[29] S. Zhang and Z. Li. Roles of nonequilibrium conduction electrons on the magnetization dynamics of ferromagnets. *Physical Review Letters*, 93:127204, 2004.

[30] R. A. Duine. Spintronics. 2009. URL `http://www.phys.uu.nl/~duine`.

[31] Z. Li J. He and S. Zhang. Current-driven vortex domain wall dynamics by micromagnetic simulations. *PHYSICAL REVIEW B*, 73:184408, 2006.

[32] R. A. Duine. Effects of nonadiabaticity on the voltage generated by a moving domain wall. *Physical Review B*, 79:014407, 2009.

[33] M. Tsoi *et al.* Excitation of a magnetic multilayer by an electric current. *Physical Review Letters*, 80(19):4281–4284, 1998.

[34] B. A. Jones Ya. B. Bazaliy and Shou-Cheng Zhang. Modification of the landau-lifshitz equation in the presence of a spin-polarized current in colossal- and giant-magnetoresistive materials. *Physical Review B*, 57(6):3213, 1998.

[35] S. E. Barnes and S. Maekawa. Current-spin coupling for ferromagnetic domain walls in fine wires. *Physical Review Letters*, 95(107204), 2005.

[36] Y. Tserkovnyak *et al.* Nonlocal magnetization dynamics in ferromagnetic heterostructures. *Reviews of Modern Physics*, 77, 2005.

[37] G. Tatara H. Kohno and J. Shibata. Microscopic calculation of spin torques in disordered ferromagnets. *Journal of the Physical Society of Japan*, 11(11), 2006.

[38] H. Kohno, G. Tatara, and J. Shibata. Microscopic calculation of spin torques in disordered ferromagnets. *Journal of the Physical Society of Japan*, 75:113706, 2006.

[39] K. Goto, H. Katsura, and N. Nagaosa. Current-induced dynamics of spiral magnet. *arXiv:0807.2901*, 2008.

[40] I. Garate, K. Gilmore, M. D. Stiles, and A. H. MacDonald. Nonadiabatic spin-transfer torque in real materials. *Physical Review B*, 79(10):104416, 2009.

[41] M. Kläui, C. A. F. Vaz, J. A. C. Bland, W. Wernsdorfer, G. Faini, E. Cambril, L. J. Heyderman, F. Nolting, and U. Rüdiger. Controlled and reproducible domain wall displacement by current pulses injected into ferromagnetic ring structures. *Physical Review Letters*, 94:106601, 2005.

[42] M. Hayashi, L. Thomas, R. Moriya, C. Rettner, and Stuart S. P. Parkin. Current controlled magnetic domain wall nanowire shift register. *Science*, 320(209), 2008.

[43] I. Fischer. Metallic magnets without inversion symmetry and antiferromagnetic quantum critical points. *Dissertation*, 2006.

[44] B. Binz and A. Vishwanath. Theory of helical spin crystals: phases, textures and properties. *Physical Review B*, 74:214408, 2006.

[45] D. Belitz, T. R. Kirkpatrick, and A. Rosch. Theory of helimagnons in itinerant quantum systems. *Physical Review B*, 73:054431, 2006.

[46] B. Binz and A. Vishwanath. Chirality induced anomalous-hall effect in helical spin crystals. *Physica B*, 403:1336, 2008.

[47] M. Lee, W. Kang, Y. Onose, Y. Tokura, and N. P. Ong. Unusual hall effect anomaly in MnSi under pressure. *Physical Review Letters*, 102:186601, 2009.

[48] J. Ye, Y. B. Kim, A. J. Millis, P. Majumdar, and Z. Tesanovic. Berry phase theory of the anomalous hall effect: Application to colossal magnetoresistance manganites. *Physical Review Letters*, 83(18), 1999.

[49] B. Binz and A. Vishwanath. Theoretical proposal predicting anomalous magnetoresistance and quadratic hall effect in the partially ordered state of MnSi. *Journal of Magnetism and Magnetic Materials*, 310:1062, 2007.

[50] A. Altland and B. Simons. *Condensed Matter Field Theory*. Cambridge, University Press, 2006.

# Deutsche Zusammenfassung

Die vorliegende Diplomarbeit befasst sich mit dem Einfluss von elektrischen Strömen auf magnetische Materialien. Verschiedene Spintronik-Experimente deuten daraufhin, dass sich mittels Spin-Transfer-Drehmomenten magnetische Strukturen durch elektrische Ströme beeinflussen lassen.

Wir konzentrieren uns in dieser Arbeit auf magnetische Materialien ohne Inversionssymmetrie, in denen eine schwache Spin-Bahnkopplung zur Ausbildung von magnetischen Helizes führt. Helimagnetische Strukturen tauchen in einer Vielzahl von Materialien auf, z.B in MnSi, $Fe_xCo_{1-x}Si$, CrSi und FeGe.

Wir betrachten insbesondere den itineranten Helimagneten MnSi, der zusätzlich zur helikalen und zur konischen Phase noch eine topologisch stabile Phase, die sogenannte A-Phase besitzt. Diese lässt sich, wie seit Kurzem bekannt ist, approximativ sehr gut durch eine Superposition von drei Helizes und einer uniformen magnetischen Komponente beschreiben.

Zunächst fassen wir einige allgemeine Eigenschaften von MnSi zusammen. Insbesondere stellen wir das magnetische Phasendiagramm von MnSi dar, in dem die Temperatur gegen das äußere angeleget Magnetfeld aufgetragen ist. Anschließend schilder wir den experimentellen Nachweis und die theoretischen Beschreibung der magnetischen Phasen.

In den darauf folgenden Kapiteln diskutieren wir den Einfluss des Stromes auf die verschiedenen magnetischen Konfigurationen. Technisch betrachtet ist unser Ansatzpunkt die Landau-Lifshitz-Gilbert Gleichung, die das reaktive und das dissipative Spin-Transfer-Drehmoment beinhaltet. Sie beschreibt die Dynamik der lokalen Magnetisierung in Anwesenheit eines Stroms. Wir charakterisieren die verschiedenen magnetischen Strukturen durch zeitabhängige Parameter und bestimmen Bewegungsgleichungen für diese.

Unser Hauptergebnis ist, dass der Strom die Richtung der Helix unbeeinflusst lässt, was ebenfalls im Experiment festgestellt wurde, aber dass der Strom einen Einfluss auf die leicht anisotrope A-Phase hat. Aus den theoretischen Berechnungen ergibt sich, dass die Anordnung der Richtungsvektoren der drei Helizes in der A-Phase rotiert und kippt. Beide Effekte sind linear im spin-polarisierten Anteil des elektrischen Stroms. Es ist wahrscheinlich, dass die Theorie, die in dieser Diplomarbeit präsentiert wird, in der Lage ist, die experimentell beobachtbare Veränderung der Position der Richtungsvektoren der Helizes unter Stromeinfluss zu erklären.

Desweiteren schildern wir den topologischen Hall-Effekt, der ein charakteristisches

Merkmal für magnetische Strukturen mit endlicher Skyrmiondichte ist. Mittels des topologischen Hall-Effekts ließ sich die A-Phase als Anti-Skyrmion-Gitter identifizieren.

Darüber hinaus betrachten wir noch einen Variationsansatz, aus dem sich die Landau-Lifshitz-Gilbert Gleichung herleiten lässt. Innerhalb dieses Ansatzes wird die topologische Struktur aufgrund eines in der Wirkung auftauchenden Berry-Phasen-Terms besonders deutlich.

Die magnetische Struktur der A-Phase wurde mittlerweile auch bei $Fe_xCo_{1-x}Si$ für $x = 0.2$ und $x = 0.25$ nachgewiesen. Dies lässt vermuten, dass die betrachtete Theorie auch für andere chirale magnetische Materialien anwendbar ist.

# Danksagung

An dieser Stelle möchte ich mich herzlich bei Herrn Prof. Dr. Achim Rosch für die Vergabe und Betreuung dieser Arbeit bedanken.

Dank gilt auch Herrn Prof. Dr. Rembert Duine für die vielfältigen und Gespräche zur Thematik, sowie Herrn Prof. Christian Pfleiderer für die guten experimentellen Ergebnisse.

Ebenfalls danken möchte ich Herrn Dr. Benedikt Binz für die sehr gute Einführung in das Thema und bei Herrn Dr. Markus Garst für die geduldige Zusammenarbeit an der Theorie über den Einfluss des Stroms auf die A-Phase.

Weiterer Dank gebührt der Arbeitsgruppe von Herrn Prof. Dr. Achim Rosch und Herrn Prof. Dr. Matthias Vojta, in der ein sehr angenehmes Arbeitsklima vorherrscht.

Meiner Familie und meinem Freund danke ich für die Unterstützung in jeglicher Hinsicht.

# Erklärung

Hiermit versichere ich, die vorliegende Arbeit selbstständig angefertigt und keine anderen als die angegebenen Quellen und Hilfsmittel benutzt sowie Zitate kenntlich gemacht zu haben.

Köln, 12. Juni 2009

(Karin Everschor)